M.S-I

FINAL REPORT

NASA CR 70530

Development of Monitoring Techniques by Acoustical Means for Mechanical Checkouts

30
~~15~~ November 1965

Contract No. NAS 8-11976

Prepared for:

NATIONAL AERONAUTICS AND SPACE ADMINISTRATION
GEORGE C. MARSHALL SPACE FLIGHT CENTER
Huntsville, Alabama

Prepared by:

S. J. Campanella, D.E.E.
D. M. Speaker

MELPAR INC
A SUBSIDIARY OF WESTINGHOUSE AIR BRAKE COMPANY
3000 ARLINGTON BOULEVARD, FALLS CHURCH, VIRGINIA

FINAL REPORT

DEVELOPMENT OF MONITORING TECHNIQUES BY ACOUSTICAL MEANS FOR MECHANICAL CHECKOUTS

Period Covered

15 May 1965 to 30 September 1965

Contract NAS8-11976

Control No. 1-5-60-00051-01 (1F)

Prepared for:

National Aeronautics and Space Administration
George C. Marshall Space Flight Center
Huntsville, Alabama 35812

Prepared by:

S. J. Campanella, D.E.E.
D. M. Speaker

Electronics Research Laboratory
Melpar, Inc.
7700 Arlington Blvd.
Falls Church, Virginia 22046

30 November 1965

FOREWORD

This report was prepared by Melpar, Inc., under Contract No. NAS8-11976, Development of Monitoring Techniques by Acoustical Means for Mechanical Checkouts, for the George C. Marshall Space Flight Center, National Aeronautics and Space Administration.

ABSTRACT

The purpose of the study described in this report was to analyze sonic signatures produced during a number of repetitive operations of S3D and F1 engine valves with the view of exploring the feasibility of mechanical means for valve checkout using sonic data as a criterion. The data studied was derived during operations of S3D fuel, lox and gas generator valves and an F1 lox valve.

The valve signals were detected by Endevco accelerometers located at various selected points on the valves and were recorded in both Direct Record and FM modes. It is worth noting that the Direct Record mode is preferred because it permits preservation of wider bandwidth than is possible with FM for a given tape speed. For example, at 60 inches per second, an extended range machine will record satisfactorily only to about 20 kc in the FM mode, while its Direct Record capability, at the same speed, is over ten times as great. For adequate analysis, the S3D valves required a frequency range of 0 to 64 kc, but an analysis band of 0 to 32 kc was adequate to preserve the essential features of the F1 lox valve patterns. Recordings were made simultaneously, on different tracks, of a given event as sensed at various valve locations. The recorded tapes were supplied to Melpar as the raw facsimile data.

The data on the tapes, played back at reduced speed, was initially analyzed, using Melpar's 100 channel fine structure spectrum analyzer to determine the frequency bands containing the sonic signature features of greatest significance to the analysis. The spectrographic patterns thus developed exhibited distinctive features vividly portraying the most subtle

details of mechanical operation. The data was subsequently reanalyzed on a parametric basis which supplied both amplitude and frequency time functions for the different valve operations that captured the significant information content and preserved it in a more efficient form suited ideally to automatic recognition of valve malfunction by pattern matching.

From the parametric analysis data it was possible to illustrate that successive operations of the same valve produce spectrographic signatures that tightly cluster about a mean pattern called the base-line pattern. The capability to easily ascertain deviations from these base-line patterns that reflect valve malfunction is rather obvious. It is a fact that two deviations were indeed found for S3D fuel valve openings and one deviation for an F1 lox valve closing. As further confidence in the fact that the base-line patterns form a basis of malfunction detection and indeed a basis for critical analysis of valve operation, it has been possible to establish a one-for-one correspondence between features of the parametric analysis and mechanical events in the valve operation.

In the case of the F1 lox valve, a finding of critical importance was that the purging noise due to persistence of actuating gas flow when the valve is not being operated, did not prevent accurate timing measurements from being performed nor did it obscure other critical features of the sonic signature. Actually, differences in the purging noise patterns, before and after the operating event, served to distinguish the open from closed state.

The effects of sensor location were studied. It was determined that the sensor location did influence the sonic signature produced and that for reliable malfunction detection, multiple sensors should be employed.

Additional study of F1 valve signatures is recommended and the prospects for an automated malfunction detection system, based on the results so far obtained, appear far better than was anticipated in advance of this program.

TABLE OF CONTENTS

		Page
ABSTRACT		1
1.	INTRODUCTION	9
2.	TECHNICAL DISCUSSION	11
	2.1 Objective	11
	2.2 Analysis Methods Employed	12
	2.2.1 General	12
	2.2.2 Fine Structure Spectrographic Analysis	13
	2.2.3 Parametric Analysis	17
	2.3 Source Data Collection Method	21
	2.4 Valve Signature Feature Analysis	22
	2.4.1 General	22
	2.4.2 S3D Fuel Valve	23
	I. Opening Event, Fuel Valve S3D	29
	II. Closing Event, Fuel Valve, S3D	33
	2.4.3 S3D Lox Valve	43
	I. S3D Lox Valve Openings	43
	II. S3D Lox Valve Closings	48
	2.4.4 S3D Gas Generator Valve	55
	I. S3D Gas Generator Valve Openings	55
	II. S3D Gas Generator Opening Event	60
	III. S3D Gas Generator Closing Event	61
	2.4.5 F1 Lox Valve	63
	I. F1 Lox Valve Opening Event	63
	II. Discussion of F1 Lox Valve Openings as Seen on Tracks 1 and 2	72
	III. Purging Noise Characteristics Before and After F1 Valve Opening Event	75
	IV. F1 Lox Valve Closing Event	77
	V. Discussion of F1 Lox Valve Closings as Seen on Tracks 1 and 2	86

TABLE OF CONTENTS (CONT'D.)

		Page
	VI. Purging Noise Characteristics Before and After F1 Valve Closing Event	94
	VII. F1 Lox Valve Feature Timing Analysis	98
2.5	Correlation of Sonic Signature Features with Mechanics of Valve Operation	102
2.5.1	S3D Fuel Valve	102
2.5.2	S3D Lox Valve	105
2.5.3	S3D Gas Generator Valve	106
2.5.4	F1 Lox Valve	107
2.5.5	Orifice Resonance	111
3.	QUALITY OF TAPES RECEIVED FROM NASA	114
4.	CONCLUSIONS	116
4.1	General	116
4.2	Signature Stability	117
4.3	Distinctive Feature Correlates	123
4.4	Influence of Sensor Locations	127
4.5	Summary of Conclusions	128
5.	RECOMMENDATIONS	130

LIST OF ILLUSTRATIONS

Figure		Page
1	Spectrum Analysis System, Block Diagram	15
2	Parametric Analysis System, Block Diagram	18
3	Spectrograms of Four Apparently Normal S3D Fuel Valve Openings, Tape N3, Track 1	24
4	Spectrograms Showing Comparison of Two Apparently Normal Openings with Two Abnormal Openings of S3D Fuel Valve, Tape N3, Track 1. (Normal Operation 2 Compared with Abnormal Operation 1; Normal 10 with Abnormal 11).	25
5	Spectrograms of Two Apparently Normal S3D Fuel Valve Openings, Tape N3, Track 2. Operations 5 and 7.	26
6	Parametric Plots of Four Apparently Normal S3D Fuel Valve Openings, Tape N3, Track 1. Operations 2, 5, 7 and 10.	27
7	Parametric Plots Showing Comparison of Two Apparently Normal S3D Fuel Valve Openings with Two Abnormal Openings, Tape N3, Track 1. (Normal Operation 2 Compared with Abnormal Operation 1; Normal 10 with Abnormal 11).	28
8	Parametric Plots of Two Apparently Normal S3D Fuel Valve Openings, Tape N3, Track 2. Operations 2 and 4.	34
9	Spectrograms of Two Typical Closings of S3D Fuel Valve, Tape N3, Track 1. Operations 2 and 5.	35
10	Spectrograms of Two Typical S3D Fuel Valve Closings, Tape N3, Track 2. Operations 2 and 5.	36
11	Parametric Plots of Two Typical S3D Fuel Valve Closings, Tape N3, Track 1. Operations 2 and 4.	37
12	Parametric Plots of Two Typical S3D Fuel Valve Closings, Tape N3, Track 2. Operations 2 and 4.	38
13	Spectrograms of Two S3D Lox Valve Openings, Tape N3, Track 1. Operations 12 and 20.	44
14	Parametric Plots of Two Typical S3D Lox Valve Openings, Tape N3, Track 1. Operations 4 and 5.	45

LIST OF ILLUSTRATIONS (CONT'D.)

Figure		Page
15	Spectrograms of Two S3D Lox Valve Closings, Tape N3, Track 1. Operations 12 and 20.	49
16	Parametric Plots of Two Typical S3D Lox Valve Closings, Tape N3, Track 1. Operations 4 and 5.	50
17	Spectrograms of Two S3D Gas Generator Valve Openings, Tape N3, Track 1. Operations 5 and 14.	56
18	Spectrograms of Two S3D Gas Generator Valve Closings, Tape N3, Track 1. Operations 5 and 14.	57
19	Parametric Plots of Two Typical S3D Gas Generator Valve Openings, Tape N3, Track 1. Operations 4 and 5.	58
20	Parametric Plots of Two Typical S3D Gas Generator Valve Closings, Tape N3, Track 1. Operations 4 and 5.	59
21	Spectrograms of Two F1 Lox Valve Openings, Tape N8, Track 1. Operations 4 and 5.	64
22	Spectrograms of Two F1 Lox Valve Openings, Tape N8, Track 2. Operations 4 and 5.	65
23	Parametric Plots of Two Typical F1 Lox Valve Openings, Tape N8, Track 1. Operations 4 and 5.	66
24	Parametric Plots of Two Typical F1 Lox Valve Openings, Tape N8, Track 2. Operations 4 and 5.	67
25	Parametric Plot of F1 Lox Valve Opening Showing Parameter Identification, Tape N8, Track 2. Operation 1.	73
26	Spectrograms of Two F1 Lox Valve Closings, Tape N8, Track 1. Operations 4 and 5.	78
27	Spectrograms of Two F1 Lox Valve Closings, Tape N8, Track 2. Operations 4 and 5.	79
28	Parametric Plots of Two Typical F1 Lox Valve Closings, Tape N8, Track 1. Operations 4 and 5.	80
29	Parametric Plots of Two Typical F1 Lox Valve Closings, Tape N8, Track 2. Operations 4 and 5.	81

LIST OF ILLUSTRATIONS (CONT'D.)

Figure		Page
30	Parametric Plot of F1 Lox Valve Atypical Closing, Tape N8, Track 2. Operation 1.	88
31	Parametric Plot of F1 Lox Valve Closing Showing Parameter Identification, Tape N8, Track 2. Operation 2.	89
32	S3D Valves with Sensor Locations Shown	103
33	Longitudinal Section of F1 Lox Valve Showing Sensor Locations for Tracks 1 and 2	108
34	Spectrogram of Acoustic Output of Air Jet Excited Pipe	112
35	Skeleton Diagram of F1 Lox Valve Opening, Track 2	131

LIST OF TABLES

Table		Page
I	S3D Engine Fuel Valve Opening Events, Tape N3, Track 1 Parametric Stability	32
II	S3D Engine Fuel Valve Closing Events, Tape N3, Track 1 Parametric Stability	41
III	S3D Engine Lox Valve Opening Events, Tape N3, Track 1 Parametric Stability	46
IV	S3D Engine Lox Valve Closing Events, Tape N3, Track 1 Parametric Stability	51
V	F1 Engine Lox Valve Opening Events, Tape N8, Track 1 Parametric Stability	69
VI	F1 Engine Lox Valve Opening Events, Tape N8, Track 2 Parametric Stability	70
VII	F1 Engine Lox Valve Closing Events, Tape N8, Track 1 Parametric Stability	82
VIII	F1 Engine Lox Valve Closings, Tape N8, Track 2 Parametric Stability	83
IX	Summary of Mean Dispersions in Percent Deviation From Mean Value Observed in S3D Valve Operation Acoustical Signatures	120
X	Summary of Mean Dispersions in Percent Deviation From Mean Value Observed in F1 Lox Valve Operation Acoustical Signatures	122

1. INTRODUCTION

This report describes the techniques employed and results achieved in the course of analysis of sonic signatures produced by repetitive operations of both S3D and F1 engine valves. The underlying purpose of the study was to determine whether such an analysis would or would not indicate the feasibility of ultimately detecting valve malfunction through automated pattern recognition devices which would employ sonic data as the basis for such decision making. The results all favor, and very highly favor, an optimistic prediction for a successful mechanical checkout technique.

The following section of this report, after discussing the objective of the work more fully, describes the analytic processes employed as well as the means used for procuring the original data. It then considers in some considerable detail the analysis of the features occurring in the sonic signatures of valve operation, both for opening and closing events. This section also reviews correlations which were found to exist between many such features and the mechanics of valve operation.

The next section, Section 3, is a brief synopsis of the quality of data tapes, eight in all, received from NASA.

Section 4 of this report is devoted principally to conclusions. In particular, Section 4 discusses the statistical stability of the various sonic signature features as they were measured over a series of operations for a given valve and the feasibility of automated sensing of malfunction.

Section 5 is a recommendations section. In essence, it proposes the extension of the analytic work just completed. The proposed extension is to be based on data derived from additional F1 engine valves and from a

variety of engines. The purpose of this analysis is to obtain additional statistical support for establishing a base-line of normal operation so that machine recognition of malfunction, which would appear as a deviation from an established pattern, could be established within a framework of unquestioned reliability.

2. TECHNICAL DISCUSSION

2.1 Objective

The central purpose of the study program was to test the thesis that acoustical monitoring of space vehicle engine valves could provide an entirely adequate and satisfactory basis for mechanical checkout of their operation. In order to establish the validity of the technique *per se*, aside from the matter of ultimate method of implementation, the experimental and subsequent analytical procedures were specifically designed to furnish answers to the following questions:

a) Do the acoustical signature patterns essentially correlate with what happens in the valve during operation? In other words, does a series of similar operations produce a series of similar patterns? And, as a starting point, will a malfunction or abnormal operation produce a recognizable alteration of the pattern?

b) Granting the validity of the foregoing, can, in a more detailed sense, the timing of successive events associated with a valve operation be measured with reasonable precision from the acoustically derived data?

c) Can the patterns be adequately defined in terms of a relatively small number of amplitude and frequency parameters? In this connection, is it possible to select specific frequency bands containing significant diagnostic information?

d) Can specific pattern details be correlated with specific mechanical events?

e) Is the range of variation of specific pattern detail, for normal operation, sufficiently small so that a pronounced variation may be considered significant?

It should be noted that while all of these questions have a direct bearing, as indicated above, on the validity of the acoustical signature as reliable diagnostic information, (c), (d), and (e) in particular also relate specifically to the feasibility of producing an automated valve checkout monitoring system employing sonic data.

2.2 Analysis Methods Employed

2.2.1 General

During the investigation the following valves were analyzed:

a) S3D Fuel, opening and closing

b) S3D Lox, opening and closing

c) S3D Gas Generator, opening and closing

d) F-1 Lox, opening and closing

The raw tape recorded data as received was slowed down and passed through two analytic processes. This data originated from sensors placed at judiciously selected points on the valves under study. The first process involved a fine structure spectrographic technique whose purposes were:

a) To determine essential pattern similarity.

b) To provide a preliminary estimate of event timing.

c) Most importantly, to indicate the frequency bands defining the spectral ranges containing significant acoustic energy and hence feature cues associated with the different events under study.

The second process was a parametric reduction of the data. In this method the original data is supplied to a parallel bank of appropriately selected bandpass filters. Amplitude functions, and, in some instances, frequency centroid functions of the filter outputs were recorded. The selection

of the frequency pass bands was based on examination of the preceding spectrographic analysis. The parametric representation, of course, does not contain information which is not present in the spectrographic reduction, but it presents it in a form which is far more readily analyzed, both by the human brain and, potentially, by automatic pattern recognition apparatus. In particular, the parametric portrayal is particularly helpful in determining:

a) Precise timing of event occurrences and durations.

b) Spectral band energy variations during valve operation.

c) Spectral band frequency variations during valve operation.

d) Correlation of specific details of sonic signature with mechanical events.

The following two sections describe the spectrographic and parametric analytic techniques in detail.

2.2.2 Fine Structure Spectrographic Analysis

As indicated earlier, the original data was first "slowed down" as a preliminary to the analysis, including both the spectrographic and parametric procedures. The slowdown was accomplished by playing the data back at reduced speed with or without intermediate rerecording as determined by the required reduction ratio. All S3D data was analyzed at 1/64th of the original speed. The F-1 data was analyzed at 1/32nd of the original. There are two reasons for employing speed reduction. First, the frequency range of interest in the original data is brought within the bandwidth of the analysis equipment. Second, by slowing down the original data it is possible to determine signature detail and timing information with considerably greater ease and reliability than would otherwise be possible.

The overall arrangement of the fine structure spectrographic analysis system is shown in block diagram form in Figure 1. The tape data, played back at reduced speed, is first filtered to remove components above 1 kc. In real time, this 1 kc band corresponds, of course, to a 32 kc range for the F-1 lox valve signatures and to a 64 kc range for the S3D valve data. The 1 kc band is then displaced upward, in effect, by heterodyning with a 1 kc fixed oscillator so that it now occupies the range of 1 to 2 kc which corresponds to the bandspread of the analyzing filter bank. Other modulation products, because of the initial low pass filtering of the data, are all outside the range of the filter bank.

The filter bank is actually the heart of the entire system. This instrument, developed and built by Melpar, Inc., contains 100 channels, each 10 cps wide at the 3 db points. Its specific value lies in the fact that it permits fine spectrographic analysis on a simultaneous basis for all channels. To achieve a similar analysis with a conventional narrow band heterodyne type analyzer would require a long, slow scan because of the appreciable buildup time requirement. The signal is simultaneously applied to all 100 channel inputs which are connected in parallel. The output of each filter is individually rectified and filtered. It is then sequentially scanned by a rotating mercury jet switch which samples the output of the entire bank 60 times each second. The switch output is applied as a horizontal deflection signal to a vertical CRT trace. This output, in addition, also amplitude modulates a 100 kc sinewave which is then supplied to the Z axis of the CRT. The effect is to intensify the higher amplitude signal brightness and so augment the distinctive features of the display. An external

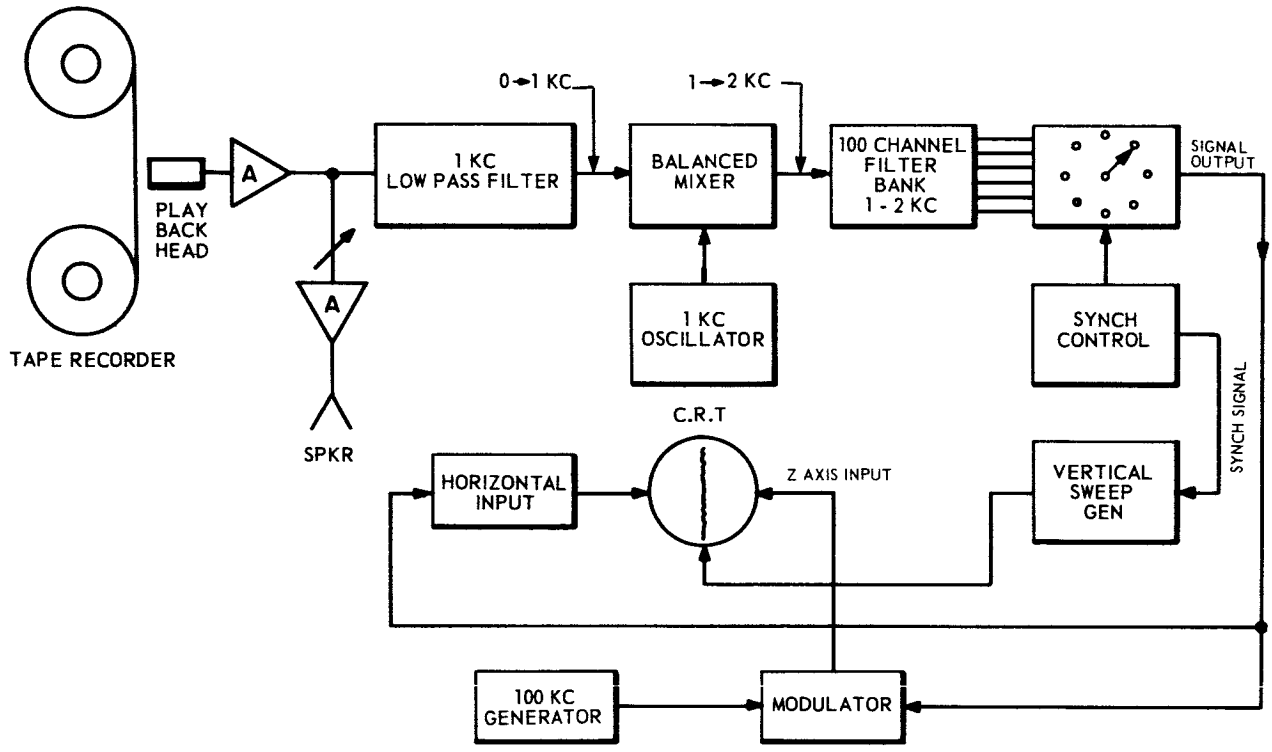

Figure 1. Spectrum Analysis System--Block Diagram

sawtooth generator provides a vertical trace for the CRT and is synchronized by a pulse from the scanning switch circuit. The synchronization insures that the start of the trace, from bottom to top, always begins at the time when No. 1 filter of the bank is being sampled. Thus, one vertical trace corresponds to one scan of the mercury switch. Means are also provided for time division so that the scan rate may be reduced from 60 per second to 30 or 15. Most of the S3D data was presented at a 60 per second scan rate, while the F-1 data was scanned at 15 sweeps per second.

At this point the CRT display consists of a vertical trace, moving from bottom to top, with energy in any given frequency channel appearing as a brightened local deflection of the trace. In order to portray the spectrographic analysis in time, a slow horizontal sweep may be superimposed on the horizontal signal input. This method is, in fact used, for preliminary visual inspection. For permanent recording, the trace is maintained in a fixed horizontal position and photographed with a motion picture camera whose film moves continuously. In this case the horizontal sweep is in effect supplied by the film motion. Typical examples of the spectrograms so produced are shown in Figures 3 & 4, and other illustrations contained in this report.

Conversion of frequency and time relationships from those appearing in the spectrograms to those corresponding to the real events is quite simple. For frequency, in the case of the S3D valves, with a slowdown ratio of 64 to 1, the total 1 kc width of the filter bank corresponds, of course, to 64 kc in "real" frequencies. Each channel then represents a "real" bandwidth

of 640 cps. For the F-1 lox valve data, the equivalent figures are 32 kc total bandwidth and 320 cps bandwidth per channel, since the slowdown ratio was 32 to 1. In all cases, the film speed was 22 inches/minute. Therefore, each second in slowed down analysis time was represented by 22/60 or 0.367 inch (0.933 cm). Conversely, one inch of original spectrogram would represent 2.72 seconds (one cm = 1.073 seconds). For the S3D valves, then one inch represented 2.72/64 = 42.6 milliseconds (one cm = 16.8 msec). For the F-1 lox spectrograms the time values per unit length would be double those above.

2.2.3 Parametric Analysis

As was pointed out in Section 2.2.1, spectrographic analysis was essential to indicating the frequency bands wherein significant acoustic data clustered most densely during the course of valve operation. However, for more refined and detailed study a different technique - parametric analysis - was invoked. The principle involved will become clear immediately on reference to the block diagram illustrating the system in Figure 2 . As for the spectrographic analysis, the data is supplied to the system in slowed down time. The signal energy is then divided into four frequency bands. The values actually employed were:

	S3D	F1
Band 1	0 to 100 cps	0 to 100 cps
Band 2	90 to 200 cps	90 to 200 cps
Band 3	250 to 400 cps	250 to 400 cps
Band 4	450 to 1000 cps *	500 to 1000 cps

* 600 to 1000 cps for Gas Generator

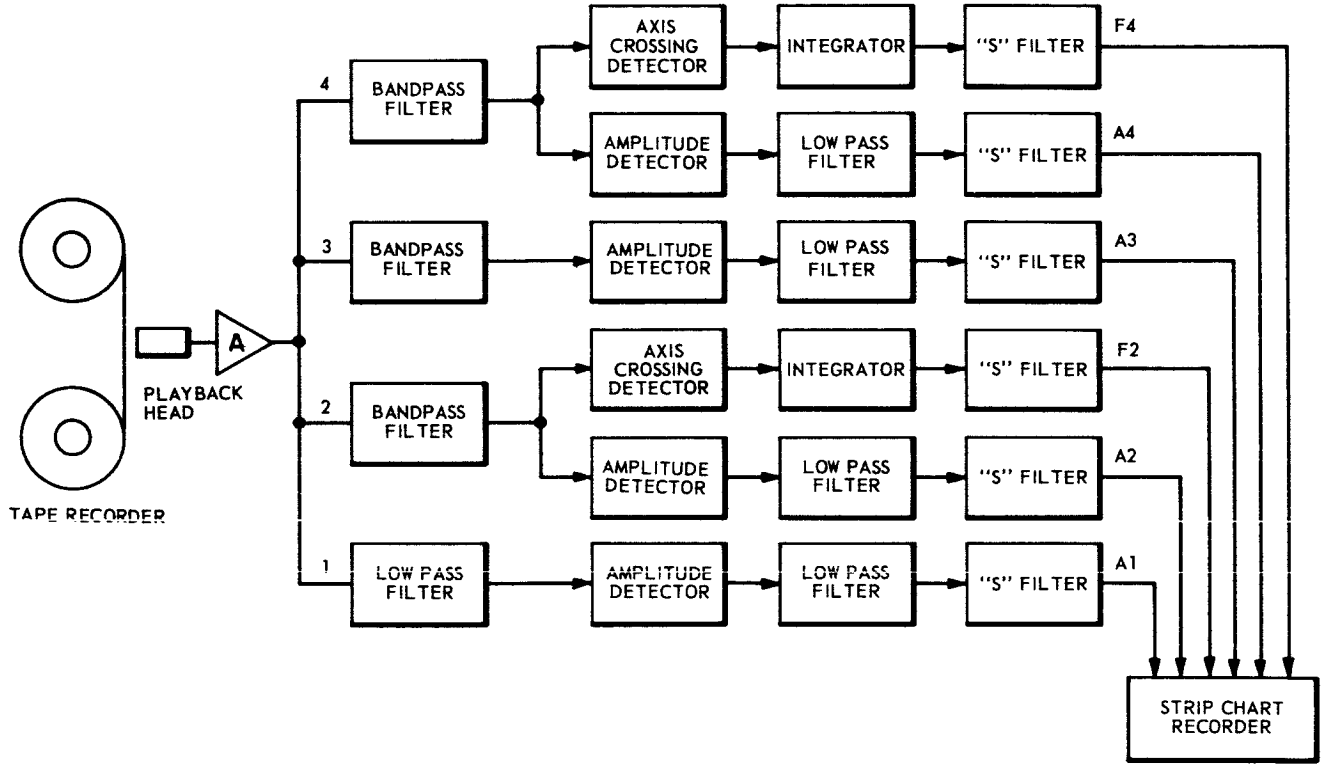

Figure 2. Parametric Analysis System--Block Diagram

It was purely fortuitous that the frequency bands of interest happened to vary so slightly for the different valves studied.

The output of each band was half-wave rectified and filtered to provide an amplitude function. In addition, the outputs of bands 2 and 4 were passed through axis crossing detectors. These detectors produce a standard, normalized DC pulse for each axis crossing. Therefore, the number of pulses per second is a measure of the axis crossings detected per second and the mean DC level produced by integrating the pulses indicates the mean frequency of the input signal.

It will be noted that there are six distinct information signals now derived from the original data and, for convenience, these are identified as follows:

Band 1 Amplitude ——— A1

Band 2 Amplitude ——— A2

Band 2 Frequency ——— F2

Band 3 Amplitude ——— A3

Band 4 Amplitude ——— A4

Band 4 Frequency ——— F4

These amplitude and frequency values are parameters in the sense that they characterize the principal features of interest in the original signal. As will appear, they define timing and other characteristics of the valve operations and serve as a basis for differentiating between normal and abnormal function.

Each of these parameters appears as a time varying DC signal which conveniently lends itself to recording in visual form by a moving pen type

chart recorder. It should be noted that the time constants of the integrators following the axis crossing detectors and of the filters following the rectifiers cannot be made too long without risking loss of definition of abrupt amplitude changes in the traces. On the other hand, sufficiently short time constant circuits permit the passage of relatively fast small amplitude variations which tend to impose an extreme jaggedness on the traces and hinder clear cut analysis of the important diagnostic features. This difficulty was overcome through the use of a special device (proprietary Melpar development) generically dubbed an "S" filter. The S filter has unique property of altering its time constant as a function of signal level change. For small changes the time constant is quite large while for large changes the time constant is small. Thus, most of the jaggedness mentioned above is eliminated while the features of real interest in the traces are adequately preserved. Reference to Figure 2 will show that an S filter has been included in each signal line to the chart recorder.

Strip chart recordings of the parameter values are called "Parametric Plots" and typical examples are illustrated in Figures 7, 8, and other figures. In each case the order of presentation from bottom to top is A_1, A_2, F_2, A_3, A_4 and F_4.

Amplitude values were measured in relative terms, using the graduation of the chart paper itself. All recordings were made at a chart speed of 5 mm/second. In terms of "real time" of valve operation, for the S3D valves each millimeter represented 3.12 milliseconds; for the F-1 lox valve it represented 6.24 milliseconds. For the F_2 parameter, each millimeter represented 1105 cps, and for the F_4 parameter each millimeter represented

1441 cps in the case of the S3D valves. The corresponding values for the F-1 lox valve plots were, of course, half of these respectively.

2.3 Source Data Collection Method

The data collection, performed by NASA, was achieved through use of Endevco accelerometers attached to various appropriately selected parts of the valve assemblies. These accelerometers incorporate lead zirconate piezoelectric elements and function, in effect, as wide range vibration pickups. The outputs of five accelerometers, at different locations, were amplified by Endevco charge amplifiers and recorded on magnetic tape at 60 ips, using three direct record channels and 2 FM channels. The tape recorder was equipped with two additional FM channels of which one was used for voice identification and the other for timing information. Valve operations were recorded in sequences of several opening and closing operations. In all, eight tapes were received from NASA which were numbered by Melpar, Inc., as N1, N2 .....N8 in serial order of receipt. The signal quality on tape N3 (containing data on the fuel, lox and gas generator valves of S3D engine) and on tape N8 (containing the data on the lox valve of F-1 engine) was particularly good and these tapes were chosen for detailed analysis.

It is worth pointing out that the Endevco accelerometers (Models 2217 and 2227) performed very well. According to the manufacturer, the models used have frequency responses more or less flat to 5 or 6 kc and resonant frequencies of 25 for the Model 2227 to 30 kc for the Model 2217. Nevertheless, no evidence of high-Q resonance peaks was observed and significant energy was found in the AM record channels at substantially higher frequencies. This is probably due to the fact that even though the transducers

resonate at the frequencies indicated above, the resonance is highly damped.

The S3D tape (N3) included a timing track consisting of a steady frequency signal (6.4 kcs) whose amplitude was stepped up or down by microswitches mechanically coupled to the valve and actuating system. Three amplitude levels were used, the lowest level corresponding to the valve closed position, the middle level indicating the valve is in transit between the closed and open states or vice versa and the maximum level indicating that the valve is fully opened. These signals are derived from microswitch data and are only approximate in their indication of the valve state. As will be demonstrated in the following, more accurate timing information is provided by the parametric patterns obtained from the acoustical signature analysis. A display of this timing track data appears on each S3D parametric plot.

2.4 Valve Signature Feature Analysis

2.4.1 General

Acoustic signatures of the lox valve on the F-1 engine and the lox, fuel and gas generator valves on the S3D engine were conducted. Because of the current importance of the F-1 engine, as opposed to the S3D engine, analysis of the F-1 lox valve is emphasized in this report. For example, parametric plots are analyzed in detail for two different sensor locations for both opening and closing events for the F-1 lox valve, whereas only one sensor location is analyzed in detail for the S3D valves. In both cases parametric plots are presented for two sensor locations. In general, in the case of all valve operations studied, parametric plots were used as the data

for final analysis and, for this reason, as well as for the clarity of presentation the plots provide, the following discussions are based principally on them rather than the spectrographic displays.

2.4.2 S3D Fuel Valve

Spectrographic portrayals of S3D fuel valve opening operations are shown in Figures 3, 4 and 5. Note that Figure 4 alludes to "abnormal" openings. "Abnormal", in this instance, alludes chiefly to a variation in event timing which is discussed later in this section. In these figures, spectrograms are shown for both track 1 and track 2 tape recordings. Track 2 was derived from a sensor mounted on the casing around the microswitch assembly and track 1 from a sensor mounted on a flange of the valve body. The track 1 data appeared to give a more balanced picture of overall valve operation and was for this reason selected for parameterization.

Reference to Figure 3 shows that while there are small differences visible among the four patterns, certain principal features remain essentially consistent. From analysis of the spectrographic content of these consistent features, the spectrum has been subdivided into four frequency ranges which are individually analyzed for signal intensity and, in two cases, centroid frequency. As previously discussed in Section 2.2, these sub-band intensities and centroid frequencies form the basis of the parametric analysis. From measurements performed on the parametric plots amplitude and frequency values which mark the time of occurrence of significant events during the valve operation were determined. Most of these are easily discernable in the parametric plots of Figures 6 and 7 for the S3D fuel valve opening. On the parametric plots, scale calibrations (original prior to photographic reduction)

E4051

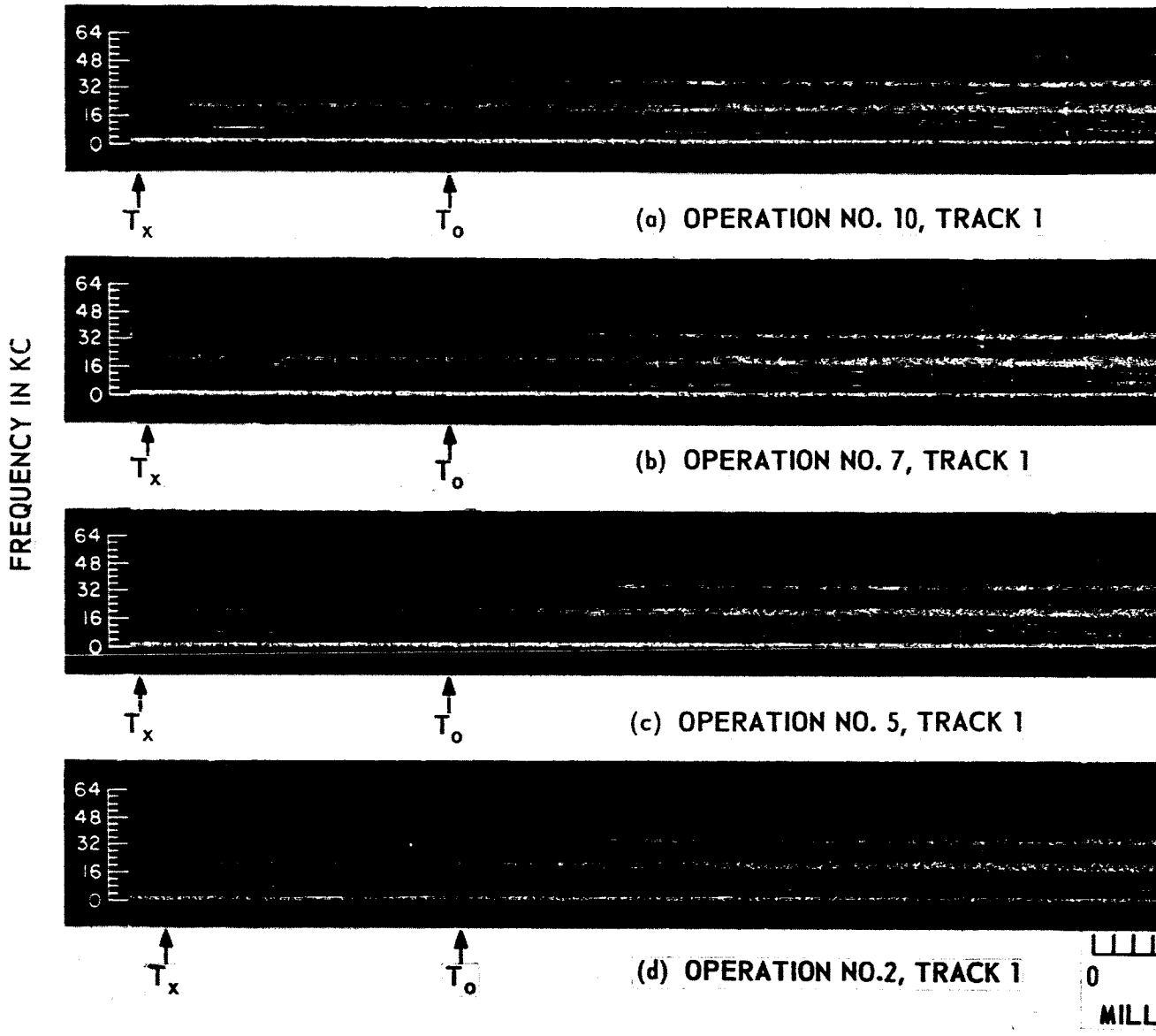
FREQUENCY IN KC
64
48
32
16
0
T_x
T_o
(a) OPERATION NO. 10, TRACK 1
(b) OPERATION NO. 7, TRACK 1
(c) OPERATION NO. 5, TRACK 1
(d) OPERATION NO.2, TRACK 1
0
MILL

24-A

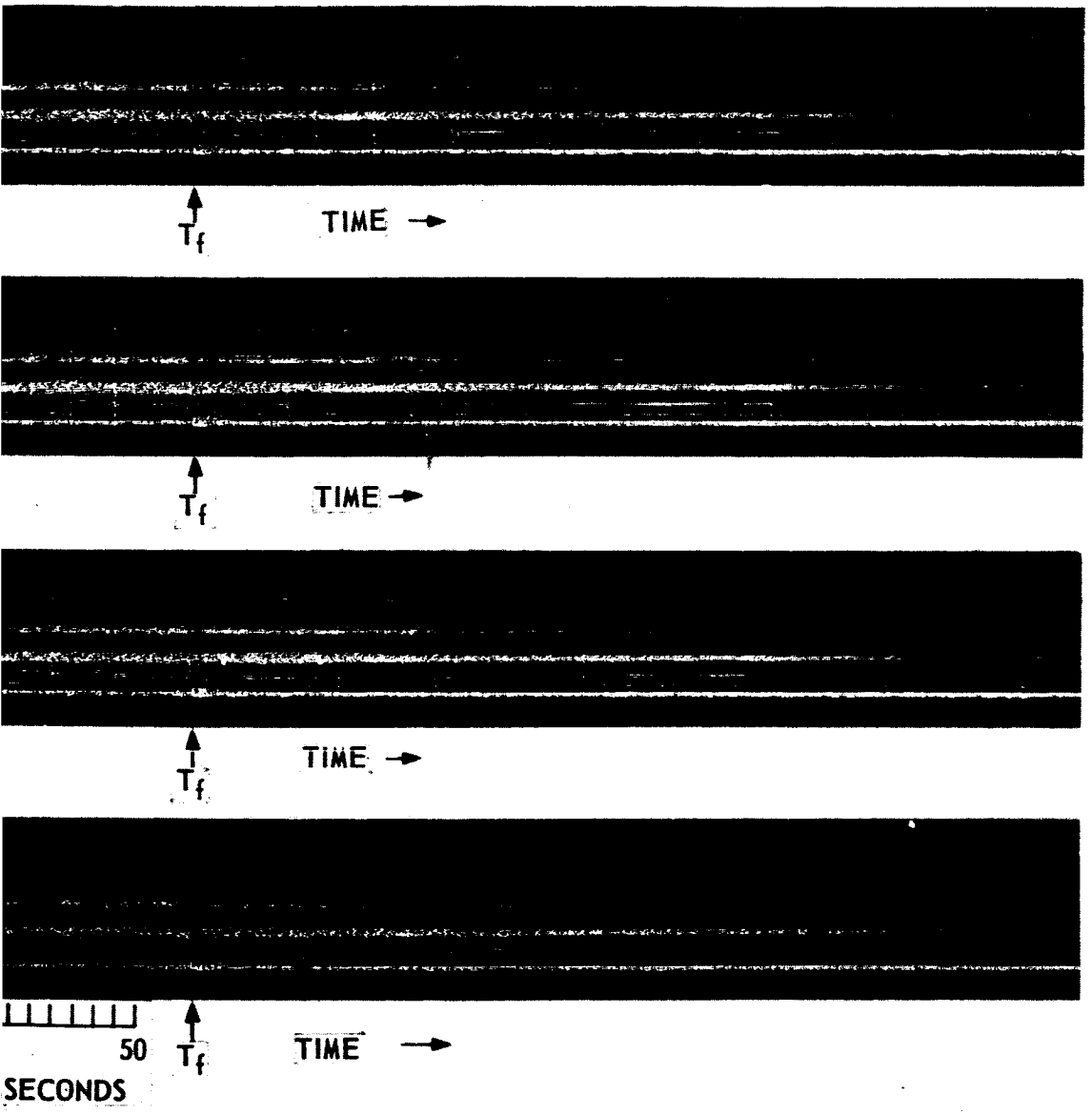

Figure 3. Spectrograms of Four Apparently Normal S3D Fuel Valve Openings, Tape N3, Track 1. Operations 2, 5, 7, and 10.

E4052

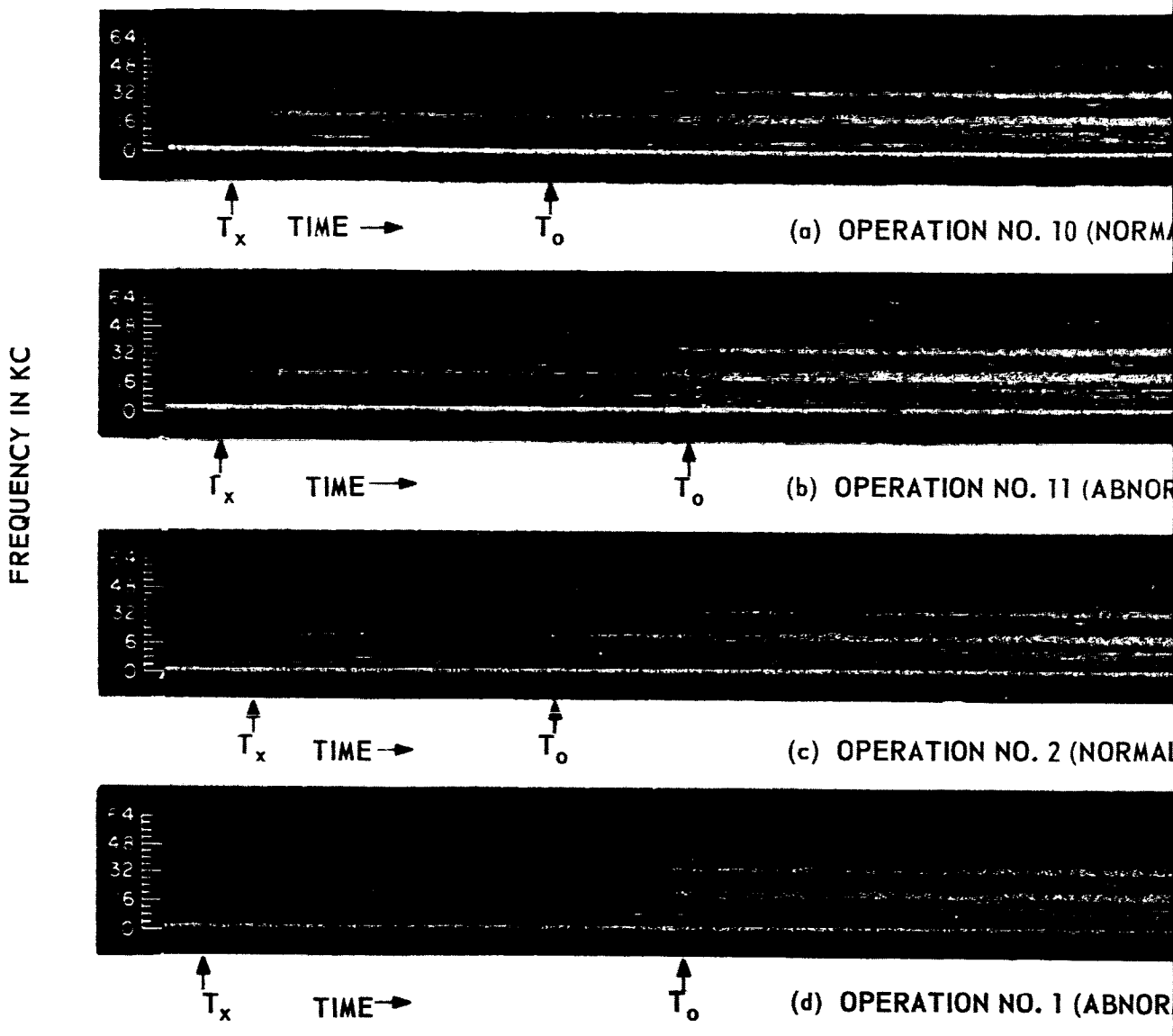
FREQUENCY IN KC
64
48
32
16
0
T_x
TIME
T_o
(a) OPERATION NO. 10 (NORMA
(b) OPERATION NO. 11 (ABNOR
(c) OPERATION NO. 2 (NORMAL
(d) OPERATION NO. 1 (ABNOR

25-A

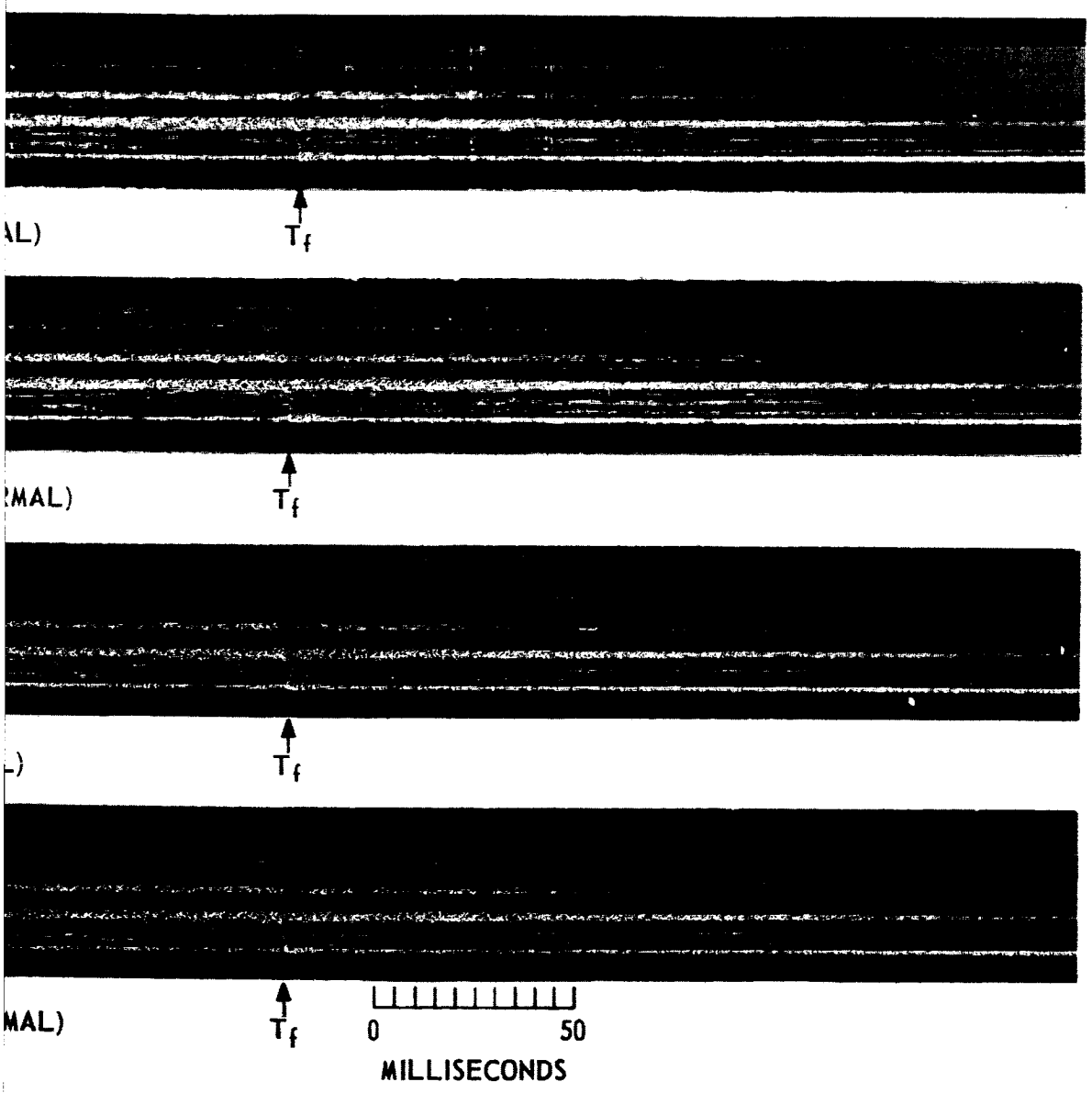

Figure 4. Spectrograms Showing Comparison of Two Apparently Normal Openings with Two Abnormal Openings of S3D Fuel Valve, Tape N3, Track 1. (Normal operation 2 compared with abnormal operation 1; Normal 10 with abnormal 11.)

E4054

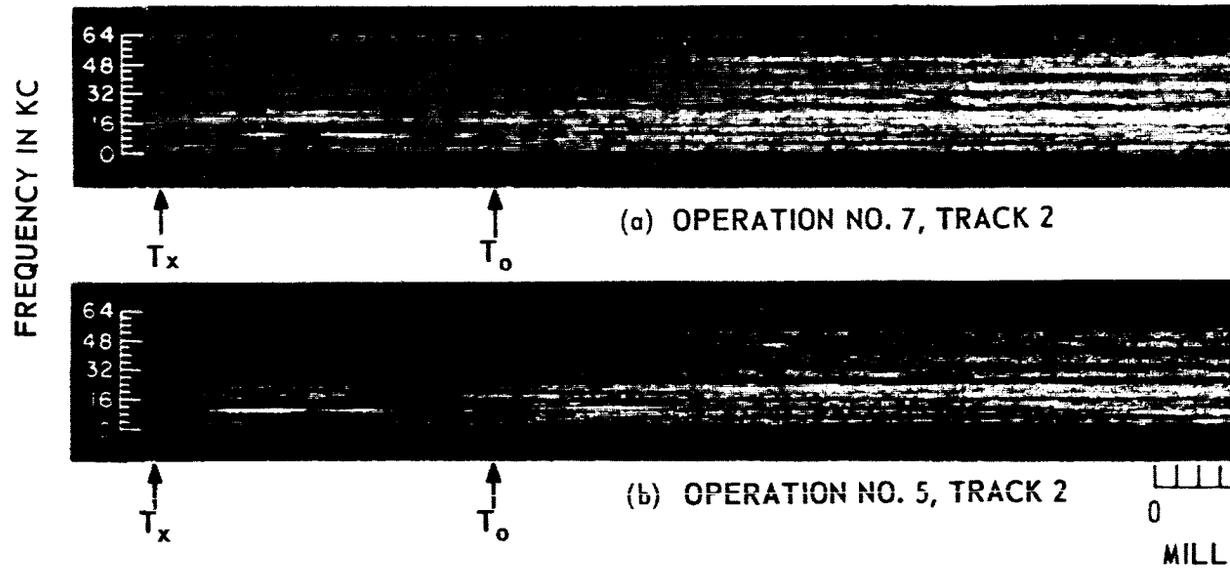
FREQUENCY IN KC
64
48
32
16
0
Tx
To
(a) OPERATION NO. 7, TRACK 2
64
48
32
16
Tx
To
(b) OPERATION NO. 5, TRACK 2
0
MILL

26-A

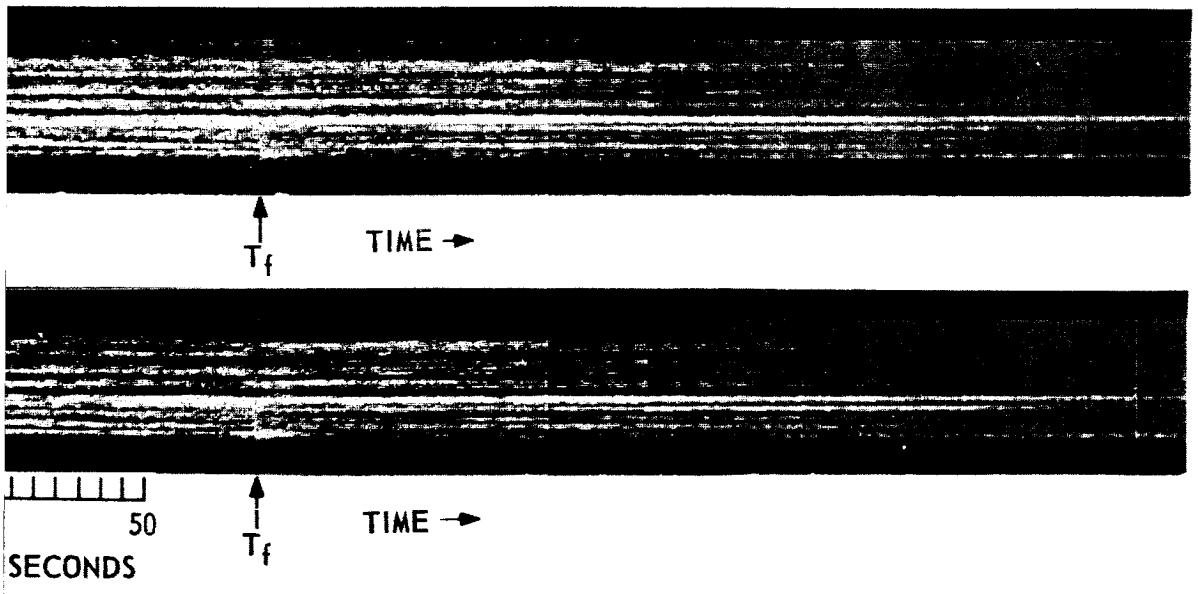

Figure 5. Spectrograms of Two Apparently Normal S3D Fuel Valve Openings, Tape N3, Track 2. Operations 5 and 7.

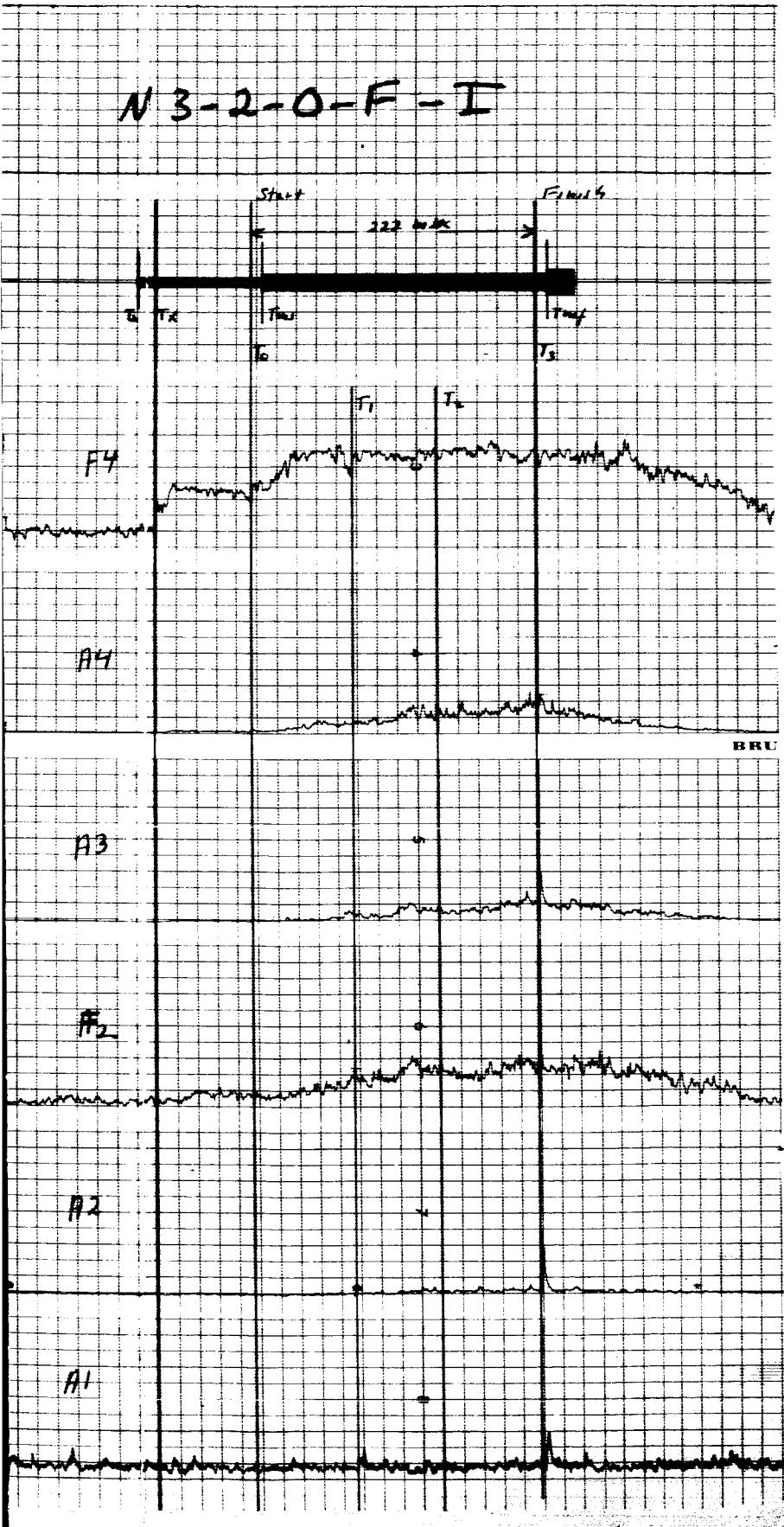
N 3-2-0-F-I
Start
Finish
222 ms
F4
A4
A3
F2
A2
A1

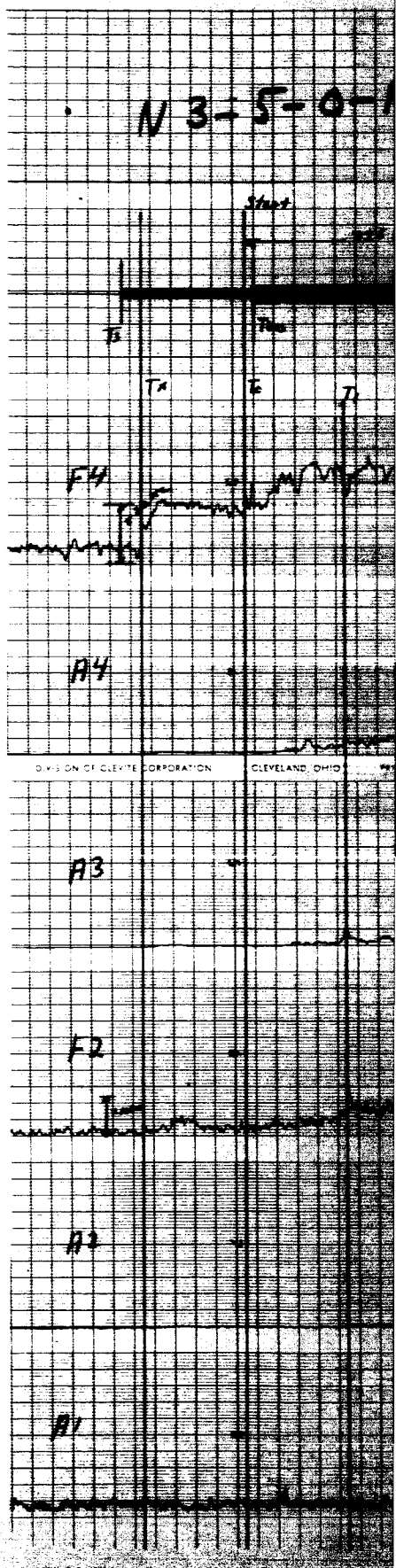
N 3-5-0-
Start
F4
A4
A3
F2
A2
A1

27A

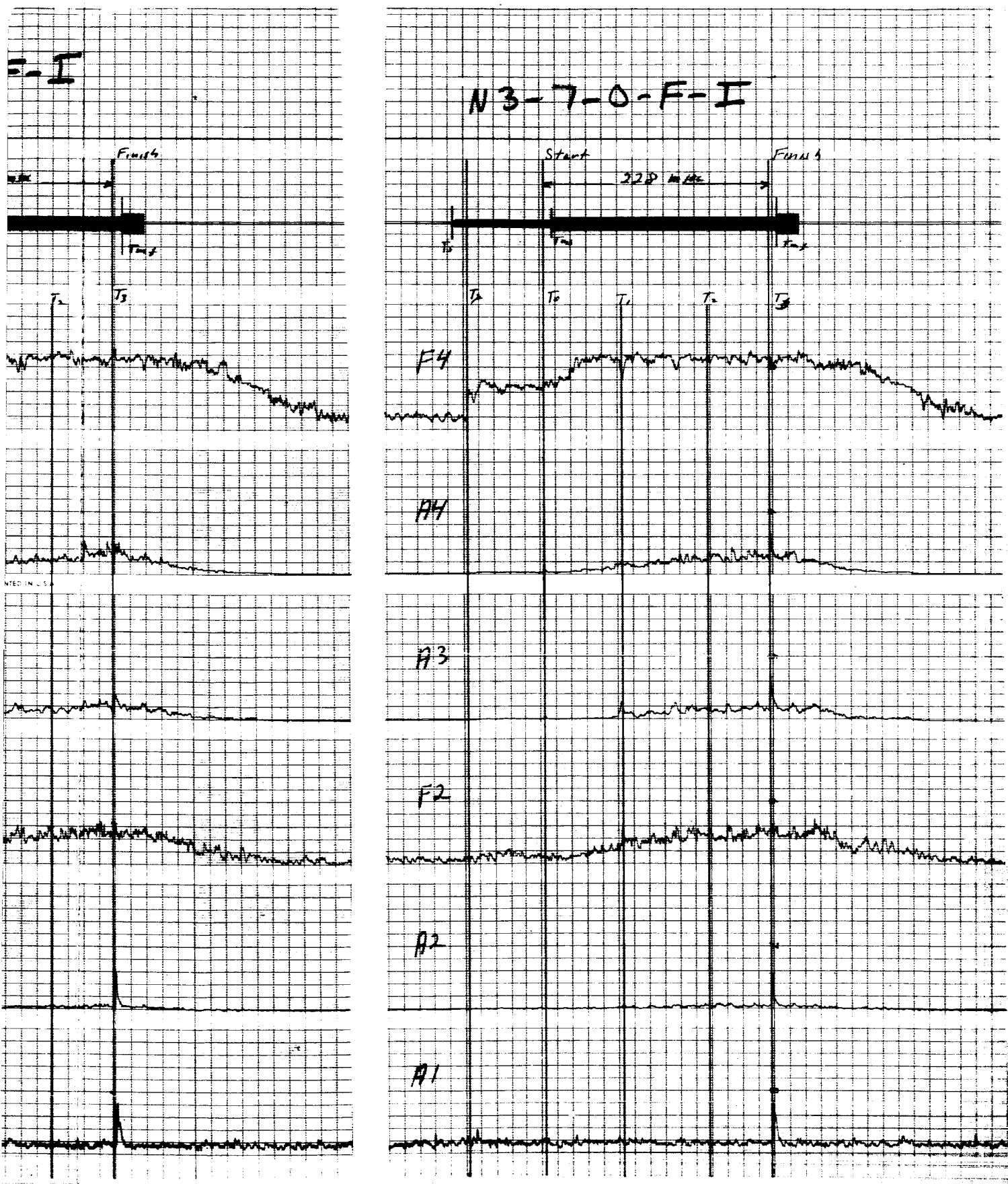
N3-7-0-F-I
Start
Finish
F4
A4
A3
F2
A2
A1

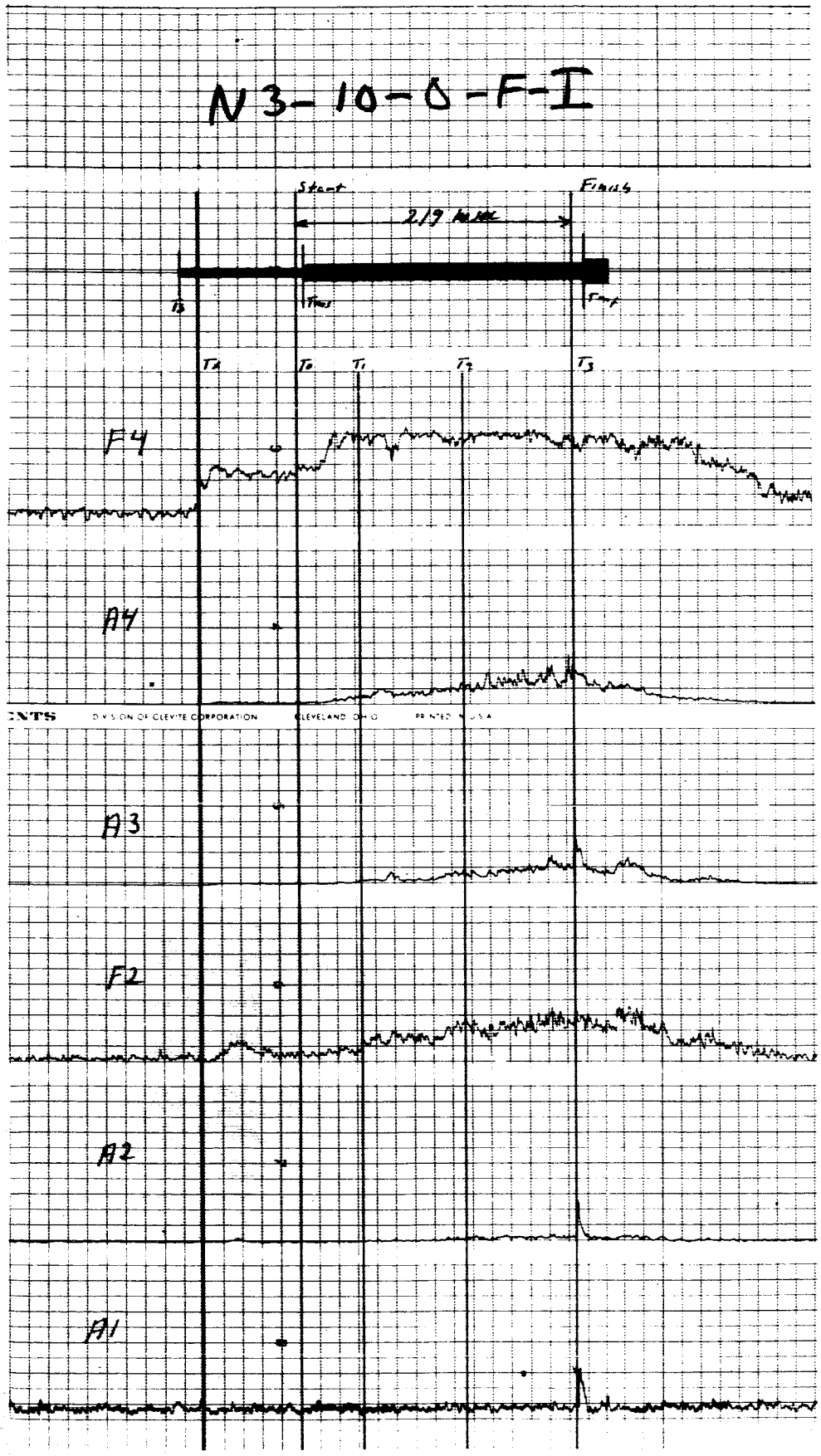

Figure 6. Parametric Plots of Four Apparently Normal S3D Fuel Valve Openings, Tape N3, Track I. Operations 2, 5, 7, and 10.

29-C

E4065

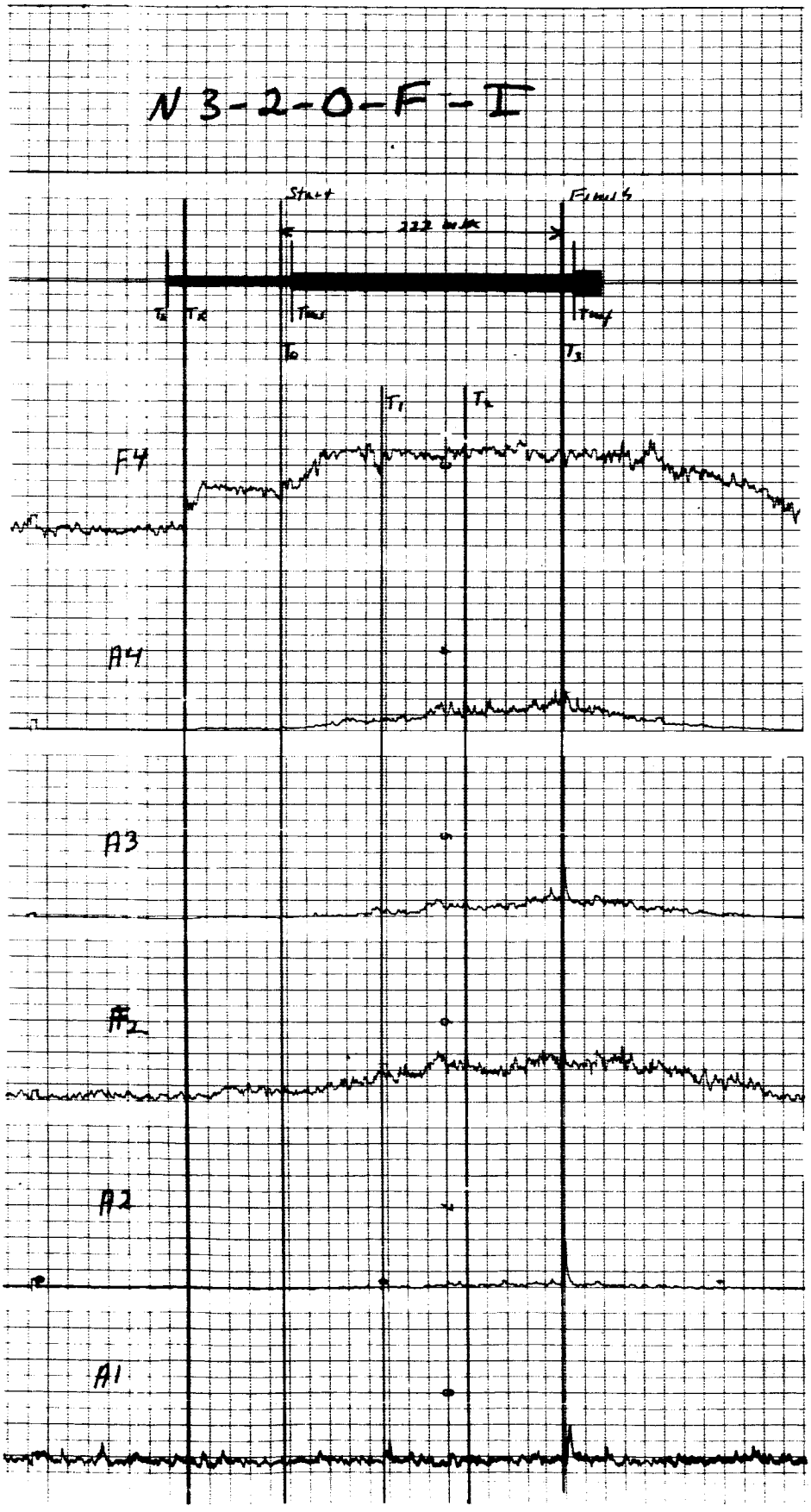
N3-2-0-F-I
Start
Finish
222 m/sec
F4
A4
A3
F2
A2
A1

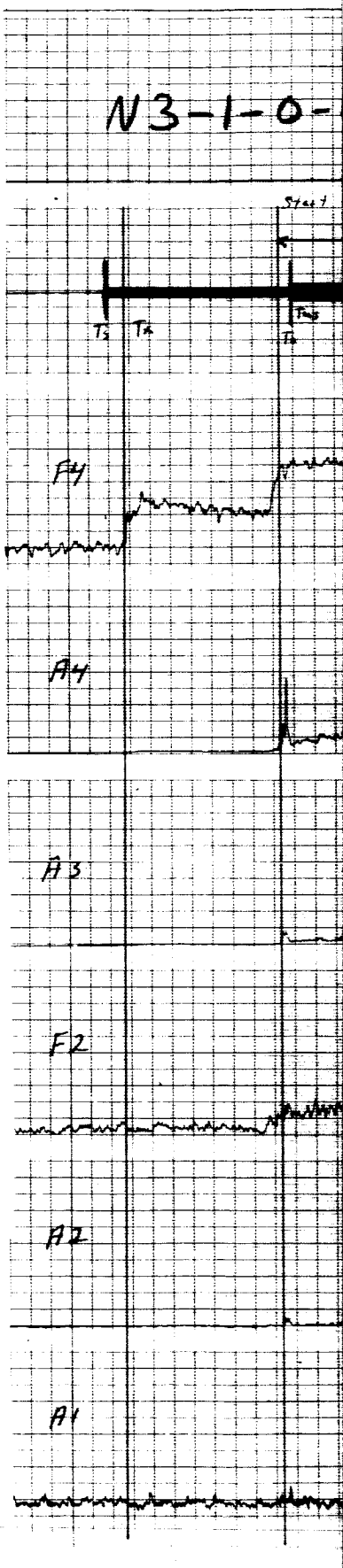
N3-1-0-
F4
A4
A3
F2
A2
A1

28A

F-I

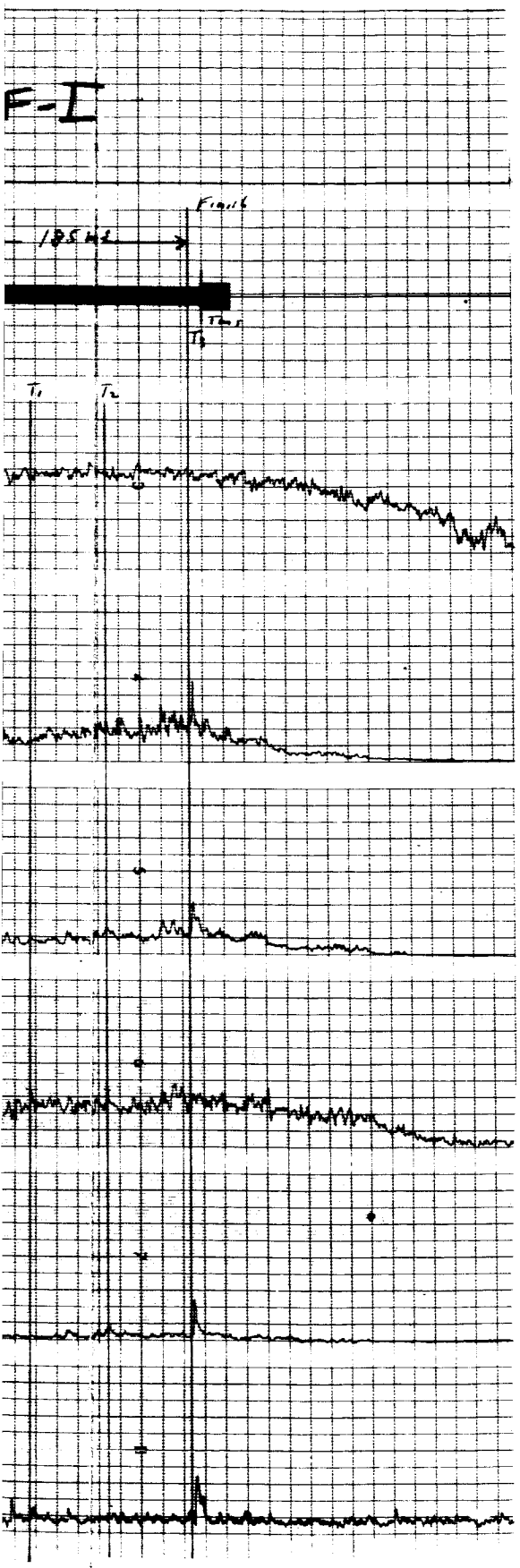

N3-11-6-F-I

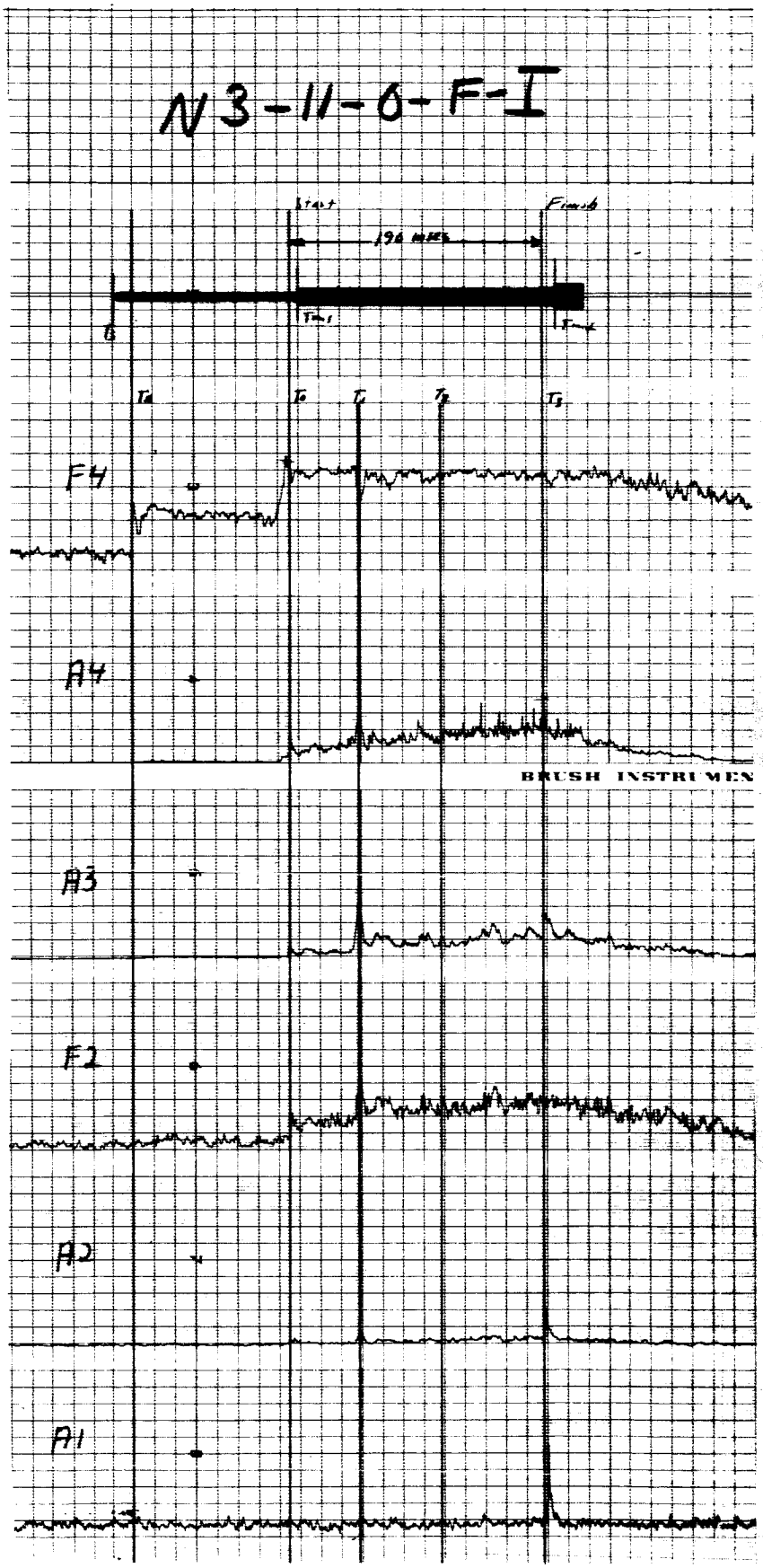

Figu
Fuel
Ope

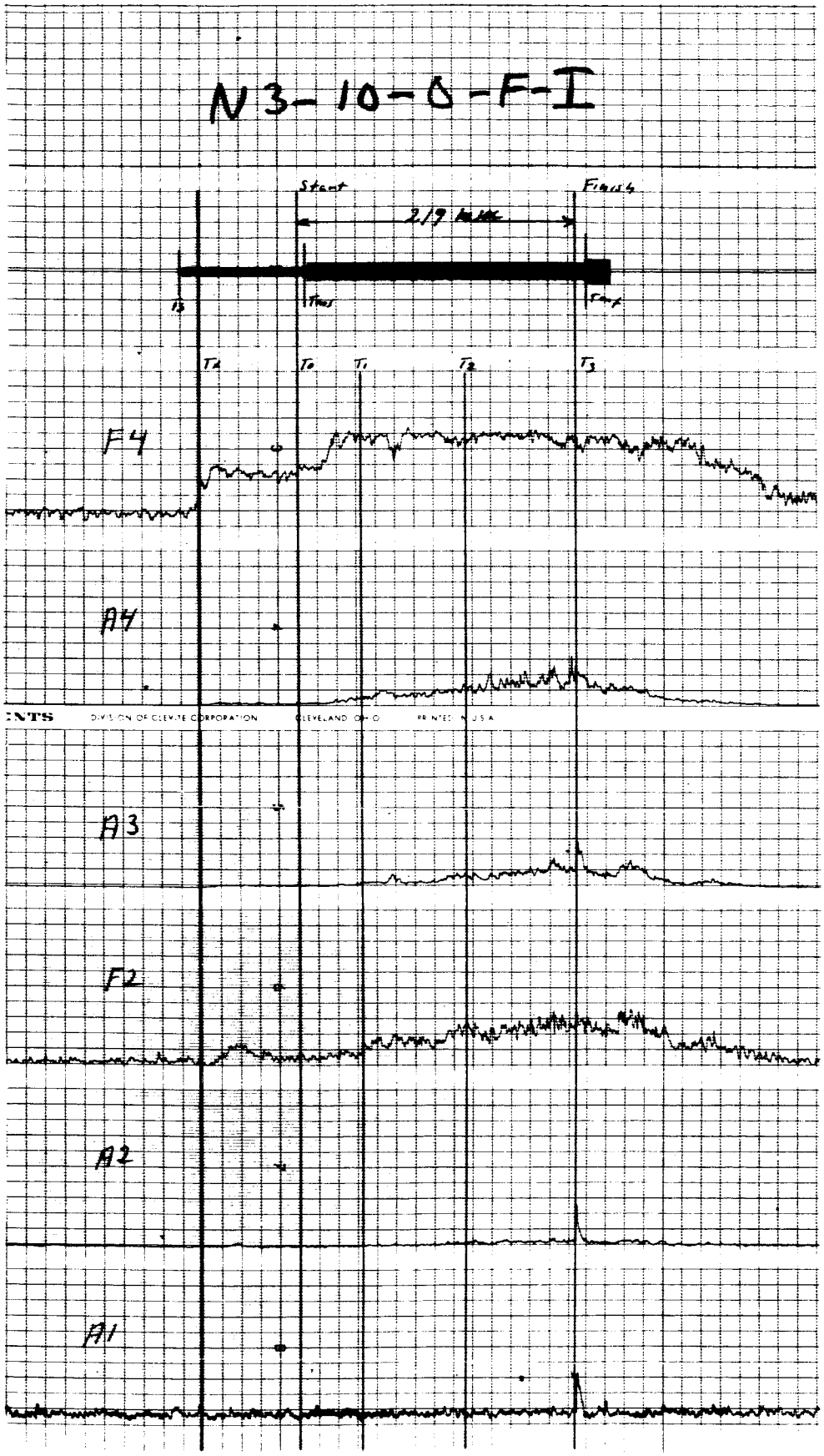

e 7. Parametric Plots Showing Comparison of Two Apparently Normal S3D Valve Openings with Two Abnormal Openings, Tape N3, Track I. (Normal ation 2 Compared with Abnormal Operation I; Normal 10 with Abnormal 11.)

are as follows for all S3D analysis.

Time: Each millimeter represents 3.12 milliseconds in real time.

Frequency: For F_2, each millimeter represents 1.105 kc and for F_4, each millimeter represents 1.439 kc. These are "real" frequencies.

Amplitude: These values are all relative. They correspond to the number of small scale divisions on the chart paper at the point of measurement.

In analyzing the plot, various time references and other parameters are assigned various symbols. These vary somewhat among the different events according to the nature of the data in the sense that a parameter which is significant in a given valve operation may not be so in the case of a different valve operation. For the S3D valve analyses the significant parameters are listed and defined below:

I. <u>Opening Event, Fuel Valve, S3D</u>

T_s - Marks onset of timing signal indicating solenoid valve operation.

T_x - Marks initial capture of F_4 signal by axis crossing detector. This is believed to indicate the first detection of gas flow through the acoustic turbulence produced by it in the inlet tube.

T_o - This is marked by the first small peak in A_2. This peak is often accompanied by peaks in A_4 and A_3 and a significant peak in F_2. This event is believed to indicate the start of valve opening.

T_1 and T_2 - Mark the first and second major peaks in F_2. These peaks are consistently observed in all fuel valve openings.

T_3 - Marks onset of only significant peak in A_1. It is accompanied by peaks in A_2 and usually in A_3. It is believed to mark the end of the opening operation, but not necessarily of total valve motion since there is believed to be some slight "overswing" past this point. (Note: In all subsequent plots the equivalent of T_3 is called T_f).

A_1T_3 - A_1 amplitude at T_3

A_2T_o - A_2 amplitude at T_o

A_2T_1 - A_2 amplitude at T_1

A_2T_2 - A_2 amplitude at T_2

A_2T_3 - A_2 amplitude at T_3

F_2T_o - F_2 frequency peak at T_o

F_2T_1 - F_2 frequency peak at T_1

F_2T_2 - F_2 frequency peak at T_2

F_2T_3 - F_2 frequency peak at T_3

A_3T_o - A_3 amplitude peak at T_o

A_3T_1 - A_3 amplitude peak at T_1

A_3T_2 - A_3 amplitude peak at T_2

A_3T_3 - A_3 amplitude peak at T_3

A_4T_o - A_4 amplitude peak at T_o

A_4T_1 - A_4 amplitude peak at T_1

A_4T_2 - A_4 amplitude peak at T_2

A_4T_3 - A_4 amplitude peak at T_3

F_4T_o - F_4 frequency peak at T_o

F_4T_1 - F_4 frequency peak at T_1

F_4T_2 - F_4 frequency peak at T_2

F_4T_3 - F_4 frequency peak at T_3

A listing of parametric values for several S3D fuel valve opening events is presented in Table I. Events 2, 5, 7, and 10 were selected as being fairly typical. Events 1 and 11 were judged to be less so and are designated as "abnormal". Means, mean deviations and percentage deviation are given for the four events judged normal. Percentage deviations for the two abnormal events from the normal means are also listed.

As indicated earlier, the two "abnormal" events were judged to be atypical with respect to event timing. The first interval of significance, (T_s-T_x), is that which occurs between the first indication of solenoid valve operation and initial detection of gas turbulence in the line via F_4. This interval, approximately 14 milliseconds, was slightly longer in the case of operations 1 and 11, but not significantly. However, note interval (T_x-T_o). This represents the time required for the gas pressure, from the point of turbulence detection, to reach a value sufficient to initiate valve motion. For the normal valves, the mean time required was 78 milliseconds with a percentage deviation of only 1.0%. For operations 1 and 11 the case was very different. The required time for operation 1 was 121 milliseconds and for 11 was 116 milliseconds. These represent percentage deviations of about 55% and 48% respectively. This measurement strongly suggests that either the valve gate or actuating mechanism had some degree of binding in the closed position and that more driving pressure buildup was hence required to start motion.

TABL
S3D ENGINE FUEL VALVE OPENIN
PARAMETRIC

Parameter Number	1	2	3	4	5	6	7	8	9	10	11	12
Event No.	T_sT_x	T_xT_o	T_oT_1	T_oT_2	T_oT_3	A_1T_3	A_2T_o	A_2T_1	A_2T_2	A_2T_3	F_2T_o	F_2T_1
2	14.7	76.5	72.0	103	1.22	15	0	0	1.5	15	4.4	9.9
5	13.9	79	76.5	127	225	21	1	2	3	15	2.9	13.2
7	14.8	78.5	72.8	0.31	223	22	1.5	3	3.5	14	2.5	14.3
10	11.6	78.6	78.5	123	2.5	16	0.1	2	2	13	3.3	6.6
$\bar{Z}$	13.7	78.1	75.0	121	223	18.5	0.65	1.75	2.5	14.3	3.3	11.0
Δ	1.1	0.85	0.6	9.0	3.0	3.0	0.6	0.88	0.7	0.75	0.6	2.8
% DEV	8.0	1.0	3.47	7.4	1.3	16	92	50	28	5.2	18	25
1	14.2	121	45.3	96.3	185	27	1	1.5	3	12	7.7	15.4
11	14.2	116	50.1	96.1	190	28	0	0	4	10	9.9	18.7
% D (1)	3.6	55	39.6	20.4	17	46	54	14	20	16	113	40
% D (11)	3.6	485	41.7	20.5	14.8	51	100	56	60	30	200	70

E I
G EVENTS, TAPE N3, TRACK 1
STABILITY

13	14	15	16	17	18	19	20	21	22	23	24	25	26
F_2T_2	F_2T_3	A_3T_o	A_3T_1	A_2T_2	A_3T_3	A_4T_o	A_4T_1	A_4T_2	A_4T_3	F_4T_o	F_4T_1	F_4T_2	F_4T_3
11.0	15.4	0.5	1	4	15	1	3	9	12	22.3	33.8	35.8	34.7
11.8	8.8	0	5	4	10	1	5	7	12	24.5	31.7	33.8	36.7
12.6	14.3	1	7	7	17	0	1	3	16	21.6	34.5	33.3	34.2
12.1	14.3	0.5	1	4	15	1	2	5	13	23.1	32.4	33.1	33.2
11.9	13.2	0.5	3.8	4.8	14.3	0.75	2.75	6	13.3	22.9	33.1	34.0	34.7
0.48	2.2	0.25	2.5	1.13	2.1	0.38	1.25	2	1.38	0.93	0.05	0.9	1.0
4.0	17	50	67	24	15	50	46	33	10	4.0	3.2	2.6	2.9
14.8	14.3	4	5	8	16	24	5	12	25	34.5	31.8	33.4	34.5
14.3	13.7	4	18	6	12	7	13	10	19	37.5	36.0	33.1	33.5
24	8.3	700	33	67	12	3200	82	100	89	51	3.9	1.8	5.8
20	3.0	700	380	25	16	933	373	67	43	64	8.8	2.6	3.5

32-B

Note, also, that the A_4 peak at the start of motion is quite prominent in operations 1 and 11, while insignificant or absent in the others. It is also worth observing that the interval (T_o-T_3) (in subsequent plots called (T_o-T_f)) is considerably shorter in the case of operation 1, being only 185 milliseconds as compared with a mean for the normals of 223 milliseconds. This interval for operation 11 is also less than the mean by a significant amount, being only 190 milliseconds.

Other timing intervals of interest are those between the microswitch indication of start motion and actual start motion and between the corresponding finish motion time marks. These intervals do not appear in the S3D fuel valve table but they do appear in the other S3D tables. In general, the start motion microswitch indication lagged the A_4 start motion indication by 6 to 9 milliseconds. It also lagged at the finish by a comparable amount, suggesting some slight overswing after the opening event was substantially completed.

For comparison, Figure 8 displays two parametric plots of typical S3D fuel valve openings as derived from track 2 data.

II. Closing Event, Fuel Valve, S3D

Spectrograms of the S3D fuel valve closings are shown in Figure 9 for track 1 and Figure 10 for track 2 data. For the parametric analysis, the first 6 closings (track 1) were selected, of which two typical samples are presented in Figure 11. Figure 12 displays the same two closings as derived from track 2 data. The principal difference between these two sets of plots is that the A_4 level was higher in the track 2 data and there was less noise in the F_4 band on this track.

E4067

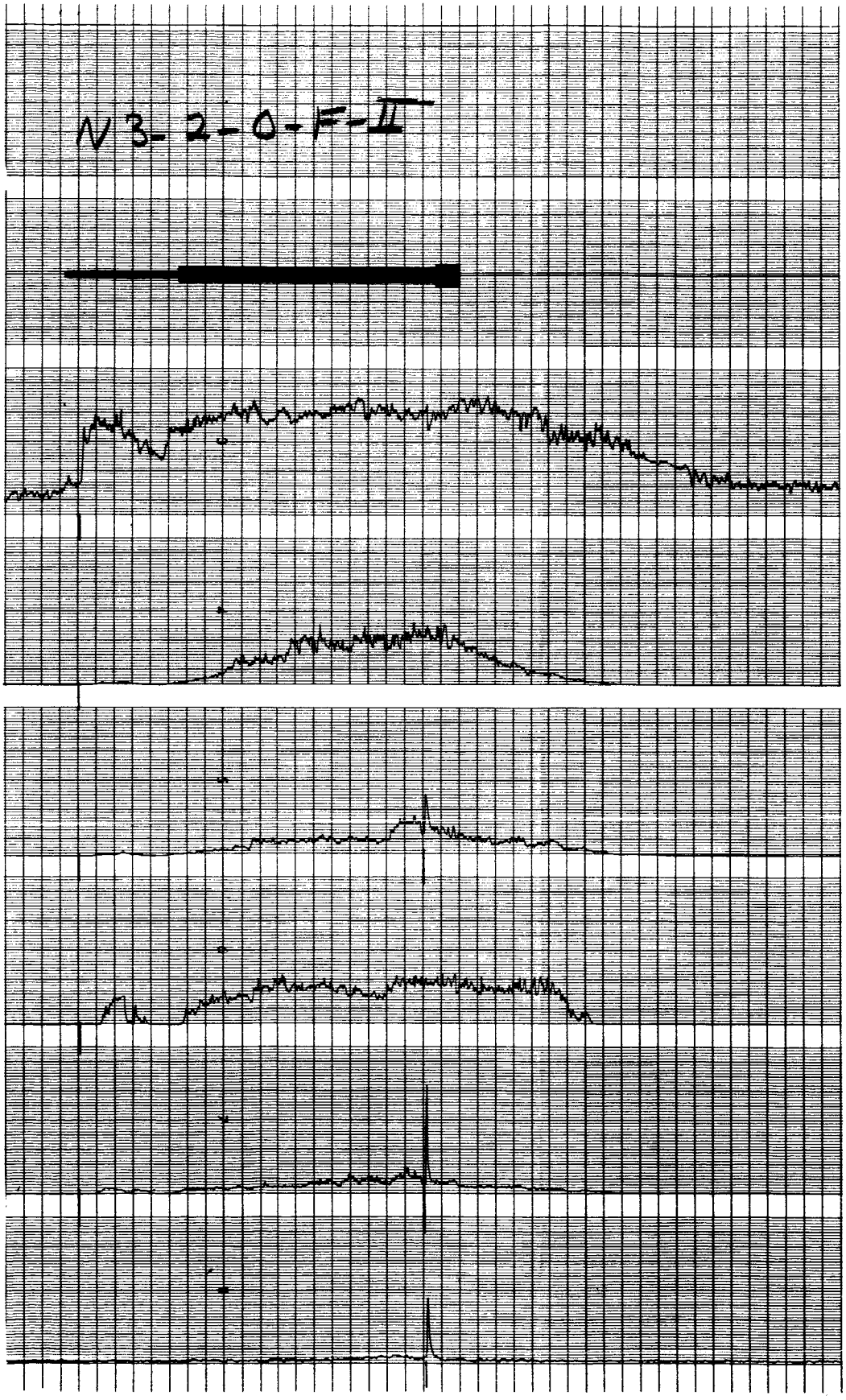

34-A

Fig

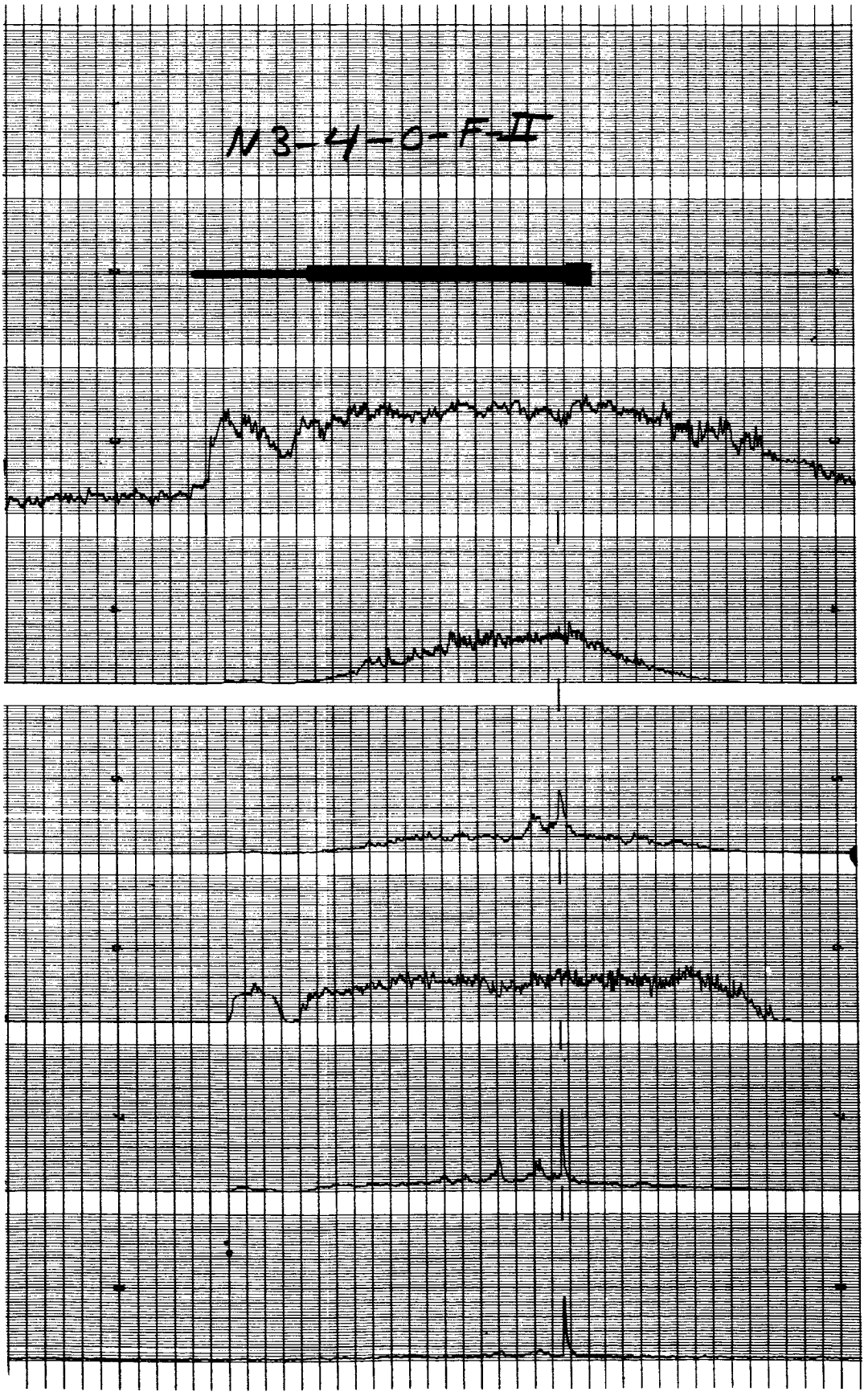

ıre 8. Parametric Plots of Two Apparently Normal S3D Fuel Valve Openings, Tape N3, Track 2. Operations 2 and 4.

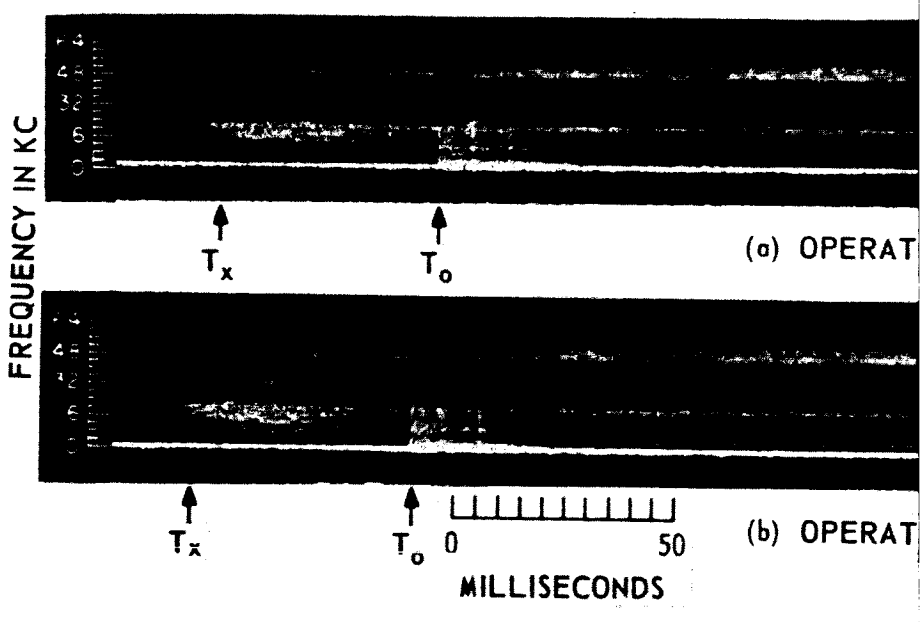
FREQUENCY IN KC
T_x
T_o
(a) OPERAT
T_x
T_o
0
50
(b) OPERAT
MILLISECONDS

Figure 9. Sp
N

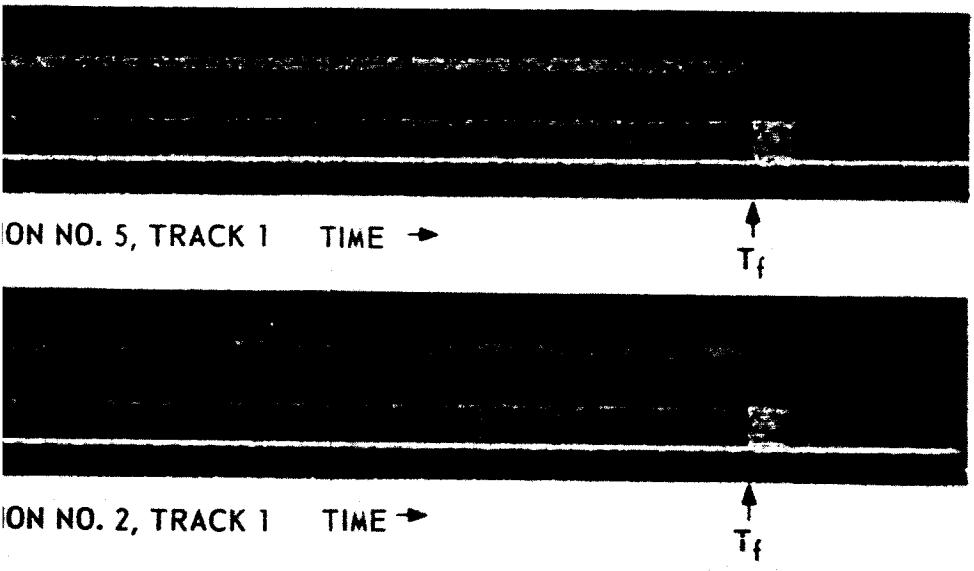

ectrograms of Two Typical Closings of S3D Fuel Valve, Tape
, Track 1. Operations 2 and 5.

E4055

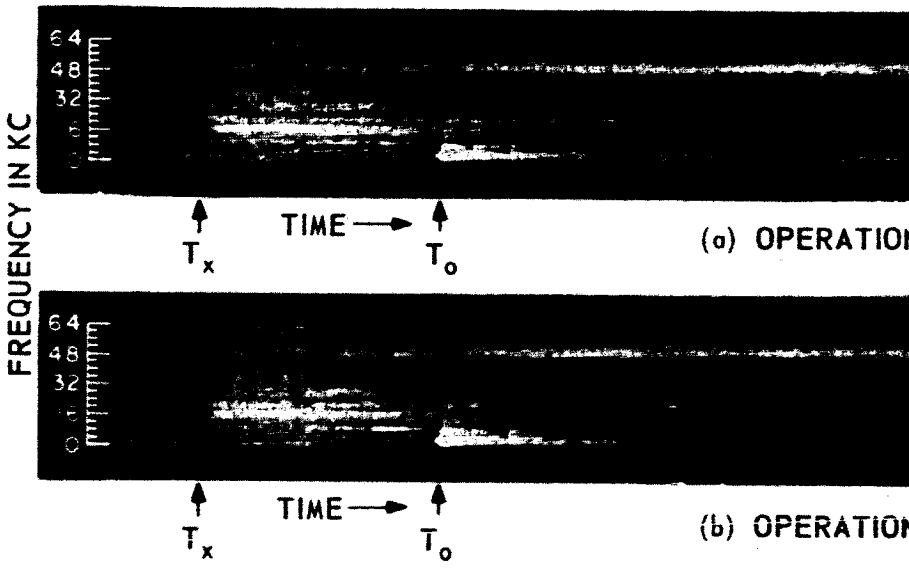

Figure 10. Spectro
Track 2

36-A

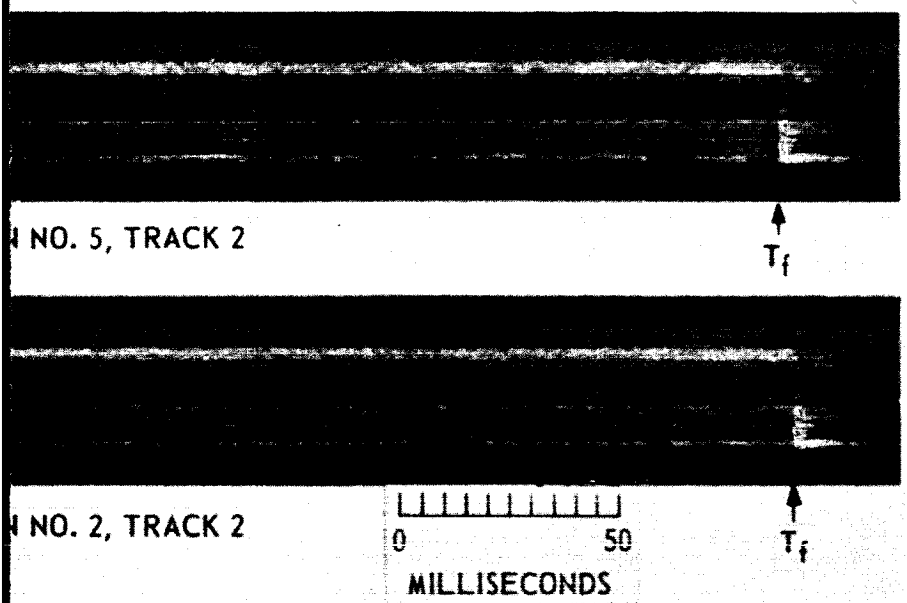

grams of Two Typical S3D Fuel Valve Closings, Tape N3,
. Operations 2 and 5.

E4066

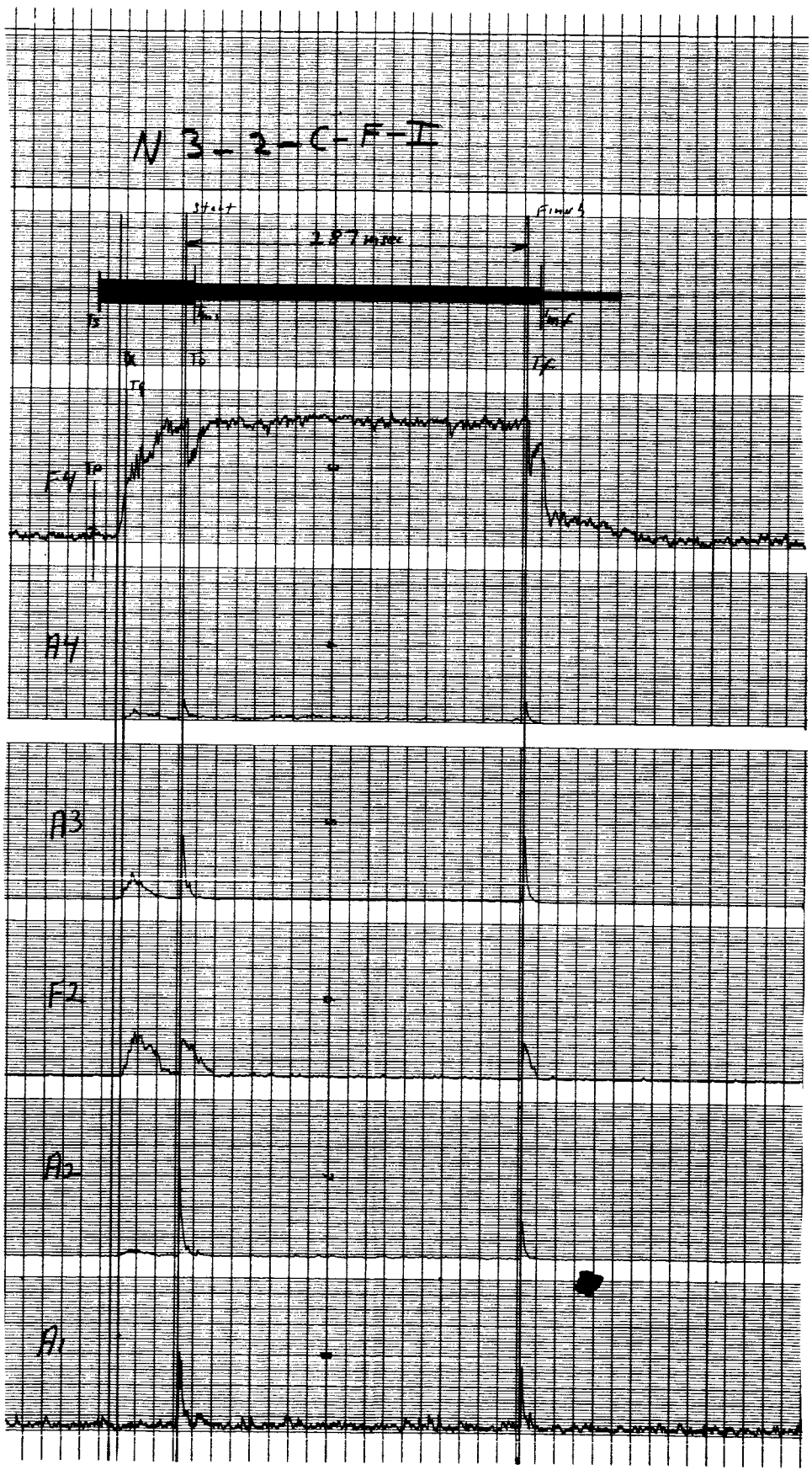

37-A

Figure 11.

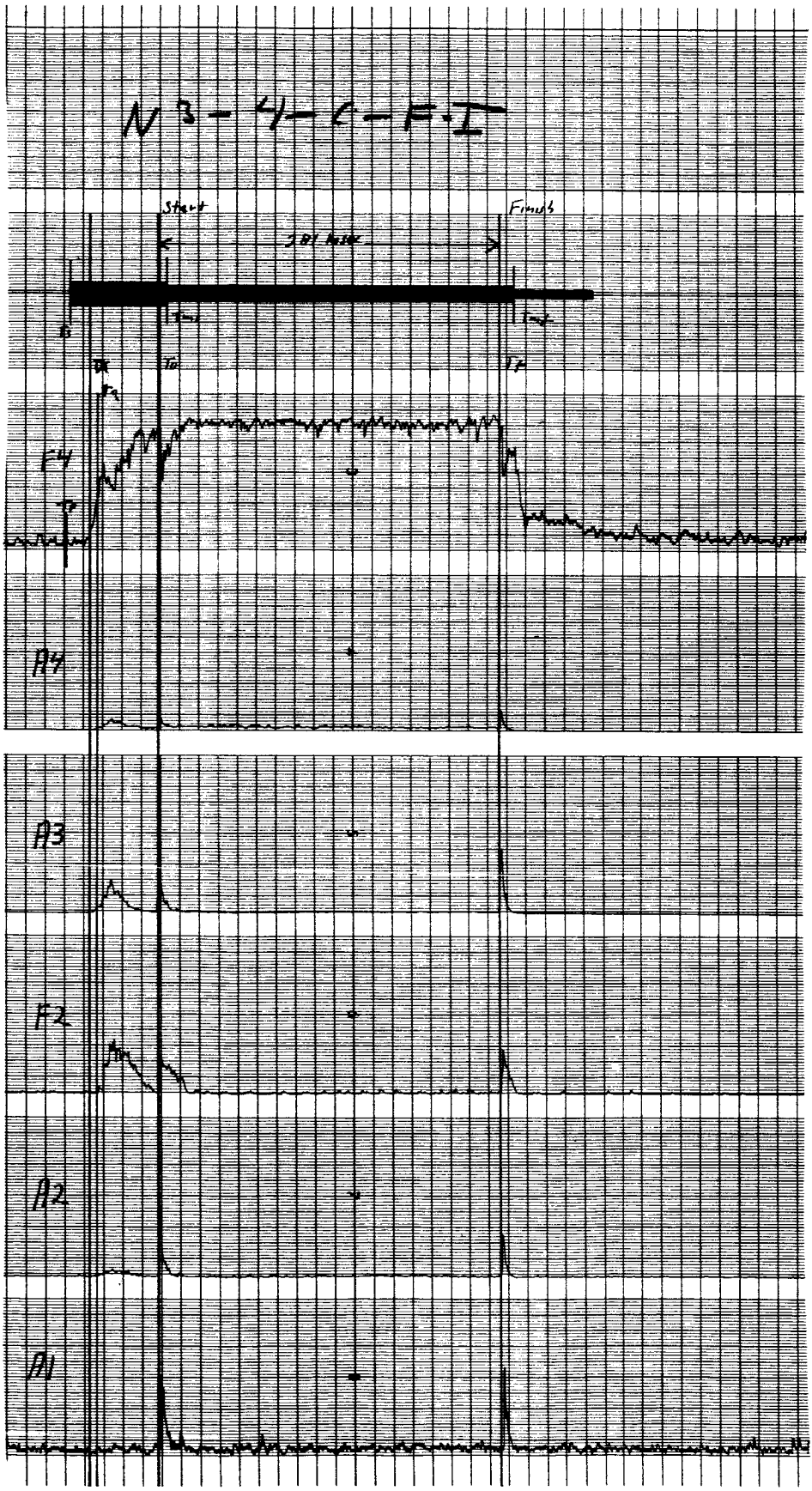

Parametric Plots of Two Typical S3D Fuel Valve Closings.
Tape N3, Track 1. Operations 2 and 4.

E4068

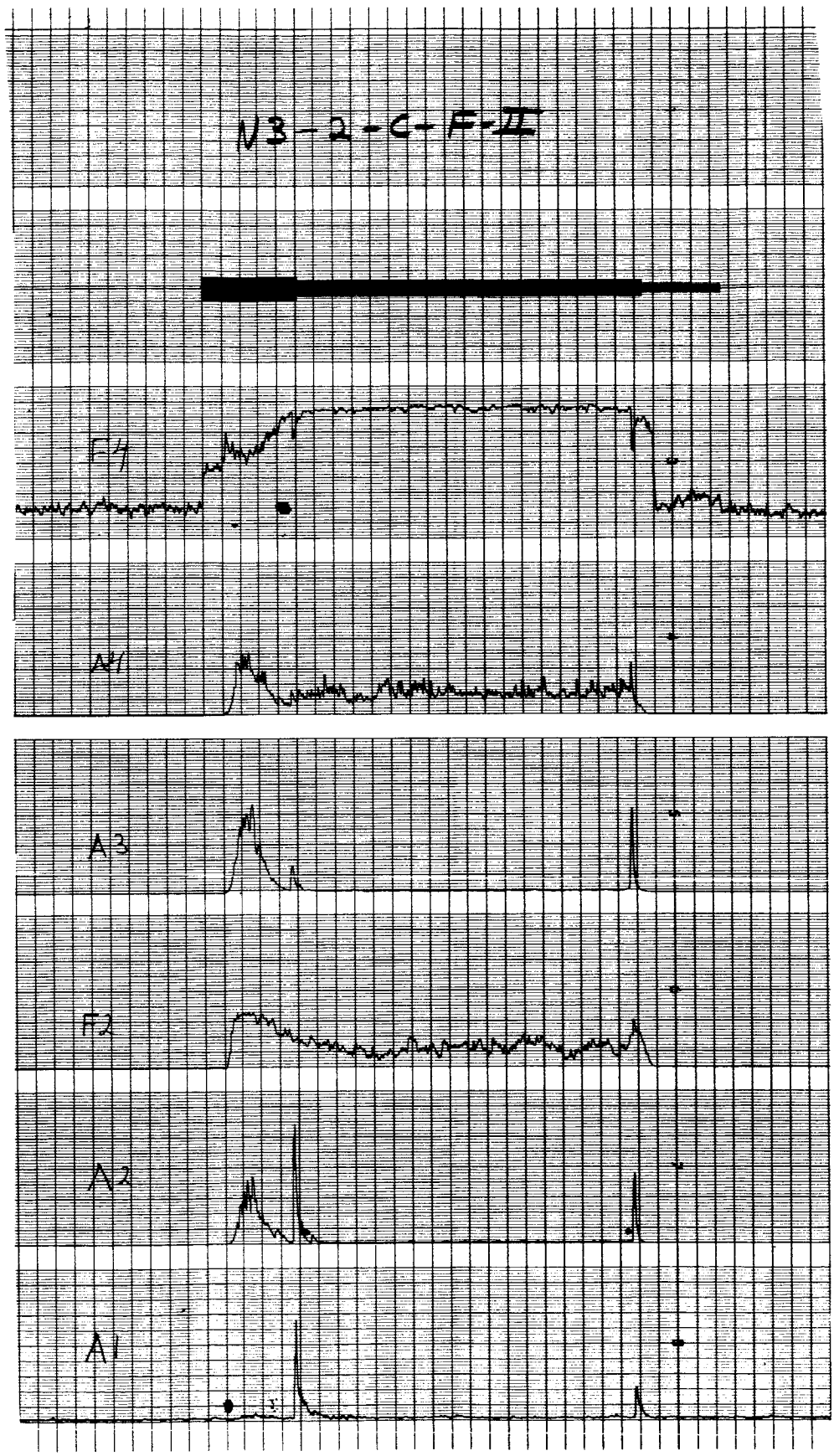

Figure

38-A

12. Parametric Plots of Two Typical S3D Fuel Valve Closings, Tape N3, Track 2. Operations 2 and 4.

In general, however, the track 1 features were quite well marked and distinctive and appear to be superior for analysis purposes. The parameters used in the S3D fuel valve closing event analysis were as follows:

T_s - Timing signal indicates operation of solenoid valve.

T_x - Corresponds to initial capture of F_4 signal. Is believed to correspond to the first detection of turbulence caused by gas flow.

T_o - Corresponds to the second major peak in A_3. It is accompanied by significant peaks in A_1, A_2 and F_2 and by a small peak in A_4. It is believed to indicate start of motion.

T_{ms} - Marks operation of microswitch intended to indicate start of closing.

T_f - This timing indication is marked by a major peak in A_3 and is believed to represent the time of valve blade seating. Associated with T_f are major peaks in A_1, A_2 and F_2 and an immediately subsequent brief but pronounced dip in F_4.

T_{mf} - Timing signal intended to denote finish of motion.

In addition, two early timing parameters, not included in the opening event analysis, are defined for the closing event. These are:

T_p - This is marked by a small but sharp rise in F_4 and is believed to be caused by mechanical transmission of the solenoid "bang" through the tubing. It usually precedes T_s by approximately one millisecond.

T_q - This is marked by the onset of the first major peak in A_3. Associated with this peak are small peaks in A_2 and A_4 as well

as an increase in F_2. The A_3 peak is usually of moderate level but is prolonged, nearly to T_o. It is believed that the signatures occurring during the interval $T_q<t<T_o$ represent takeup of free play in the actuating linkage prior to the start of valve gate motion.

A_1T_o - Amplitude of A_1 peak at T_o.

A_1T_f - Amplitude of A_1 peak at T_f.

$\int A_2(<T_o)$ - Area under A_2 during the interval $T_q<t<T_o$.

A_2T_o - Amplitude peak of A_2 associated with T_o.

A_2T_f - Amplitude of A_2 peak at T_f.

F_2T_q - F_2 frequency peak just after T_q.

F_2T_o - F_2 frequency peak just after T_o.

F_2T_f - F_2 frequency peak just after T_f.

$\int A_3(<T_o)$ - Area under A_3 during T_q-T_o interval.

A_3T_o - Amplitude of A_3 peak at T_o.

A_3T_f - Amplitude of A_3 peak at T_f.

A_4T_o - Amplitude of A_4 peak at T_o.

A_4T_f - Amplitude of A_4 peak at T_f.

F_4T_p - Peak frequency of F_4 at T_p.

$\overline{F_4}(T_o-T_f)$ - Frequency centroid of F_4 during the interval $T_o<t<T_f$.

Time, frequency and amplitude measurements of 6 closing events of the S3D fuel valve are presented in Table II. The most striking features of the plots are:

a) Major amplitude peaks in A_1, A_2 and A_3 which mark the start and finish of motion.

TABLE II
S3D ENGINE FUEL VALVE CLOSING
PARAMETRIC ST

Parameter Number	1	2	3	4	5	6	7	8	9	10	11
Event No.	T_sT_p	T_sT_x	T_oT_x	T_oT_{ms}	T_oT_f	T_fT_{mf}	T_xT_q	$A_1(T_o)$	$A_1(T_f)$	$\int A_2<T_o$	A_2T_o
1	1.5	14.5	58.0	7.3	287	11.3	4.4	23	16	2	29.5
2	1.4	16.4	55.1	5.9	282	11.0	4.9	21	22	1	28
3	1.5	15.3	57.2	1.9	281	11.7	5.0	19	26	1	28
4	2.25	9.3	53.2	7.0	263	11.6	3.71	21	25	2	25.5
5	1.25	16.1	55.0	8.2	276	11.6	3.5	26	28	1.5	21
6	1.25	17.3	53.5	7.8	276	12.7	5.16	22	27	1.5	23
$\bar{Z}$	1.79	14.8	55.2	7.1	278	11.6	4.5	22	24	1.54	26
$\bar{\Delta}$	0.4	1.9	1.6	0.6	6	0.3	0.5	1.67	3.33		2.7
% DEV.	22.3	12.8	3.3	8.4	2.1	2.6	11.2	7.6	13.9	24	10.3

EVENTS, TAPE N3, TRACK 1
ABILITY

12	13	14	15	16	17	18	19	20	21	22
A_2T_f	F_2T_q	F_2T_o	F_2T_f	$\int A_3<T_o$	A_3T_o	A_3T_f	A_4T_o	A_4T_f	F_4T_p	$F_4(T_oT_f)$
12	11.8	11.2	9.45	4.5	21	21	6	3	7.36	42.5
12	10.2	9.8	8.8	4.5	20	21	6	7	5.46	45.8
16	13.7	10.8	7.7	5	22.5	23.5	2	2	8.26	45.6
18.5	13.7	10.7	11.3	5	14.5	24.5	3	0	6.95	45.8
13	15.4	10.3	10.2	4.5	12	20	5	7	5.40	46.3
17.5	11.1	10.3	11.6	4	21	25	3	2	6.57	45.8
15	12.6	10.5	9.9	4.2	18.7	22.7	4.2	3.5	6.67	45.3
2.7	1.6	0.38	1.2	0.67	3.44	2.0	1.5	2.34	0.84	0.93
18	12.8	3.7	12.1	16	18	8.8	36	67	12.6	2.1

b) The activity in A_2, F_2 and A_3 prior to start of motion of the valve blade which, as pointed out, suggests free play in the actuating mechanism.

c) The fairly steady mean frequency of F_4 of about 45.3 kc starting with the first detection of turbulence at T_q and persisting until the end of valve motion.

d) The reasonably consistent duration of closing time, averaging 278 milliseconds, with a percentage deviation of only 2.1%. (Note: This deviation is due to variability in the functioning of the valve and is greatly in excess of the time measurement error of the acoustical event parametric analysis technique. The inherent timing accuracy of the technique is considerably better than one millisecond.

As in the case of the S3D fuel valve openings, the microswitch timing indications for the start and finish of motion are seen to lag by a small amount the actual occurrences of these events as seen in the acoustical event parametric analysis. The lag period is somewhat shorter for the opening (mean is 7.1 milliseconds) than for the closing (mean is 11.6 milliseconds) with mean percentage deviations not greater than 9%..

It is appropriate to point out that, as viewed on the chart, a peak in A_1 will seem to lag a corresponding peak in A_3 or A_4 slightly. This effect is caused by the longer buildup time of the narrower passbands of the filters used for processing the lower frequency parameters and appears consistently in all of the valve parametric plots in this report.

E4056

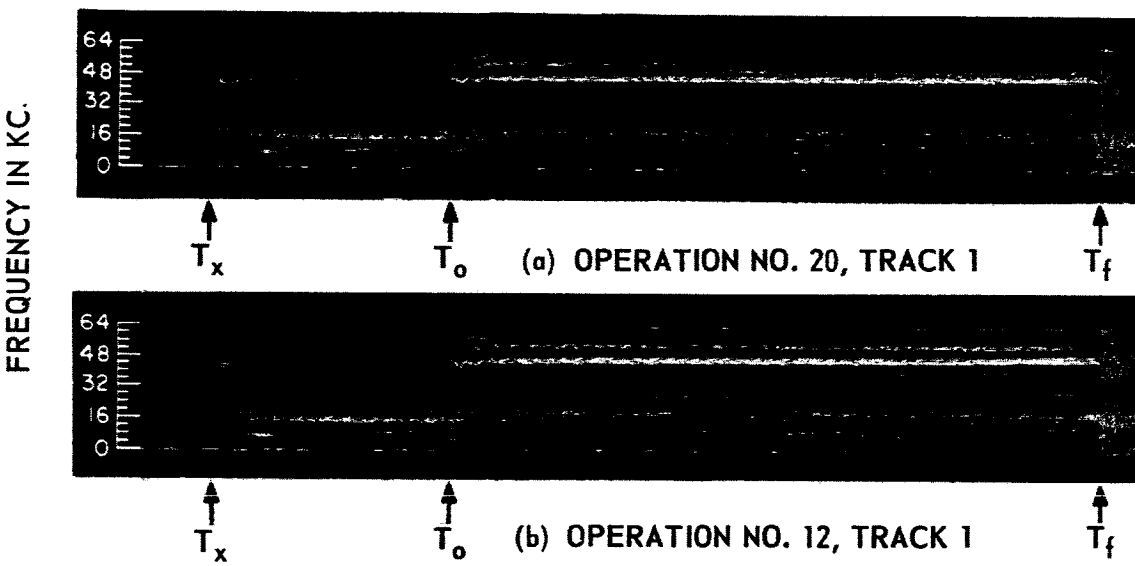
FREQUENCY IN KC.
64
48
32
16
0
T_x
T_o
(a) OPERATION NO. 20, TRACK 1
T_f
64
48
32
16
0
T_x
T_o
(b) OPERATION NO. 12, TRACK 1
T_f

44-A

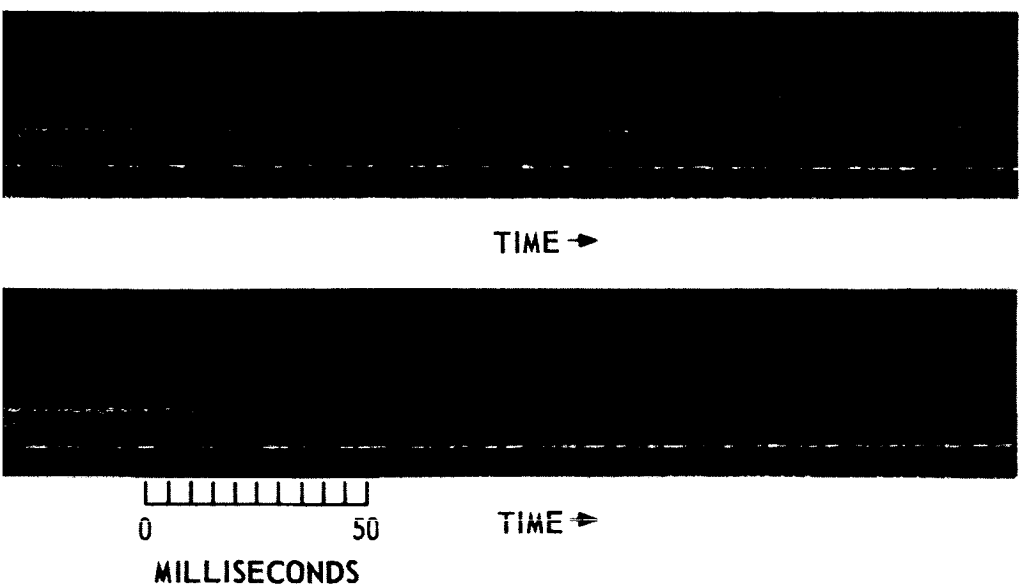

igure 13. Spectrograms of Two S3D Lox Valve Openings, Tape N3, Track 1. Operations 12 and 20.

E4069

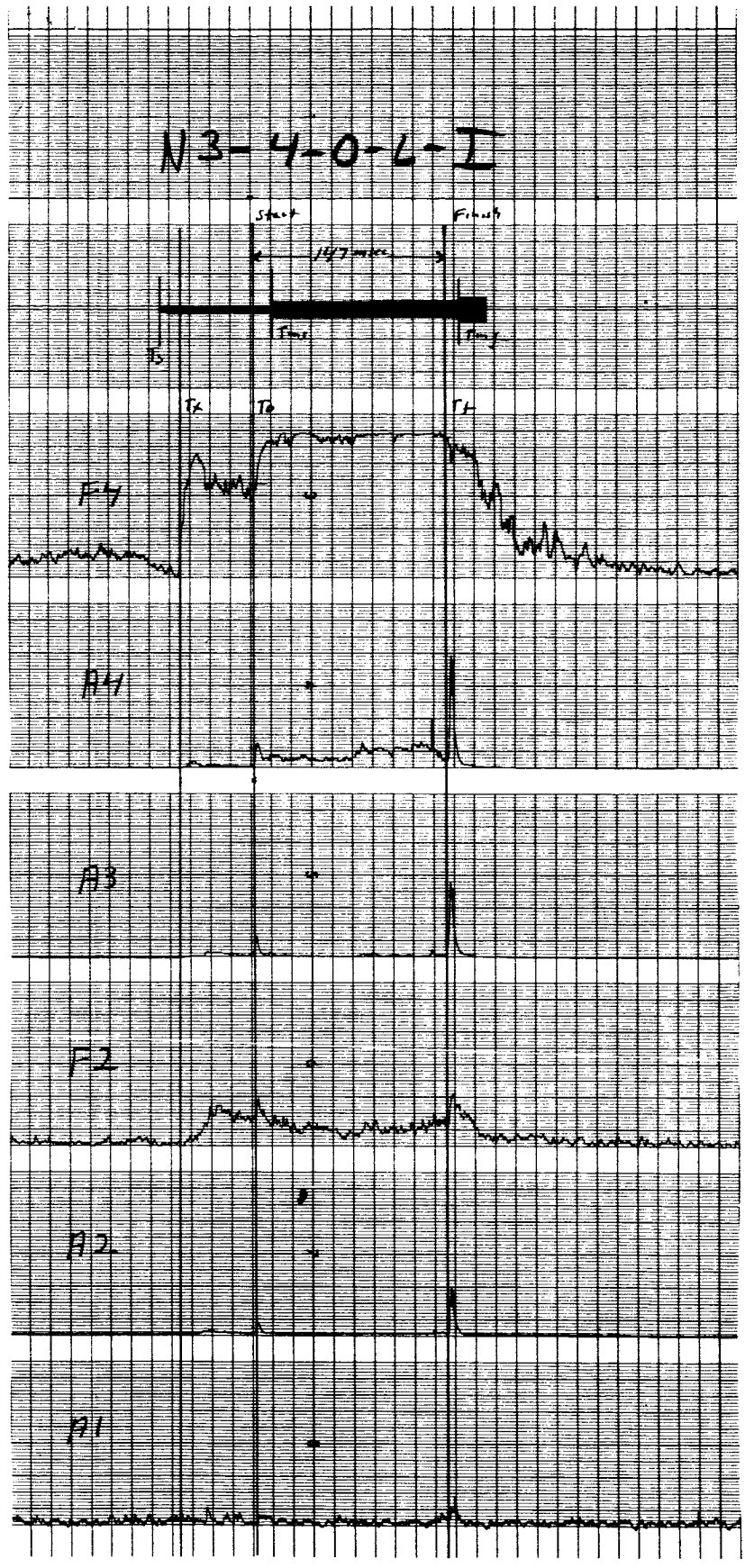

Figure 14. Parametric Plot
Tape N3, Track

45-A

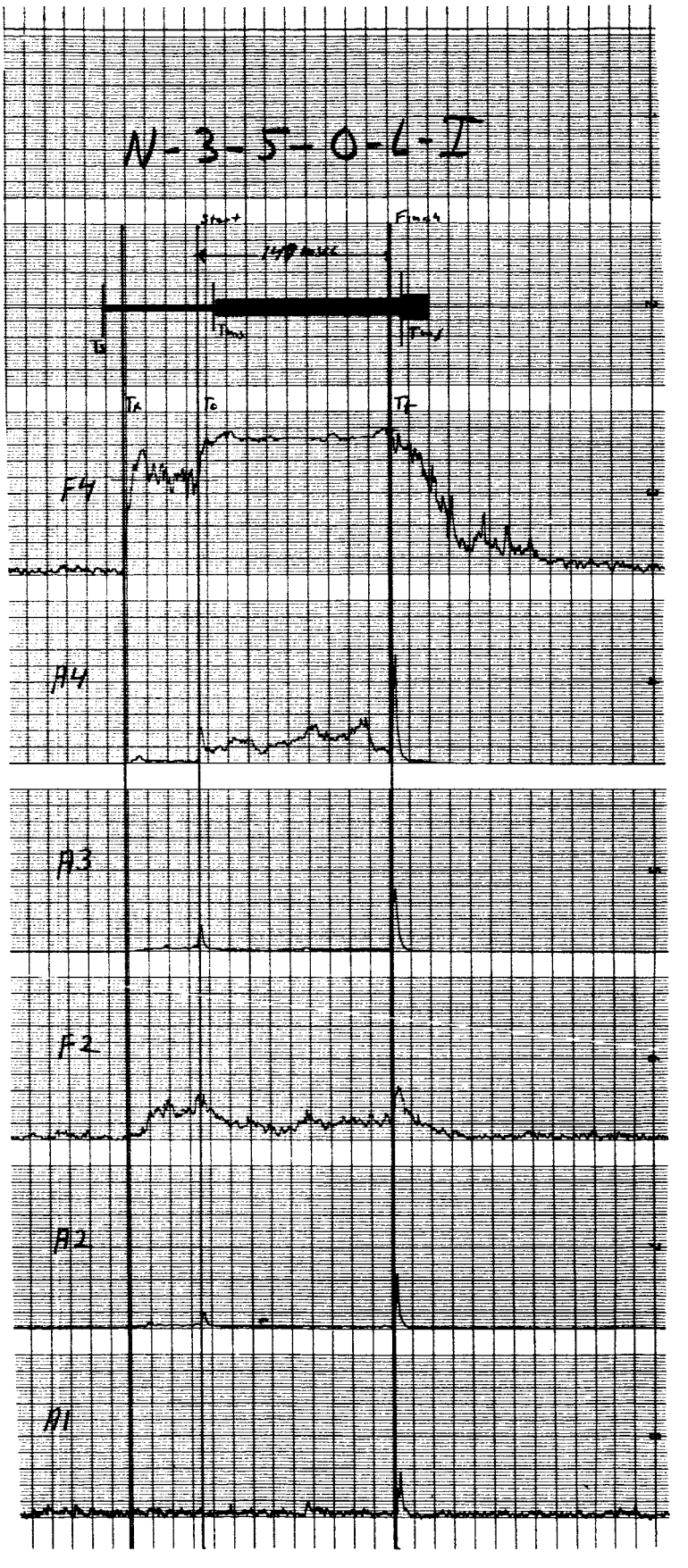

s of Two Typical S3D Lox Valve Openings,
l. Operations 4 and 5.

TABLE III
S3D ENGINE LOX VALVE OPENING EVENTS,
PARAMETRIC STABILITY

Parameter Number	1	2	3	4	5	6	7	8	9	10	11
Event No.	T_sT_x	T_xT_o	T_oT_{ms}	T_oT_f	T_fT_{mf}	A_1T_o	A_1T_f	$\int A_2 < T_o$	A_2T_o	A_2T_f	$F_2(T_xT_o)$
1	16.6	63.0	13.7	135	9.5	7.5	6.5	2.5	27	20	10.3
2	15.1	54.5	16.3	153	7.3	2	18	6	6	17	10.9
3	14.9	57.2	14.6	157	8.4	1	8	2	6	20	8.5
4	15.1	53	13.1	147	7.6	3	9	4	4	15	11.0
5	17.7	56.6	13.5	149	8.3	3	14	3	5	17	11.0
6	14.6	60.5	14.3	139	9.8	23	12	2.5	22	16	9.65
$\bar{z}$	15.6	57.5	14.3	147	8.5	6.9	11.3	3.3	11.7	17.5	10.2
$\bar{\Delta}$	.9	2.9	.8	6.3	.7	5.8	3.4	1.1	8.6	1.7	0.78
% Dev.	5.8	5.0	6.3	4.3	8.2	84	30	33.4	73	9.5	7.7

TAPE N3, TRACK 1

12	13	14	15	16	17	18	19	20	21	
F_2T_o	F_2T_f	A_3T_o	A_3T_f	A_4T_o	$\overline{A_4}(T_oT_f)$	A_4T_f	$\overline{F_4}(T_xT_o)$	$\overline{F_4}(T_oT_f)$	F_4T_f	
11.1	13.2	17	18	31.5	4	44	30.5	47.0	50.8	
11.7	13.0	6.5	21.	10.5	5	40	31.4	50.6	48.5	
11.8	13.1	7	24.5	8	5	24.5	31.2	49.2	47.4	
12.6	14.1	6.5	24	7	4.5	35	32.1	50.4	50.9	
12.8	14.9	7.5	18	11	7	37	32.1	48.7	51.6	
11.3	10.6	11.5	21	17	12	40	29.5	45.5	48.2	
11.9	13.1	9.3	21.1	14.2	6.3	36.7	31.2	48.5	49.6	
0.55	0.92	3.3	2.1	6.7	2.1	4.7	0.73	1.6	1.5	
4.6	7.0	35	10	47	33.4	12.8	2.4	3.2	3.1	

A_1T_o - Amplitude of A_1 associated with T_o.

A_1T_f - Amplitude of A_1 associated with T_f.

$\int A_2(<T_o)$ - Area under A_2 during the interval $T_x \leq t \leq T_o$.

A_2T_o - Amplitude of A_2 peak associated with T_o.

A_2T_f - Amplitude of A_2 peak associated with T_f.

$F_2(T_x-T_o)$ - F_2 frequency peak during the interval $T_x \leq t \leq T_o$.

F_2T_o - F_2 frequency peak associated with T_o.

F_2T_f - F_2 frequency peak associated with T_f.

A_3T_o - Amplitude of A_3 peak associated with T_o.

A_3T_f - Amplitude of A_3 peak associated with T_f.

A_4T_o - Amplitude of A_4 peak associated with T_o.

$\overline{A_4}(T_o-T_f)$ - Mean amplitude of A_4 during the interval $T_o \leq t \leq T_f$.

A_4T_f - Amplitude of A_4 peak associated with T_f.

$\overline{F_4}(T_x-T_o)$ - F_4 frequency centroid during the interval $T_x \leq t \leq T_o$.

$\overline{F_4}(T_o-T_f)$ - F_4 frequency centroid during the interval $T_o \leq t \leq T_f$.

F_4T_f - F_4 frequency peak following T_f.

The outstanding features observed in the S3D lox valve opening parametric plots were:

a) A fairly consistent opening time of 147 milliseconds (mean) with a percentage deviation of only 4.3%. Note that this was about 76 milliseconds shorter than the mean opening time for the fuel valve.

b) T_{ms} and T_{mf} consistently lagged the start and finish times. Again, the T_{mf} lag suggests a slight overswing of the arm which actuates the microswitch for the finish indication.

c) The F_4 frequency centroids before and after T_o possess means which are 31.2 and 48.5 kc respectively with deviation percentages of less than 3.5%.

In general, the S3D lox valve opening events were fairly uniform and no single event deviated sufficiently from the others as to justify labeling it as "abnormal". Recall that specific abnormal events were observed in the fuel valve opening series.

II. S3D Lox Valve Closings

Spectrograms of S3D lox valve closings are shown in Figure 15. Parametric analyses were made of the first six closings which corresponded to the first six openings detailed in Table III. The closing event parametric plots displayed in Figure 16 are of operations 4 and 5 and are derived from track 1 data. These are the same operations for which opening plots are shown.

The results of the parametric analysis of the S3D lox valve closings are presented in Table IV and the parameter definitions are as follows:

T_s - Start of timing signal marking operation of solenoid valve.

T_x - Abrupt increase in F_4 representing first detection of turbulence caused by gas flow.

T_o - Very abrupt start of series of major peaks in A_4 and accompanied by very large peaks in A_3 and A_2. Fairly large peaks also occur in A_1. There is also a large rise in F_2 and a small increase in F_4. T_o is believed to mark the start of motion.

E4057

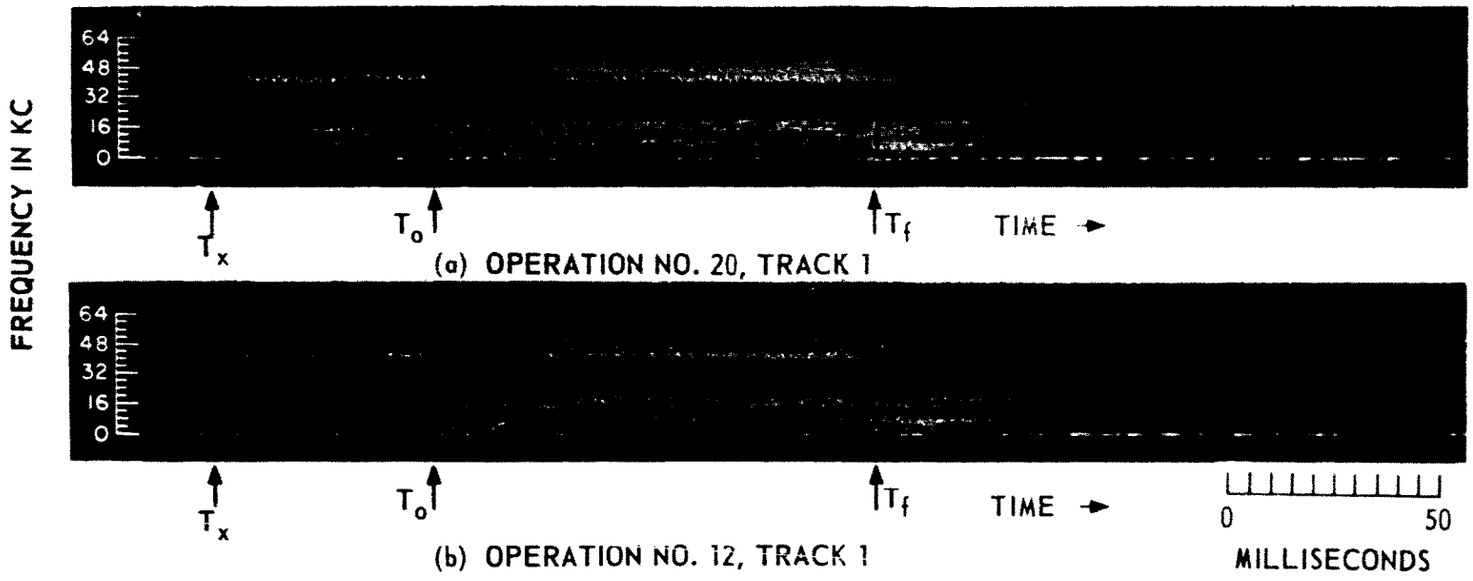

Figure 15. Spectrograms of Two S3D Lox Valve Closings, Tape N3, Track 1. Operations 12 and 20.

E4070

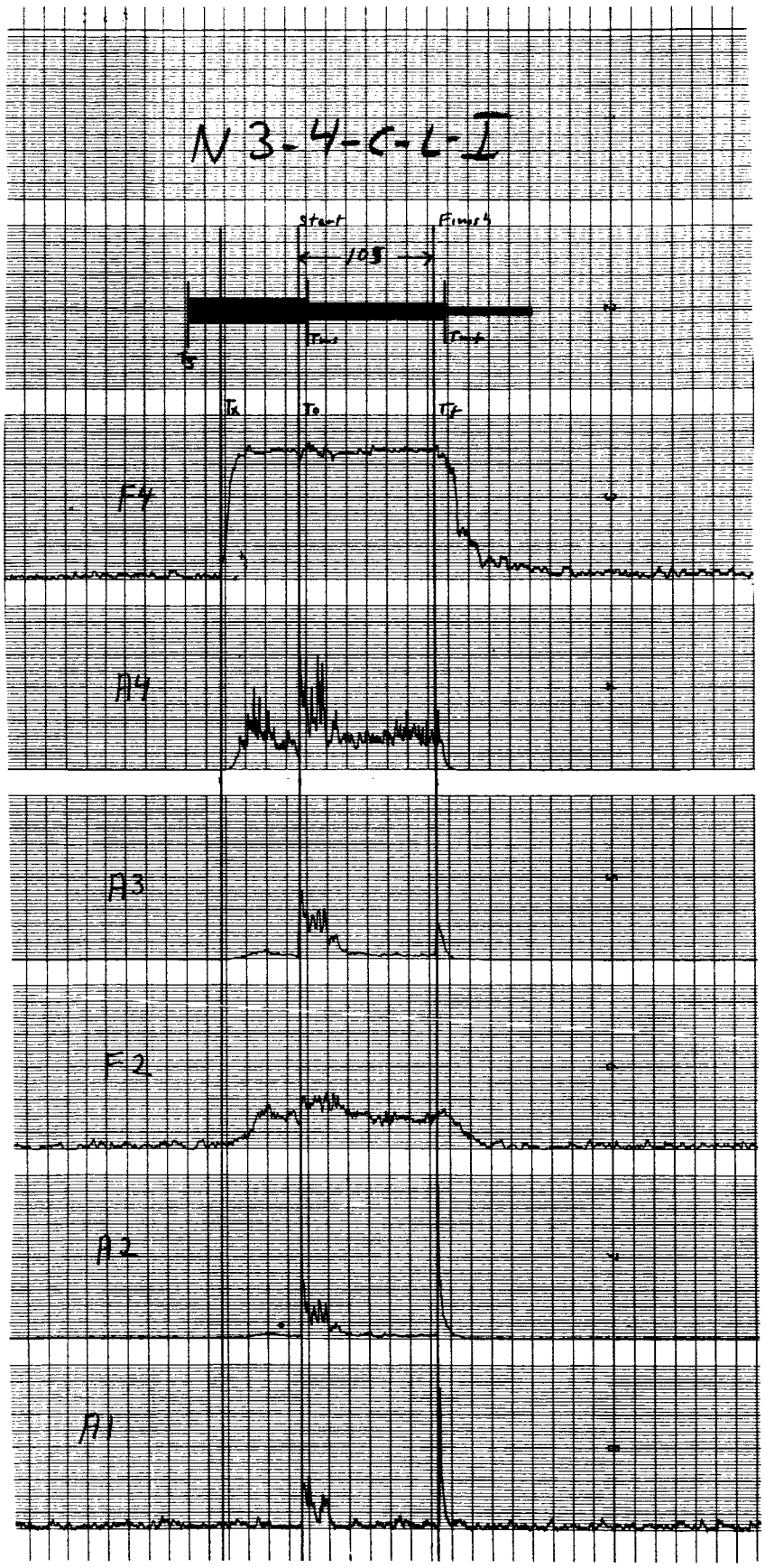

Figure 16. Parametri
Tape N3, T

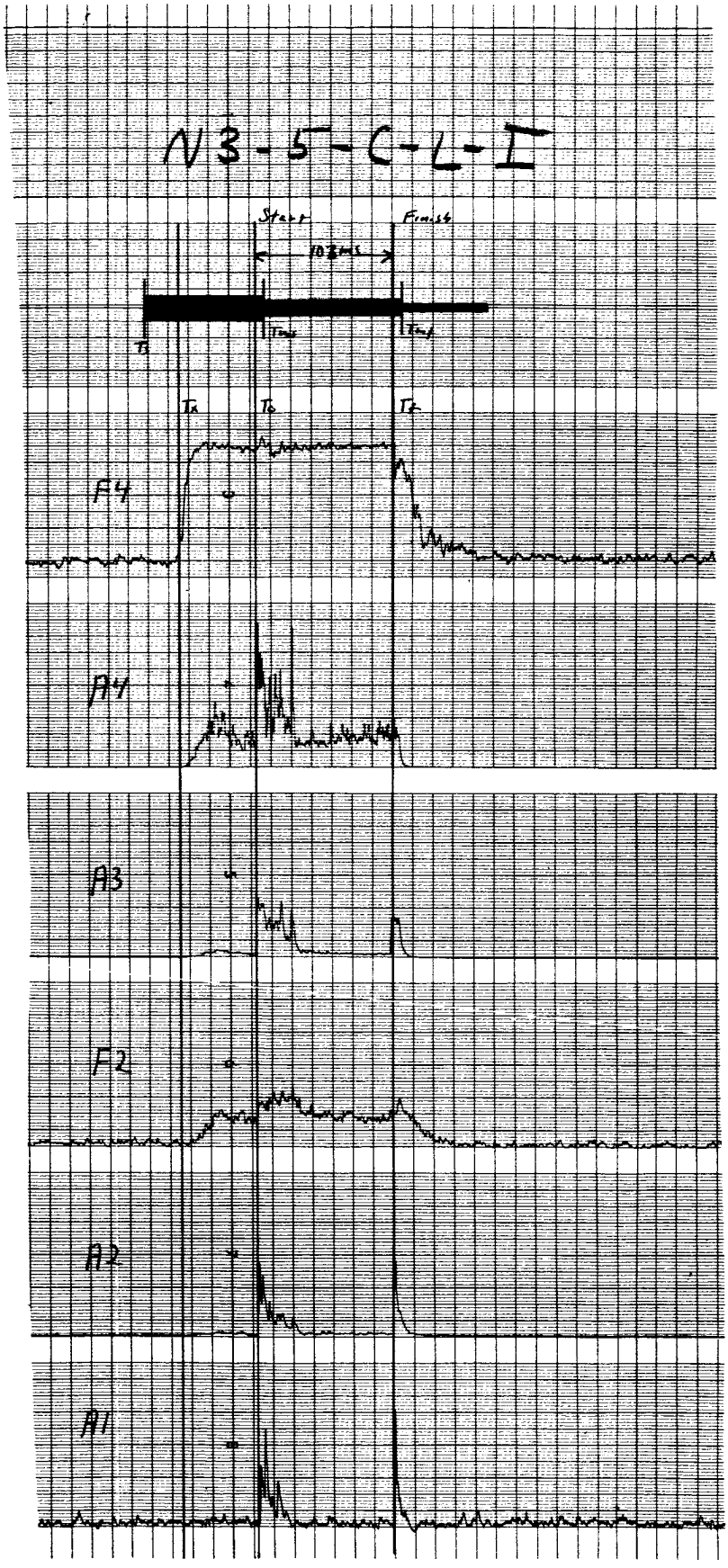

: Plots of Two Typical S3D Lox Valve Closings,
rack 1. Operations 4 and 5.

2

TABLE IV
S3D ENGINE LOX VALVE CLOSING EVENTS, TAPE
PARAMETRIC STABILITY

Parameter Number	1	2	3	4	5	6	7	8	9	10	11	12
Event No.	T_sT_x	T_xT_o	T_oT_{ms}	T_oT_f	T_fT_{mf}	A_1T_o	A_1T_f	A_2T_o	A_2T_f	$F_2T_xT_o$	$\overline{F_2}T_o$	F_2T_f
1	23.1	53.4	7.1	107	9.3	21	20.5	29.5	40	10.3	11.5	9.75
2	23.0	61.0	7.4	104	9.2	12	41.5	29	45	10.4	10.03	9.75
3	21.6	60.5	7.5	108	8.6	13	44	13	44	11.1	12.2	8.86
4	24.1	60.0	8.2	105	6.7	14	44	16	44	11.3	12.9	10.7
5	23.7	60.2	6.8	106	9.0	18	36	23	23	10.6	11.8	11.3
6	23.2	62.5	7.5	109	8.1	21	28	30	44	9.6	12.1	12.2
$\overline{x}$	23.1	59.5	7.4	107	8.5	16.5	37.2	23.5	40	10.5	11.8	10.4
$\overline{\Delta}$	.6	2.1	.3	1.5	.7	3.5	8.5	6.2	5.7	0.45	0.65	0.97
% Dev.	2.6	3.6	4.1	1.4	8.2	21	22.8	26.3	14	4.3	5.5	9.3

N3, TRACK 1

13	14	15	16	17	18	19	20	21	22	23	24
$\int A_3 < T_o$	A_3T_o	$\overline{A_3}T_oT_f$	A_3T_f	$A_4T_xT_o$	$\int A_4 < T_o$	A_4T_o	$\overline{A_4}T_oT_f$	A_4T_f	$\overline{F_4}T_xT_o$	F_4T_o	$\overline{F_4}T_oT_f$
4.5	32	4	16.7	17	7	45	9	9	44.3	41.7	45.5
3.5	25	4	10	17	6	50	9	13	44.3	41.1	45.8
3.5	27	4	10.4	12	6	40	7	14.5	45.2	42.4	46.7
4.5	18	5	10.8	14	7.5	35	7	18	44.6	41.9	46.1
3.5	16	4	12	15	7	44	8	18	45.2	43.3	45.7
3.5	27	4.5	12	14	6.5	46	9	21.5	44.8	43.1	45.3
3.8	24.2	4	12	15	6.7	43.4	8	15.7	44.7	42.2	45.9
.4	4.8	.25	1.6	1.5	.5	3.9	.8	3.5	0.33	0.68	0.38
19.7	6.4	6	13.2	8.8	7.5	8.9	10	22	0.7	1.6	0.8

2

T_{ms} - Timing signal indicates operation of microswitch denoting start of motion.

T_f - Marked by very large peaks in A_2 and A_1 and accompanying prominent peaks in A_3 and A_2. T_f is usually followed, within a few milliseconds, by a peak in F_2 which thereafter declines. T_f is believed to correspond to seating of the valve blade.

T_{mf} - Timing signal indicates operation of microswitch denoting finish of motion.

A_1T_o - Amplitude of A_1 peak associated with T_o.

A_1T_f - Amplitude of A_1 peak associated with T_f. With the exception of the first operation A_1T_f is substantially greater than A_1T_o.

A_2T_o - Amplitude of A_2 peak immediately following T_o.

A_2T_f - Amplitude of A_2 peak associated with T_f. Without exception A_2T_f appreciably exceeds A_2T_o.

$F_2(T_x\text{-}T_o)$ - Maximum frequency excursion of F_2 during the interval $T_x<t<T_o$.

$\overline{F_2}T_o$ - F_2 frequency centroid immediately following T_o.

F_2T_f - Maximum F_2 frequency peak following T_f. This occurs within 10 milliseconds following T_f.

$\int A_3(<T_o)$ - Area under A_3 during the interval $T_x<t<T_o$.

A_3T_o - A_3 amplitude peak following T_o.

$\overline{A_3}<T_f$ - Mean amplitude of A_3 after settling down to plateau during the interval $T_o<t<T_f$. This plateau occupies about the last two-thirds of the closing time.

A_3T_f - Peak amplitude of A_3 associated with T_f.

$A_4(T_x-T_o)$ - Peak amplitude of A_4 during the interval $T_x<t<T_o$.

$\int A_4(<T_o)$ - Area under A_4 during T_x-T_o interval.

A_4T_o - Amplitude of A_4 peak associated with T_o.

$\overline{A_4}(T_o-T_f)$ - Mean amplitude of A_4 after settling down to plateau during T_o-T_f interval. As in the case of the comparable parameter for A_3, this plateau occupies roughly the last two-thirds of the closing time.

A_4T_f - A_4 peak amplitude associated with T_f.

$\overline{F_4}(<T_o)$ - F_4 frequency centroid during T_x to T_o interval. This is similar in character to an F_4 centroid during the corresponding interval in the opening event of the same valve.

F_4T_o - Moderate F_4 frequency peak above preceding centroid level occurring shortly after T_o.

$\overline{F_4}(<T_f)$ - F_4 frequency centroid during most of T_o to T_f interval. This centroid is slightly higher in frequency than $\overline{F_4}<T_o$. It is worth noting that this second centroid also corresponds to an equivalent in the opening event.

The generalizations made previously about the S3D lox valve opening events are essentially valid for the closings as well. For example:

a) The closing times for the six events analyzed were reasonably consistent with a mean value of 107 milliseconds and a percentage mean deviation of only 1.4%. A feature of some interest is the following: although the S3D fuel and lox valves are quite similar in terms of construction and operating principles, the

mean opening time for the fuel valve was somewhat shorter than the closing time (223 milliseconds as compared with 278 milliseconds). However, for the lox valve the situation was reversed in that the closing time was the shorter (107 milliseconds for the closing and 147 for the opening). Both the opening and closing times were shorter, in the case of the lox valve, than their equivalents for the fuel valve.

b) T_{ms} and T_{mf} lagged the start and finish times (mean lags were 7.4 and 8.5 milliseconds respectively).

c) The F_4 frequency centroid after T_o was slightly, but not significantly, higher than that before T_o. The former was 45.9 kc and the latter 44.7 kc. Mean percentage deviations were less than 1%.

The chief differences between the S3D lox valve opening and closing events, other than operating time, are:

a) The closing event is characterized, in part, by appreciable energy indications in both the A_4 and A_3 traces during the interval $T_x < t < T_o$. Attention is called to the T_q timing parameter used in connection with the fuel valve opening. It will be recalled that T_q appeared between T_x and T_o and was marked by a significant A_3 peak. It is believed that the A_3 and A_4 activity, during the comparable interval for the lox valve closing, have a similar significance in indicating a taking up of free play in the valve actuating system just prior to the start of motion of the blade.

b) At the start of motion both A_3 and A_4 display high amplitude components of relatively long period prior to settling down to fairly steady values (plateaus mentioned earlier). This strongly suggests a rather pronounced vibratory motion of the spring compliance and component mass of the moving system which is damped relatively early in the course of the event. Note that the A_4 signal is actually an amplitude modulation of F_4 which does not appear as such in the F_4 trace because the latter is derived from an axis crossing detector which does not reflect amplitude variations. The F_4 signal itself apparently represents an orificial signature excited by gas flow. Its frequency remains substantially constant both prior to and during valve motion.

2.4.4 S3D Gas Generator Valve

I. S3D Gas Generator Valve Openings

Two examples of gas generator opening event are shown spectrographically in Figure 17 and two of the closing event are displayed in Figure 18. At first glance it is obvious that the durations of the openings and closings are both considerably shorter than their counterparts in the fuel and lox valves. This is indeed confirmed by parametric analyses, typical examples of which are shown in Figure 19 (opening event) and in Figure 20 (closing event).

This report does not contain tabulated parametric data for the gas generator valve. However, such data was measured and recorded for the first six operations of the valve. The timing parameters were identical

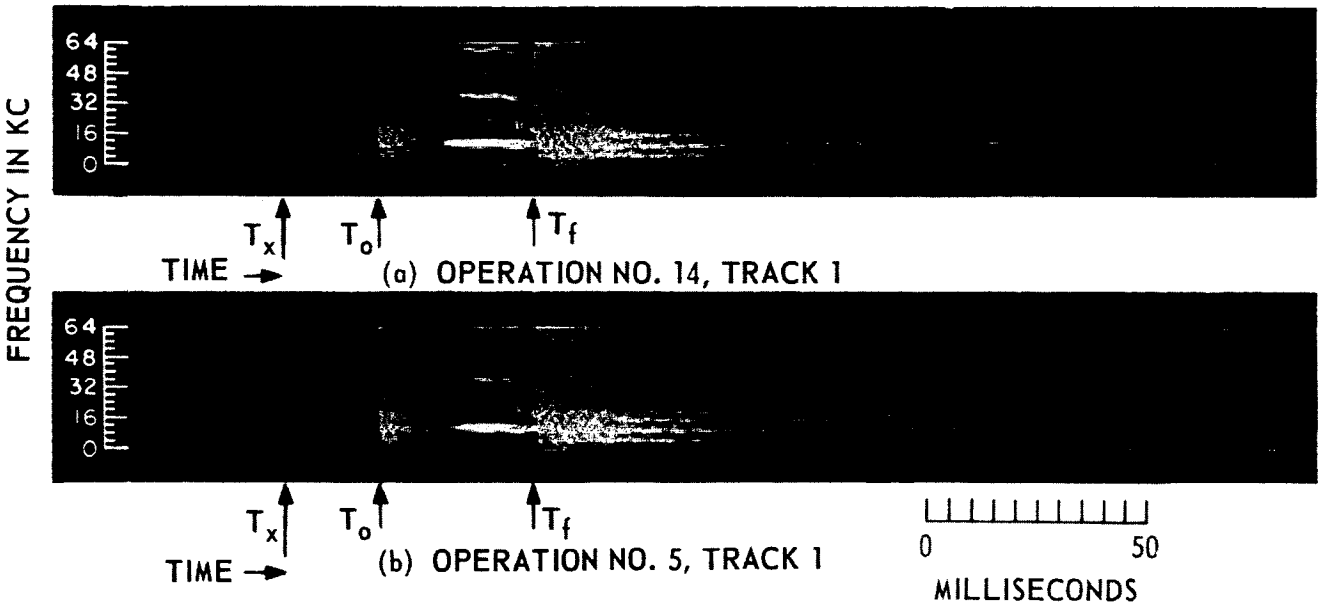

Figure 17. Spectrograms of Two S3D Gas Generator Valve Openings, Tape N3, Track 1. Operations 5 and 14.

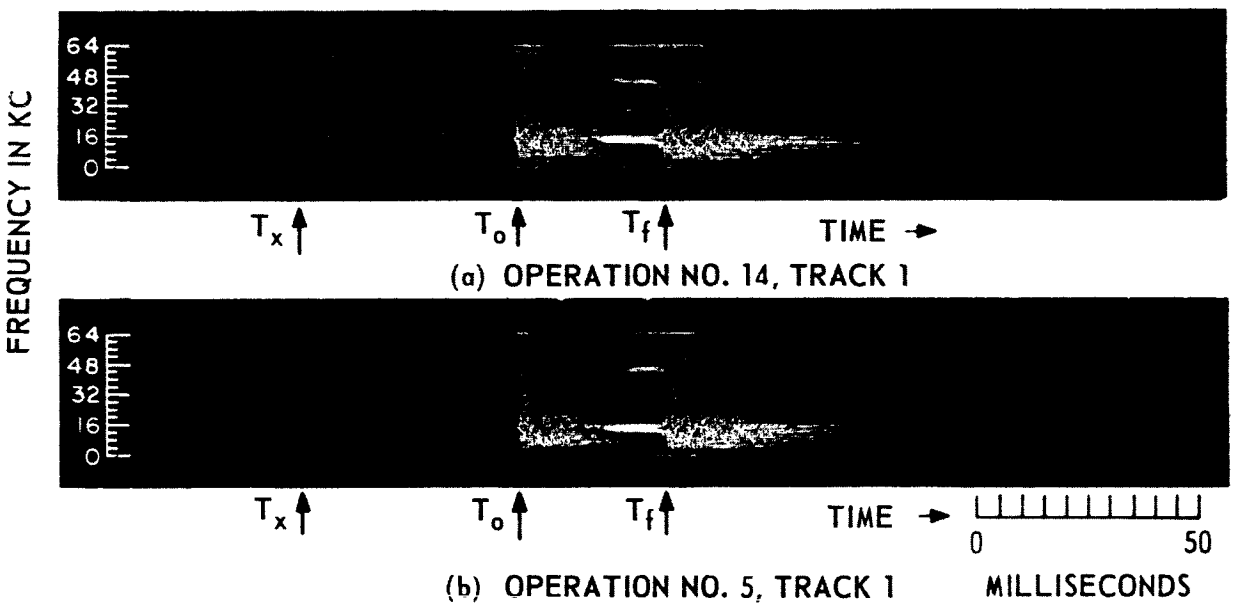

Figure 18. Spectrograms of Two S3D Gas Generator Valve Closings, Tape N3, Track 1. Operations 5 and 14.

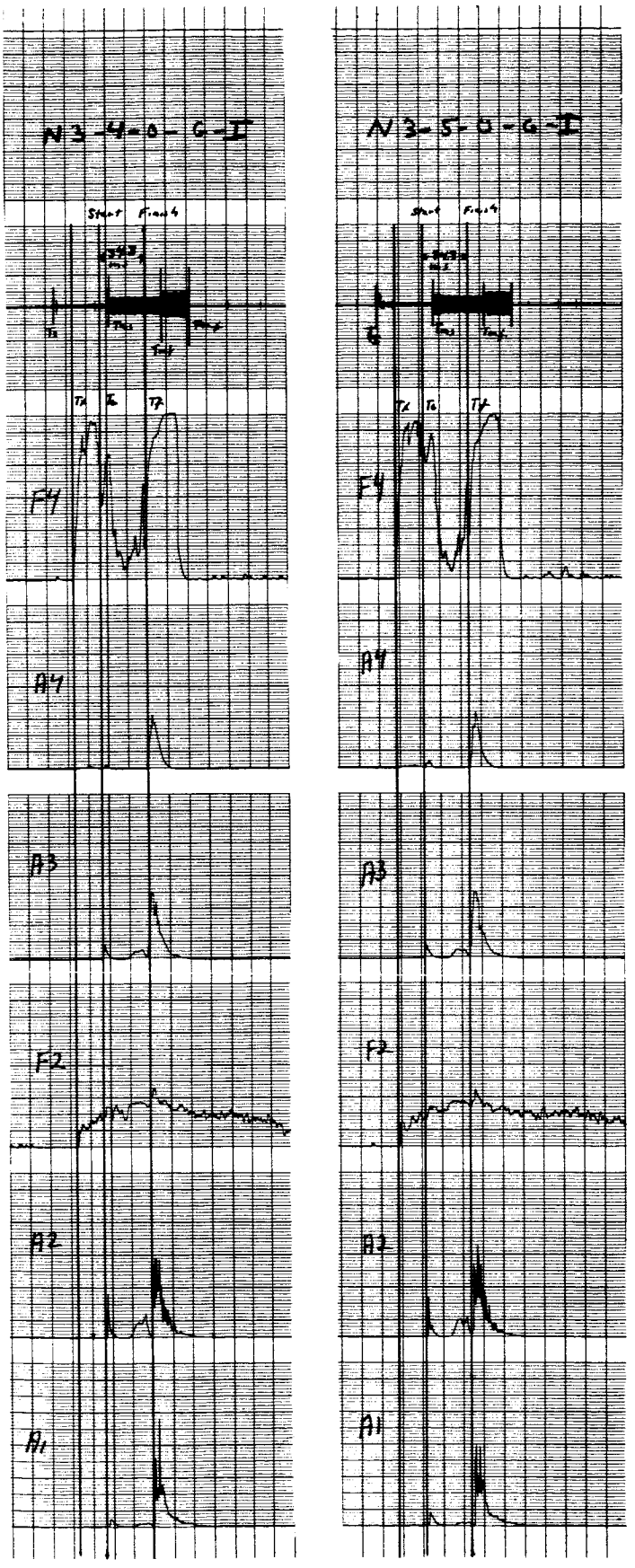

Figure 19. Parametric Plots of Two Typical S3D Gas Generator Valve Openings, Tape N3, Track 1. Operations 4 and 5.

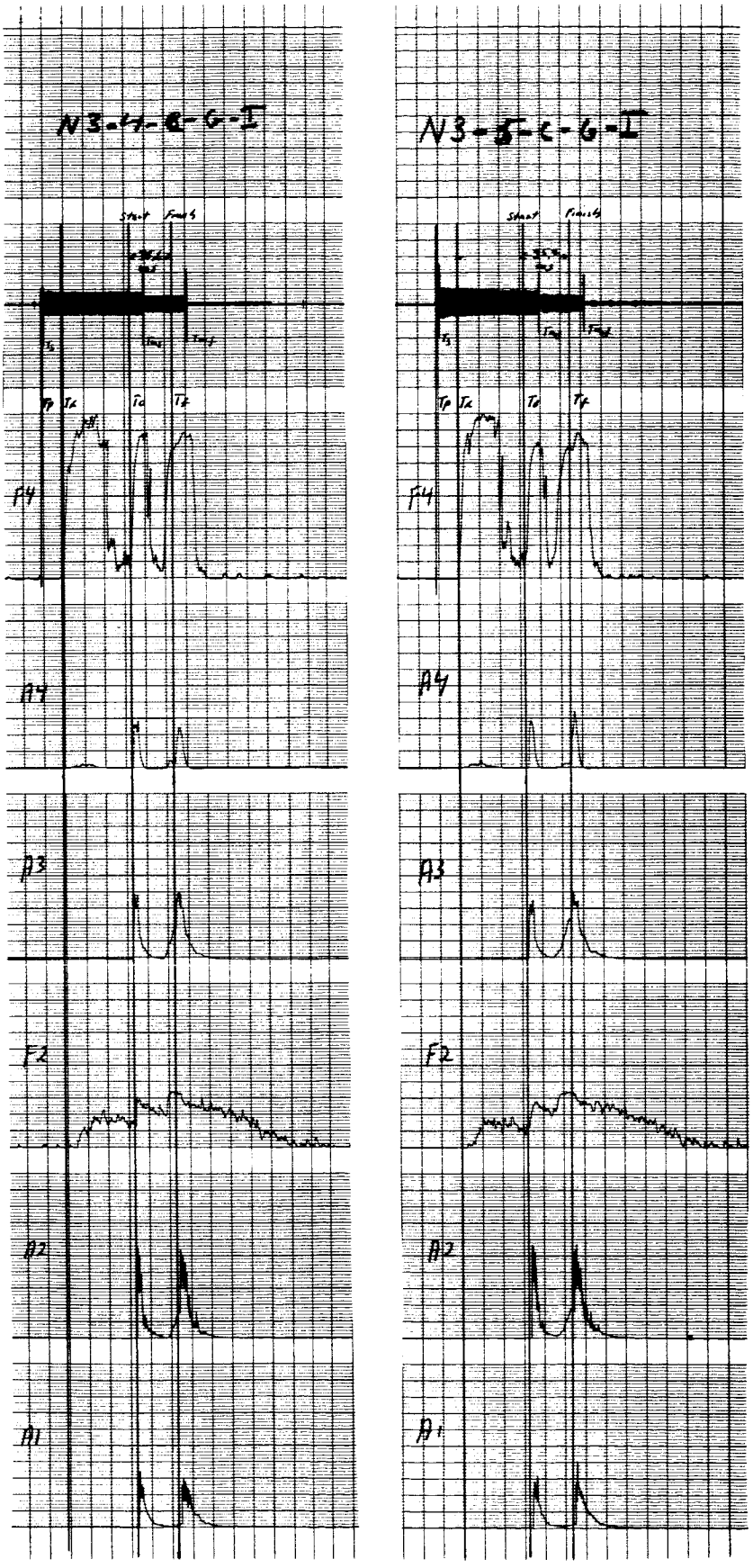

Figure 20. Parametric Plots of Two Typical S3D Gas Generator Valve Closings, Tape N3, Track 1. Operations 4 and 5.

with those employed for the lox valve with the exception that a T_p time mark was added to the closing analysis. The A and F parameters were essentially similar to those previously employed. The salient parametric features observed are described below for the opening and closing events. Reference to the appropriate parametric plots will be helpful in connection with the following discussion.

II. S3D Gas Generator Opening Event

a) The opening time (T_o to T_f interval) for the S3D gas generator valve was quite brief in comparison with either the fuel or lox valve. The mean time for six operations was only 33.4 milliseconds with a percentage deviation of 4.4%. Of the six openings, the first (28.4 milliseconds) was markedly shorter than the others which fell within the range of 33.2 to 35.6 milliseconds. This was considered, on the whole, to represent fairly consistent performance.

b) An unusual feature of the gas generator valve opening operation proved to be the time required from solenoid valve operation to start motion, i.e., the interval from T_s to T_o. This interval was a long one, with a mean of about 35.7 milliseconds - longer in fact than the motion time itself.

c) The start of the blade motion was simultaneously indicated by relatively small peaks in A_1, A_3 and A_4 and by a major peak in A_2.

d) The finish of blade motion was marked by major peaks in all amplitude parameters, particularly in A_2 and A_3.

e) The end of the F_4 trace displays a peak which is often monochromatic at a mean frequency of 58 kc with a mean deviation of about 6.5%. The significant feature of this plateau is that it begins a few milliseconds after T_f and, for this reason is clearly not caused by mechanical operation of the gas generator valve. The source must be caused by gas flow through an orifice such as the bleed valve.

f) As was the case for the other valves, the microswitch indications consistently lagged the parametric signatures for the start and finish of gate motion.

III. S3D Gas Generator Closing Event

a) Like the opening time, the closing time of the gas generator valve was short compared with the equivalent interval for the fuel and lox valves. Specifically, for the six closings analyzed, the mean time was 34.7 milliseconds with a percentage deviation of 5%. (It was virtually identical with the mean opening time of 44.0 milliseconds). Again, the performance was considered quite uniform in this respect.

b) As in the case of the opening event, the interval from solenoid operation to start motion - the T_s to T_o period - was longer than the actual valve motion time, but more strikingly so for the closing. The mean T_s to T_o interval was 63.5 milliseconds as derived from the sum of the mean T_s-T_x and T_x-T_o values. This means that the time required for the valve to start motion from the operation of the solenoid was nearly double the time

consumed by the motion itself.

c) The start of blade motion was indicated by large simultaneous peaks in A_1, A_2, and A_3 and significant, though somewhat smaller peaks in A_4. These peaks were accompanied by a rather fast increase in F_2 and F_4.

d) The finish of blade motion was also marked by major peaks in all amplitude parameters. A major difference between the parameter indications for the opening and closing events was that, for the closing, the amplitude peaks denoting start and finish of motion were nearly equal for a given parameter. For the openings, the second peak, marking the end of motion, was invariably larger, often by a considerable factor.

e) As with the opening event, the F_4 trace displays a peak just subsequent to T_f. This peak, unlike the smooth, regular appearance of the opening event correlate, is considerably more irregular in frequency and has a rather lower mean frequency for the six events - 50.5 kc as compared with 58 for the opening. However, since it begins after the finish of motion, it is clearly due to gas flow excitation.

f) The lag of microswitch indications for start and finish of motion occurs for the closing event of this valve as for those previously discussed.

g) A feature, not appearing in the opening event, is a small F_4 peak occurring between 3 and 4 milliseconds prior to the solenoid operate indication. The time of occurrence of this peak is

called T_p. The event is believed due to mechanical transmission of solenoid "bang" along the tubing. The timing would suggest a slight delay in the microswitch indication. As will be recalled, a signature corresponding to F_4T_p was also observed for the closing event of the S3D fuel valve.

2.4.5 F1 Lox Valve

All of the F1 lox valve data which was analyzed was derived from NASA Tape No. 8. The signals on this tape were, on the whole, well recorded and quite clean. Data from track 1 and track 2 were both employed in this analysis which covered five opening and five closing events.

I. F1 Lox Valve Opening Event

Spectrograms of the F1 lox valve openings are shown in Figure 21 as derived from track 1 and in Figure 22 as derived from track 2. Examination of these shows that both purging noise and operating signatures are readily distinguishable. This is an important finding in view of the initial concern that purging noise might obscure the valve operating signatures. That the purging noise and valve operating acoustical signatures are distinct and separable is evident in the spectrograms and in parametric analyses discussed in the following. Parametric plots of two F1 lox valve openings as derived from track 1 are displayed in Figure 23. Plots of the same events, as derived from track 2, are shown in Figure 24. The calibration of these plots, and all other F1 plots, differs from that of the S3D plots only in respect to timing. Since the F1 data speed reduction was 32/1, instead of 64/1, each millimeter represents twice the time interval that it did on the S3D plots - that is, on the F1 plots each millimeter = 6.24 milliseconds. The parametric opening event

E4060

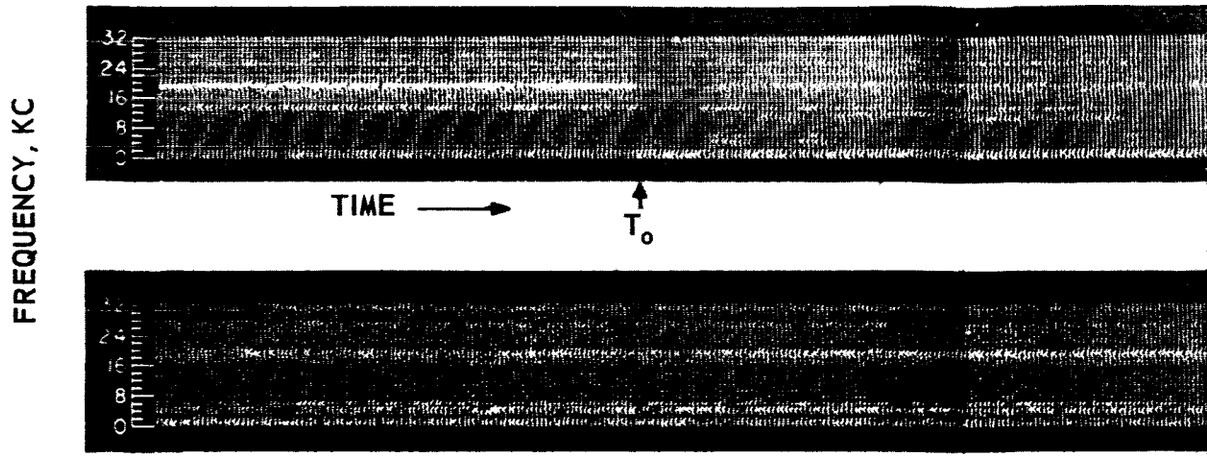

(a) OPERATION NO

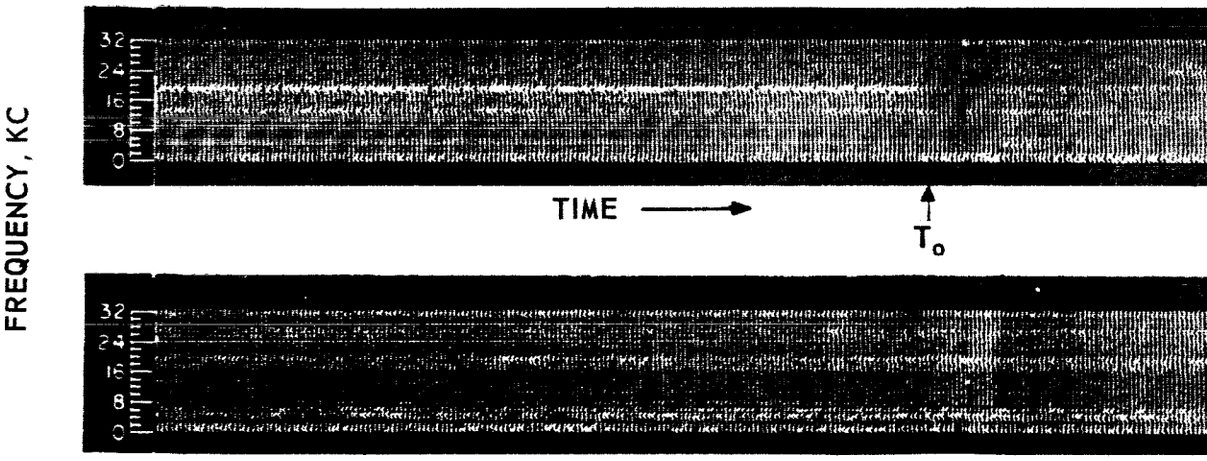

(b) OPERATION NO

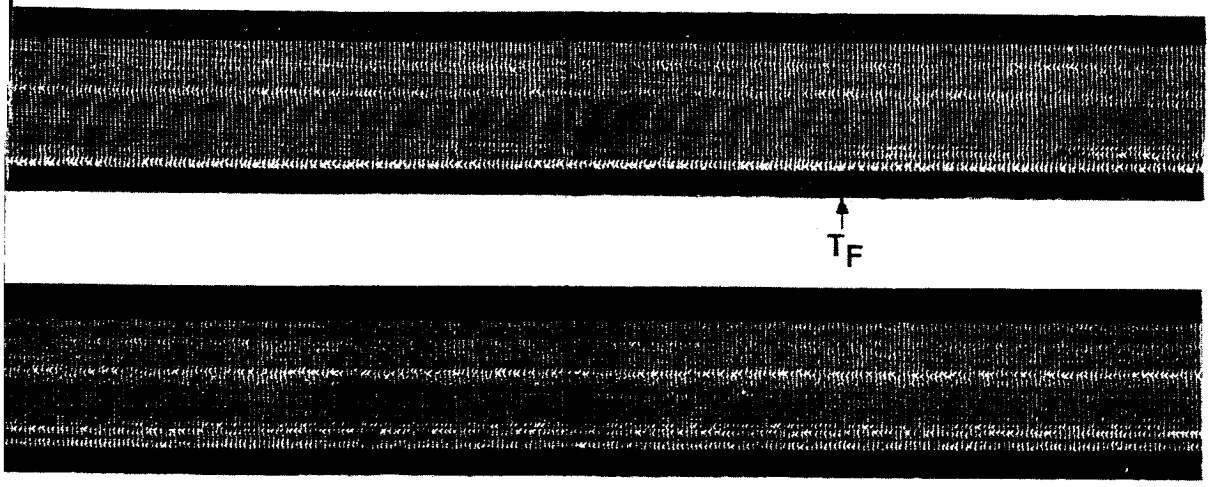

). 5, TRACK 1

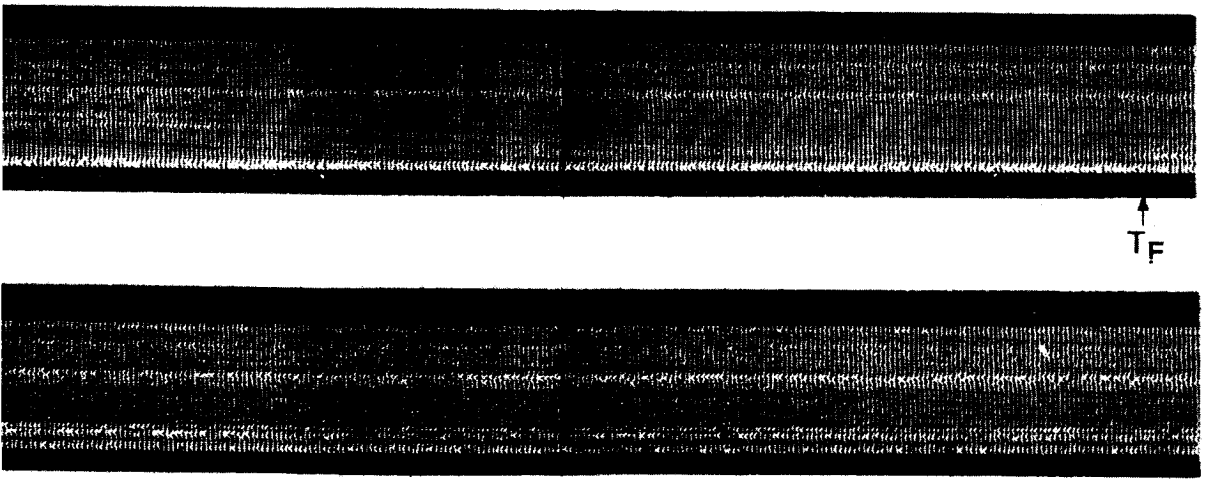

). 4, TRACK 1

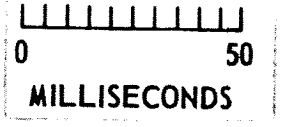

Figure 21. Spectrograms of Two F-1 Lox Valve Openings, Tape N8, Track 1. Operations 4 and 5.

E4062

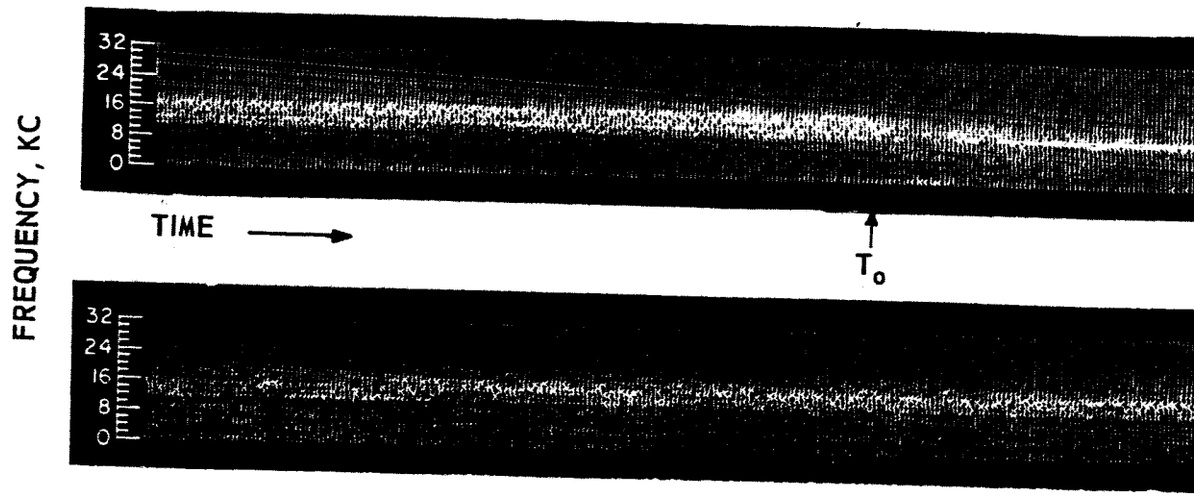

(a) OPERATION NO.

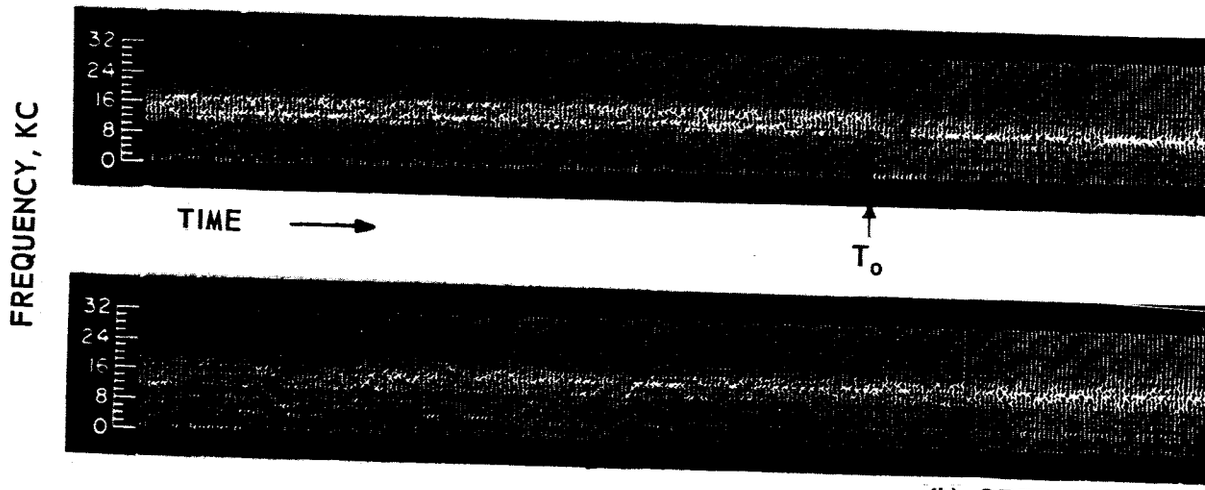

(b) OPERATION NO.

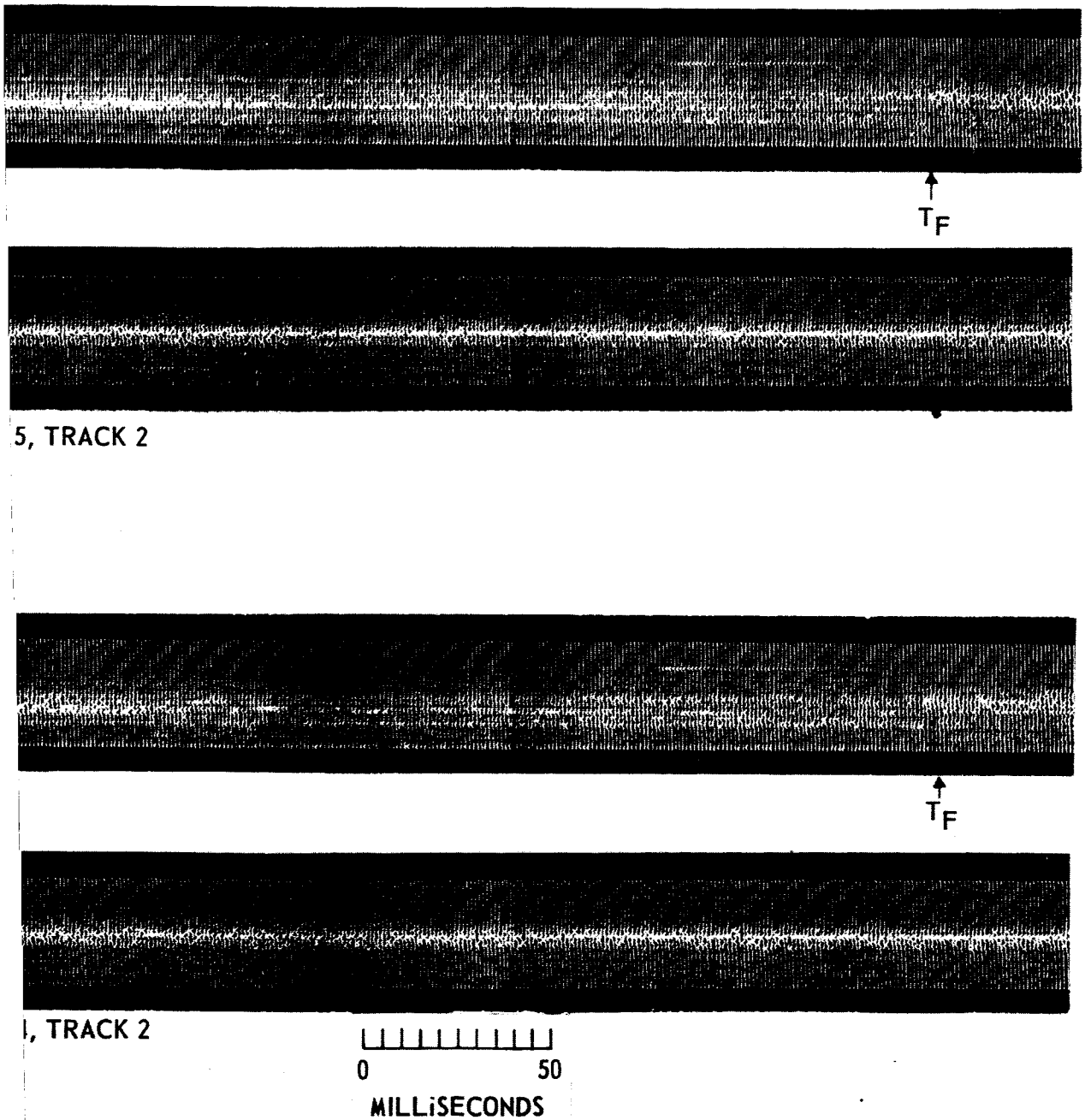

Figure 22. Spectrograms of Two F-1 Lox Valve Openings, Tape N8, Track 2. Operations 4 and 5.

E4073

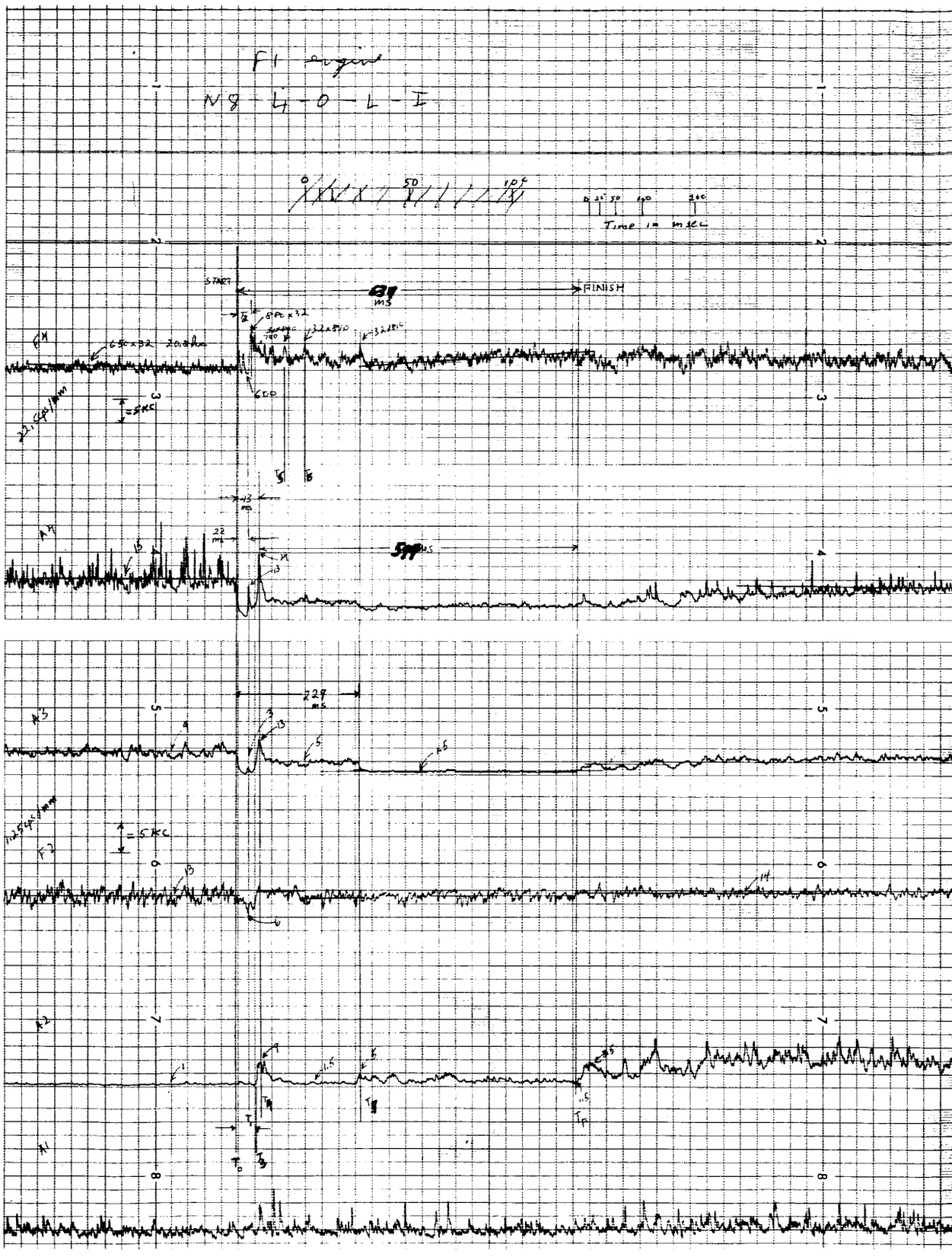

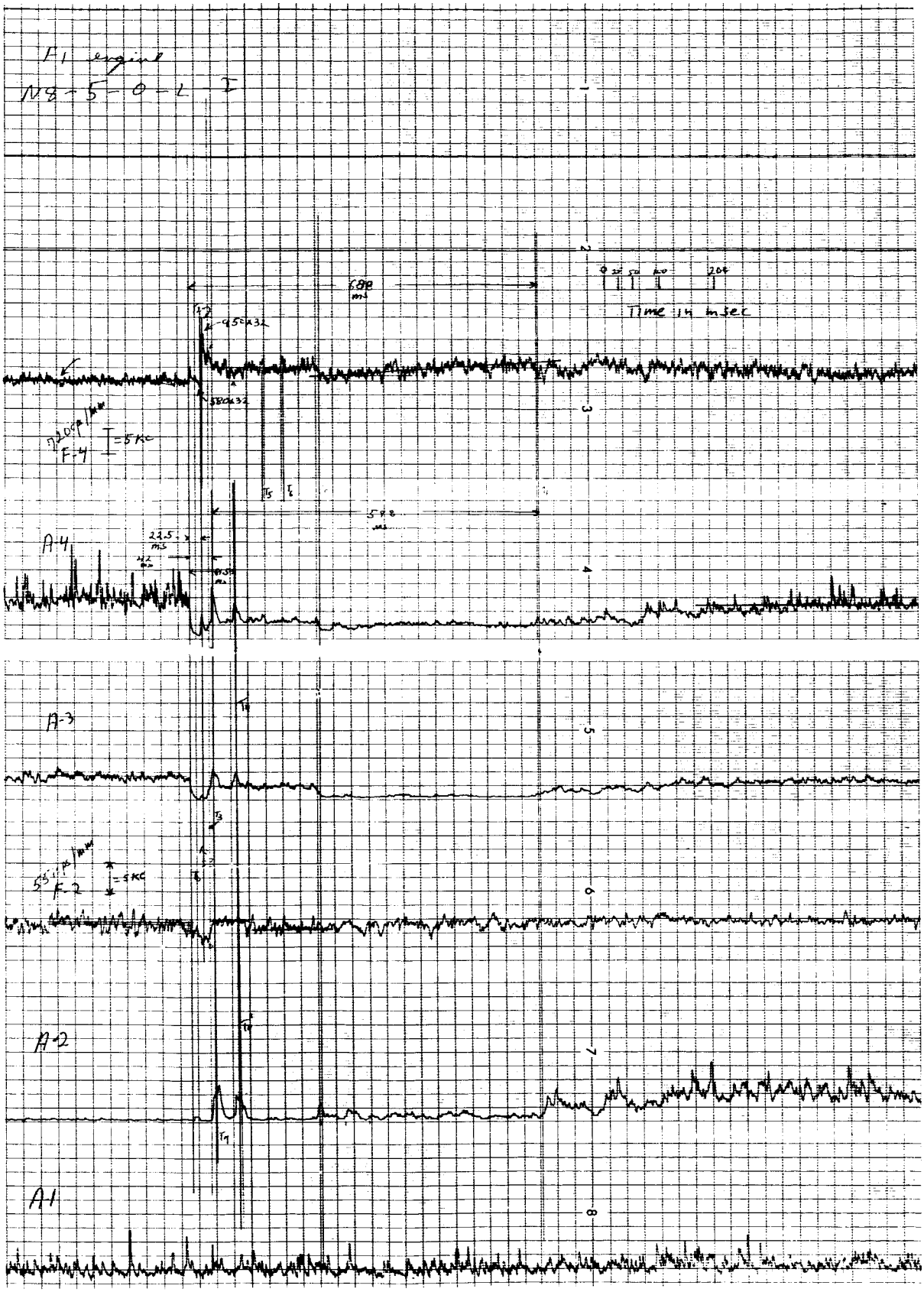

Figure 23. Parametric Plots of Two Typical F-1 Lox Valve Openings, Tape N8, Track 1. Operations 4 and 5.

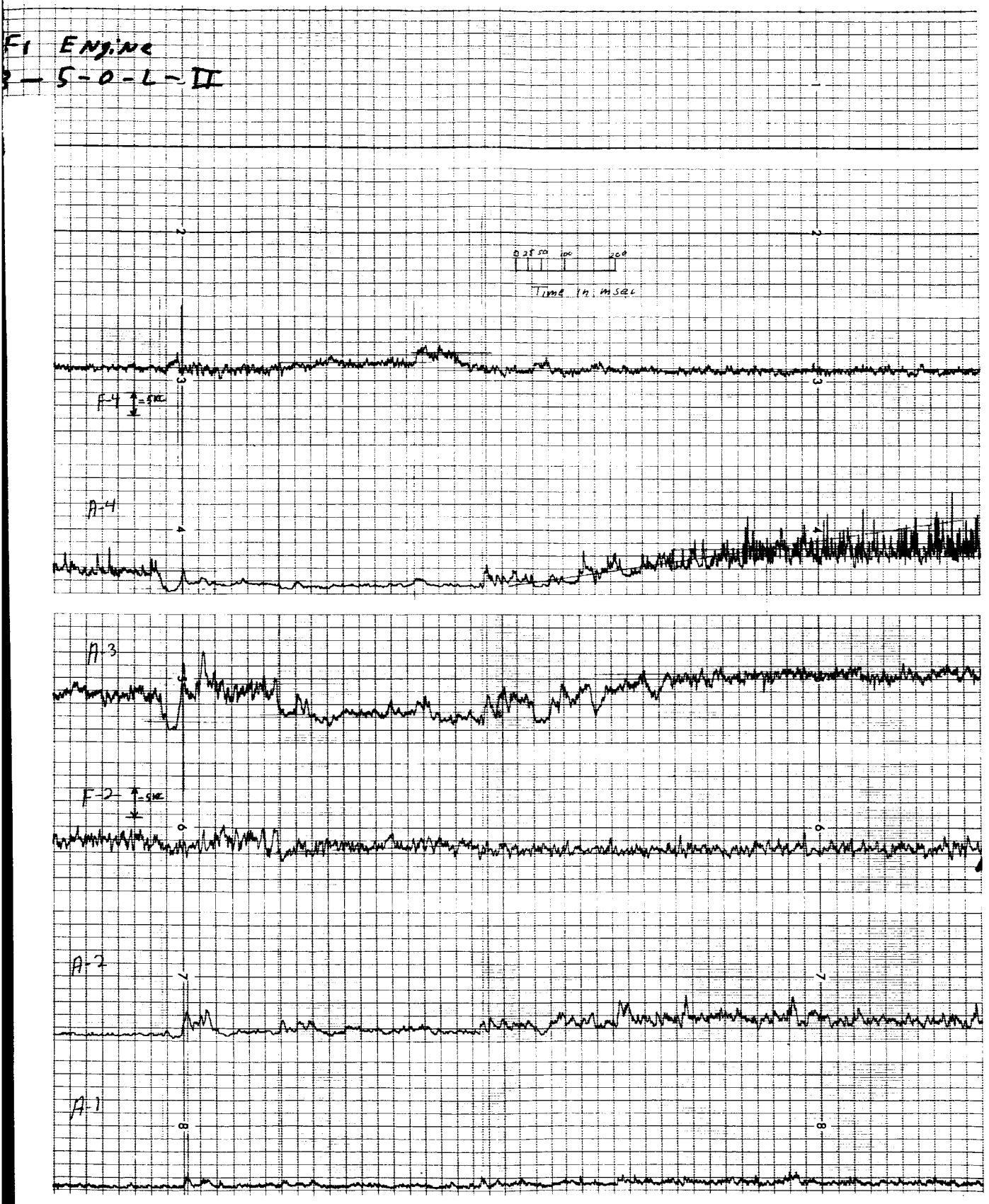

Figure 24. Parametric Plots of Two Typical F-1 Lox Valve Openings, Tape N8, Track 2. Operations 4 and 5.

data is displayed in tabular form in Table V for track 1 and in Table VI for track 2. Definitions of parameters follow:

The parametric analysis for the F1 lox valve is founded on the parameters designated A1, A2, A3, A4, F2 and F4.

A1 is the envelope amplitude of the spectral energy falling in the frequency band from 0 to 3200 cps.

A2 is the envelope amplitude of the spectral energy falling in the frequency band from 2880 cps to 6400 cps.

A3 is the envelope amplitude of the spectral energy falling in the frequency band from 8000 to 12,800 cps.

A4 is the envelope amplitude of the spectral energy falling in the frequency band from 16,000 cps to 32,000 cps.

F2 is the frequency centroid in the band from 2880 to 6400 cps, (same band from which A2 is derived).

F4 is the frequency centroid in the 16,000 cps to 32,000 cps, (same band from which A4 is derived).

(a) Track 1 Plots for F1 Lox Valve Opening

This track is recorded from a sensor located on the housing that covers the sequencing valve assembly.

T_o - Standard time reference from which all intervals were measured. T_o is marked by the initiation of a period of silence or near silence appearing in well marked form both in A4 and A3. This interval is known to correspond to the operation of the 4-way valve which actuates the lox valve by reversing the direction of gas flow. T_o, in the F1 analysis, is taken as the start of

TABLE V
F1 ENGINE LOX VALVE OPENING EVE
PARAMETRIC STAB

Parameter Number	1	2	3	4	5	6	7	8	9	10	11	12
Event No.	ΔT_o	T_1	T_1'	T_1''	T_2	T_3	T_F	P_1	P_2	P_3	P_4	$\overline{A2}(<T_o$
1	40	46	28.1	32	47.5	226	640	23.8	37.5	43	81.2	1
2	40	44	25.0	32	43	226	638	19.4	37.5	47	84.4	1
3	43	47	33.0	32	46	228	635	18.0	31.0	30	N	1
4	39	43	26.2	32	47	229	637	22.0	31.0	30	71.9	1
5	37	43	24.4	32	49	237	638	23.0	37.5	47	N	1
$\bar{a}$	39.2	44.6	27.3	32	46.5	229	638	21.3	35	39	79	1
$\bar{\Delta}$	1.6	1.4	2.5	0	1.6	3.0	1.2	2.0	3.1	10	5	0
% Dev.	4.1	3.1	8.5	0	3.4	1.3	0.2	9.4	8.9	25	6.3	0

Parameter Number	22	23	24	25	26	27	28	29	
Event No.	$\overline{A3}(<T_o)$	$\overline{A3}(\Delta T_o)$	$A3(P_1)$	$\overline{A3}\Big\|_{T_1}^{T_3}$	$\overline{A3}\Big\|_{T_3}^{T_F}$	$\overline{A3}(>T_F)$	$\overline{A4}(<T_o)$	$\overline{A4}(\Delta T_o)$	A
1	6.5	1.5	3.8	5	1.2	6.0	14	3.0	8
2	8.2	0.8	1	5	1.5	6.5	14	3.0	9
3	6.0	0.5	0	5	1.5	6.5	10	2.0	1
4	9.0	1.5	2.8	5	1.5	6.5	15	3.5	13
5	8.8	1.0	2.0	5	1.0	6.5	15	3.5	9
$\bar{a}$	7.7	0.94	1.9	5	1.3	6.4	13.6	3.0	8
$\bar{\Delta}$	1.1	0.3	1.1	0	0.2	0.2	2.5	0.4	2
% Dev.	14.3	32	58	0	15.5	3.1	18.5	13.5	36

NTS, TAPE N8, TRACK 1
LITY

13	14	15	16	17	18	19	20	21
$A2(T_2)$	$\overline{A2}\Big\|_{T_2}^{T_3}$	$\overline{A2}\Big\|_{T_3}^{T_F}$	$A2(>T_F)$	$\overline{F2}(<T_o)$	$\overline{F2}\Big\|_{T_2}^{T_3}$	$\overline{F2}\Big\|_{T_3}^{T_F}$	$F2(T_1'')$	$\Delta F2\Big\|_{T_2}^{T_3}$
9	1.7	2.0	10	5.5	5.8	5.9	3.3	1.0
9	1.5	3.5	10	5.5	5.6	6.0	3.9	0.5
7.5	1.5	2.0	10	5.4	5.9	6.0	3.9	1.0
9	1.5	2.0	11	5.7	5.9	5.5	3.6	1.1
12	1.3	2.0	11	5.8	5.5	5.5	3.3	1.3
9.3	1.5	2.3	10.4	5.6	5.7	5.8	3.6	0.98
1.0	0.1	0.5	0.5	0.1	0.1	0.2	0.3	0.2
10.7	6.6	2.2	4.8	1.8	1.8	3.5	8.3	20

30	31	32	33	34	35	36	37	38	39	40
(P_1)	$\overline{A4}\Big\|_{T_1}^{T_3}$	$\overline{A4}\Big\|_{T_3}^{T_F}$	$\overline{A4}(>T_F)$	$\overline{F4}(<T_o)$	$F4(T_1')$	$\overline{F4}\Big\|_{T_1}^{T_3}$	$\overline{F4}\Big\|_{T_3}^{T_F}$	$F4(P_4)$	$\overline{F4}(>T_F)$	$\Delta F\Big\|_{T_3}^{T_F}$
.5	6.5	5.0	12	20.8	28.2	23.4	22.9	20.0	22.3	2.74
	6.5	5.3	12	20.8	29.4	23.4	22.9	20.7	22.0	2.18
.0	6.5	5.5	12	21.0	27.8	23.6	22.8	N	22.0	3.6
	7.0	5.3	12	20.8	28.2	23.0	22.5	19.5	22.3	2.9
	6.5	5.1	12	20.3	30.4	23.0	22.8	N	22.0	3.4
.0	6.6	5.2	12	20.7	28.8	23.3	22.8	20.1	22.1	3.0
.9	0.16	0.16	0	0.2	0.88	0.22	0.1	0.26	0.14	0.52
	2.4	3.1	0	1.0	3.1	1.0	0.5	1.3	0.6	17.5

2

TABLE
F1 ENGINE LOX VALVE OPENING
PARAMETRIC

Parameter Number	1	2	3	4	5	6	7	8	9	10	11	12	13
Event No.	ΔT_o	T_1	T_2	T_3	T_4	T_F	T_R	T_1'	P_1	$A1(T_2)$	$\overline{A1}\Big\|_{T_o}^{T_F}$	$\overline{A2}(<T_o)$	$\overline{A2}(\Delta T$
1	42.5	50	57.5	232	N	630	1120	40.6	130	8	1.5	2.0	2.0
2	42.5	44	50	228	505	623	1210	30	120	6	2.0	2.5	2.0
3	40	44	50	231	500	623	1246	36	115	5.5	2.0	2.3	2.0
4	39	47	51	232	494	623	1206	36	113	6.5	2.0	2.5	2.1
5	40	44	49	225	495	618	1190	34	110	5.4	2.0	2.5	2.0
$\bar{a}$	40.8	44.6	51.5	230	499	624	1197	35.3	118	5.7	1.9	2.4	2.0
$\bar{\Delta}$	1.4	2.0	2.4	2.4	3.2	3.0	31	2.7	6	0.8	0.1	0.16	0.02
% Dev.	3.5	4.5	4.7	1.0	0.6	0.5	2.6	7.5	5.1	14	5.3	6.7	1.0

Parameter Number	23	24	25	26	27	28	29	30	
Event No.	$\overline{A3}(<T_o)$	$A3(T_2)$	$\overline{A3}\Big\|_{T_1}^{T_3}$	$\overline{A3}\Big\|_{T_3}^{T_F}$	$\overline{A3}(>T_F)$	$\overline{A3}(\Delta T_o)$	$\overline{A4}(<T_o)$	$\overline{A4}(\Delta T_o)$	$\overline{A4}$
1	15.5	29.5	21.3	12.5	26.5	9	8.3	2.0	4.
2	19	23.0	22.5	13.0	27.2	7.5	8.8	1.8	4.
3	18.5	21.0	22.5	10.0	26.5	6.0	8.0	2.0	3.
4	20	33.0	22.8	13.0	27.5	8.0	9.0	2.0	4.
5	19	31	23.0	12.0	27.5	8.0	9.0	2.0	4.
$\bar{a}$	18.4	28.0	22.3	12.0	27.0	7.7	8.6	2.0	4.
$\bar{\Delta}$	1.2	4.3	0.5	0.9	0.44	0.8	0.38	0.04	0.
% Dev.	6.5	15.3	2.2	7.5	1.6	10.5	4.4	2.0	6.

VI
EVENTS, TAPE N8, TRACK 2
STABILITY

14	15	16	17	18	19	20	21	22	
$A2T_2$)	$\overline{A2}(<T_3)$	$\overline{A2}(<T_F)$	$\overline{F2}(<T_o)$	$\overline{F2}\Big\|_{T_o}^{T_2}$	$F2(T_2)$	$\overline{F2}\Big\|_{T_2}^{T_3}$	$\overline{F2}\Big\|_{T_3}^{T_F}$	$\Delta F2$	
16	3.5	4.0	8.26	7.43	5.5	8.8	8.15	2.4	
12	4.0	5.0	8.81	7.15	5.45	8.8	8.25	1.65	
12	3.5	4.0	8.7	7.15	5.5	9.0	7.75	1.1	
19	4.0	4.5	9.0	7.71	6.17	9.4	8.20	1.9	
11	3.5	4.5	8.7	7.43	5.8	8.8	7.71	1.2	
14	3.7	4.4	8.5	7.37	5.66	8.95	7.90	1.65	
2.8	0.12	0.32	0.3	0.18	0.24	0.18	0.25	0.4	
20	3.3	7.3	3.5	2.4	4.3	2	3.2	24	

31	32	33	34	35	36	37	38	39	40
$\Big\|_{T_1}^{T_3}$	$\overline{A4}\Big\|_{T_3}^{T_F}$	$\overline{A4}(>T_F)$	$\overline{F4}(<T_o)$	$\overline{F4}\Big\|_{T_1}^{T_3}$	$\overline{F4}\Big\|_{T_3}^{T_4}$	$\overline{F4}\Big\|_{T_4}^{T_F}$	$F4(T_1')$	$F4(T_1)$	$\overline{F4}(>T_F)$
4	3.0	18	17.3	16.5	18.0	18.0	18.6	18.0	16.5
5	3.5	19	17.0	16.6	18.1	19.8	19.4	17.8	16.7
9	3.0	19.4	17.3	16.7	18.0	20.2	20.6	17.7	16.7
5	3.3	19	17.3	17.1	18.5	20.0	20.4	17.3	16.9
0	3.5	18	16.0	16.9	18.3	20.7	20.4	16.1	16.7
2	3.3	18.6	17.0	16.8	18.2	19.7	19.9	17.4	16.7
26	0.20	0.56	0.38	0.18	0.18	0.7	0.7	0.4	0.12
2	6.1	3	2.2	1.1	1.0	3.6	3.5	2.3	0.7

the overall operation and precedes the actual start of motion.

ΔT_o - This is the duration of the silence interval. It probably represents the time required for gas flow reversal.

T_1 - Time of major peak in A4. This occurs very shortly after the end of ΔT_o.

T_1' - Marked by major peak in F4.

T_1'' - The time at which F2 passes its minimum value to move up to a plateau.

T_2 - Marks initial major peak in A2.

T_3 - Time at which plateaus in both A3 and A4 shift downward.

T_f - Marks termination of plateaus in both A2 and A3.

P_1 - Marks the time of occurrence of a small amplitude peak during ΔT_o. It is usually also seen in both A3 and A4.

P_2 - Period between peaks appearing in initial A2 plateau.

P_3 - Period of fluctuations seen in A2 during the interval $T_3 < t < T_f$.

P_4 - Period of fluctuations seen in F4 subsequent to T_f.

The other parameters have the same meanings that they did in the preceding tables in that they represent amplitude or frequency values at the times or during the intervals indicated.

(b) Track 2 Plots for F1 Lox Valve Openings

This track is recorded from a sensor that is mounted on the valve body close to Purge Port Y. The meanings of the timing symbols are the same as those used in the track 1 Table with the following exceptions:

T_1'', P_2, P_3 and P_4 are not used in connection with the track 2 analysis.

P_1 is used but with a different meaning. It is a measure of the slow fluctuations shown in A3 following T_f.

T_4 is used in track 2 analysis, but not in track 1. This marks the time at which the F4 plateau preceding T_f terminates. The value of F4 rises at this point to a somewhat higher centroid during the T_4 to T_f interval.

T_R - The time required for A4 to return to a steady state value subsequent to T_f. It appears to represent a period of recovery in the N_2 driving system.

As in the case of the track 1 table, all time marks are measured from T_o as a reference. In both tables, T_f is considered to mark the finish of the events. Figure 25 is a parametric plot of an F1 lox valve opening derived from track 2 data with most of the symbols used marked directly on the plot for identification. Wherever values are given, the figures are mean figures, not those pertaining to the particular event portrayed.

II. Discussion of F1 Lox Valve Openings as Seen on Tracks 1 and 2

Viewed as a whole, the opening event represents a parametrically definable transitional epoch between statistically stationary but distinctly different states excited by random purging noise. During the time the lox valve is closed, prior to operation of the four-way control valve, purging noise energy appears principally in A3 and A4. This is true of both tracks. A1 displays somewhat more activity in track 1 than in track 2, but its information content in either case, for the entire event, is relatively low. A2 energy is low during the interval prior to T_o for both tracks, but this trace does display significant features subsequently. The frequency of the purging noise in the A2 band prior to T_o, displayed in the F2 trace, shows random

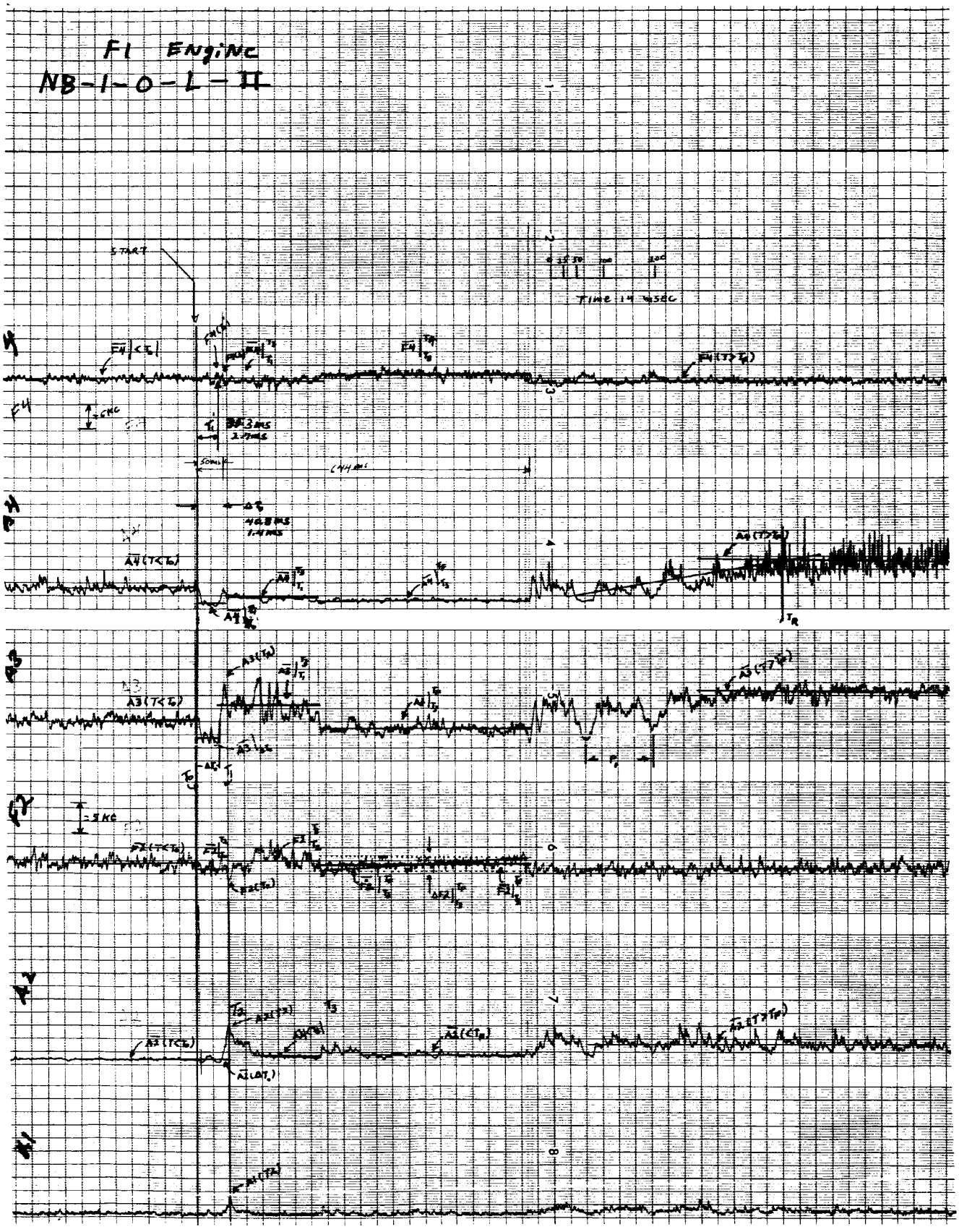

Figure 25. Parametric Plot of F-1 Lox Valve Opening Showing Parameter Identification, Tape N8, Track 2. Operation 1.

variations about a centroid value of 5.6 kc for track 1 and 8.5 kc for track 2. These values reflect the predominant resonances detected at the different sensor locations. Similar centroids are observed for F4 with means of 20.7 kc for track 1 and 17.0 kc for track 2. At T_o, when the four-way valve is actuated, the amplitudes of both A3 and A4 are seen to drop to relatively low levels which persist during the so-called "silence" period previously designated as ΔT_o. Immediately following the silence, marked peaks are observed in both A3 and A4 in addition to an abrupt frequency rise in F4 which then drops back to a lower value. It is believed that actual valve motion begins immediately after these peaks which represent a pressure buildup just prior to start motion. Note that at this point both A3 and A4 not only drop in mean value from their pre-T_o levels, but also display a very large reduction of instantaneous random excursion and assume reasonably steady plateaus. These plateaus persist until T_3 at which time each drops to a lower, fairly constant level. It is believed, on the basis of relative elapsed time, that this represents contact between the driving rod at the end of the poppet shaft and the sequence valve rocker arm. The signals continue past this point without significant change, except for a very slight rise in F4, until T_f. T_f is marked by the appearance of random excursions in A4 and A3 together with an increase of mean level. A similar pattern appears in A2. In general, these effects are more conspicuous in track 1 than in track 2. Subsequent to T_f, believed to mark the finish of valve motion, the dominant feature of the plots is the resumption of purging noise signals which are now the only source of excitation.

III. Purging Noise Characteristics Before and After F1 Valve Opening Event

The main differences among these purging noise patterns before and after the valve opening operation (recall that flow reversal takes place) as they appear in track 1 and track 2, are:

A1 - Track 1 shows relatively large random excursions throughout total event and appears to possess little information value. Track 2 displays random perturbations of markedly lower amplitude, and also contributes little information to signature recognition.

A2 - Tracks 1 and 2 are very similar with respect to this parameter. The pre-T_o purging noise signal is very low for both tracks, being slightly higher for track 2. The post-T_f signals are considerably larger for both tracks, showing relatively high amplitude perturbations containing long period components.

A3 - The pre-T_o patterns for both tracks display considerable random activity with the mean value for track 2 appreciably greater than that of track 1 (18.4 as compared with 7.7). The post-T_f patterns again show the characteristic random perturbations, but the mean levels are rather different. The track 2 level rose to 27.5 and the track 1 level fell slightly to a mean of 6.4.

A4 - The pre-T_o traces for both tracks show the expected random activity as do the post-T_f patterns. The pre-T_o perturbations are rather greater for track 1 than for track 2 as is also the mean value (13.6 against 8.6). The post-T_f A4 trace for track 1 resumes its random character with rather smaller excursion

amplitude than for the pre-T_o period with a very slightly lower mean value (12). On the other hand, the post-T_f perturbations for track 2 are greater than those for the pre-T_o period and the mean level climbs relatively slowly before reaching a final steady state average which is appreciably higher (20.7) than as was during the pre-T_o period. The time required for the steady state average level to be reached is comparable with the valve operation time - about 553 milliseconds after T_f.

F2 - Prior to T_o both the track 1 and track 2 traces display some degree of random variation of relatively small amplitude about mean centroids of 5.6 kc for track 1 and 8.5 kc for track 2. Subsequent to T_f, the F2 centroids on tracks 1 and 2 respectively become 6.2 kc and 7.7 kc. These shifts in F2 purging noise centroid values are sufficient to easily classify the valve as being either opened or closed.

F4 - The pre-T_o F4 traces are very similar to those for F2 but with the mean track 1 centroid at 20.7 kc and the track 2 mean at 17.0 kc. Subsequent to T_f, the track 1 centroid becomes 22.1 kc and the track 2 centroid is 16.7 kc. As was true for the F2 purging noise traces, the pre- and post-event F4 frequency levels indicate the F1 lox valve state (open or closed). This is particularly true for the track 1 signal in which the difference between the levels is well marked.

IV. F1 Lox Valve Closing Event

Spectrograms of F1 lox valve closings Nos. 4 and 5 as derived from track 1 data are displayed in Figure 26 and from track 2 data in Figure 27. Parametric plots of the same events (closings 4 and 5) are shown in Figure 28 for track 1 data and in Figure 29 for track 2 data.

As was true for the opening event, it is equally clear for the closing that the purging noise in no way impaired the clarity of the sonic operating signatures. This is evident on even cursory inspection of the spectrograms and even more so on examination of the parametric plots. The importance of this cannot be over estimated because it means that event timing can be determined with great precision and that signature features can readily be distinguished, thus providing a firm basis for accurate identification of normal valve function and reliable detection of malfunction.

The closing parametric plots were recorded in the same way as the opening plots and same time calibration applies to them. That is, each millimeter = 6.24 milliseconds. The sensor locations corresponding to track 1 and track 2 were also the same. The parametric data for the closing events is displayed in Table VII for track 1 and in Table VIII for track 2. The meanings of the A1, A2, F2, A3, A4 and F4 parameters are the same as those identified in connection with the opening event. Definitions of time indications follow:

E4061

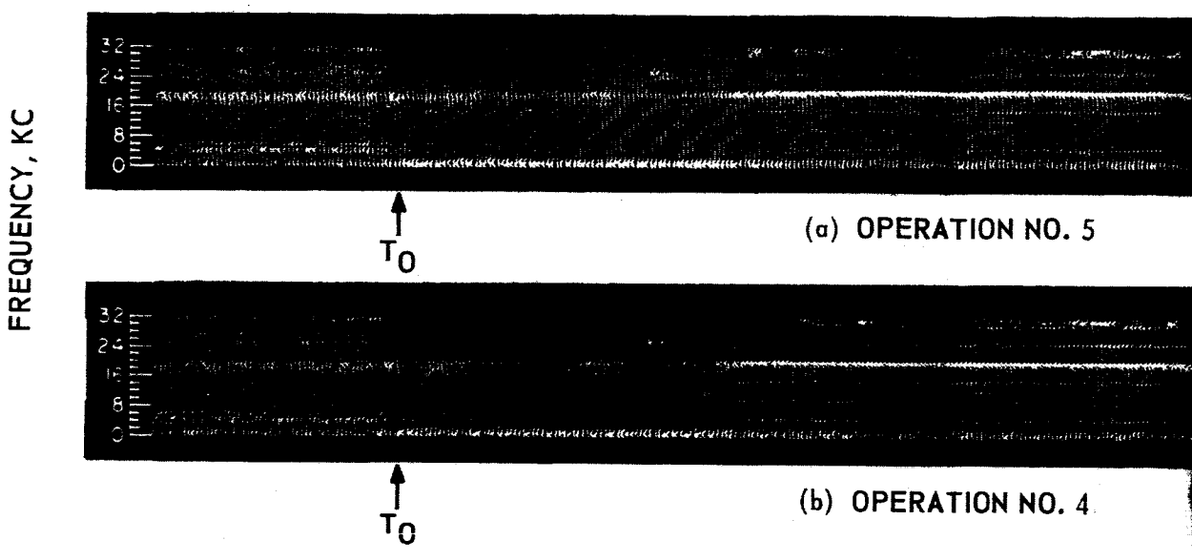
FREQUENCY, KC
32
24
16
8
0
T_O
(a) OPERATION NO. 5
32
24
16
8
0
T_O
(b) OPERATION NO. 4

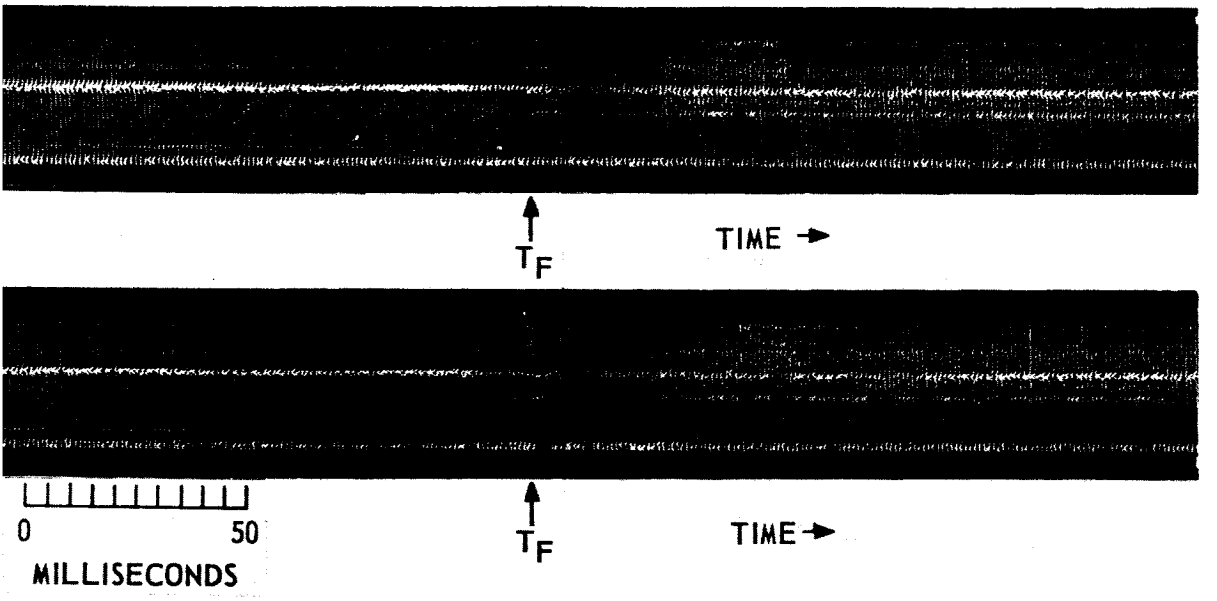

Figure 26. Spectrograms of Two F-1 Lox Valve Closings, Tape N8, Track 1. Operations 4 and 5.

E4063

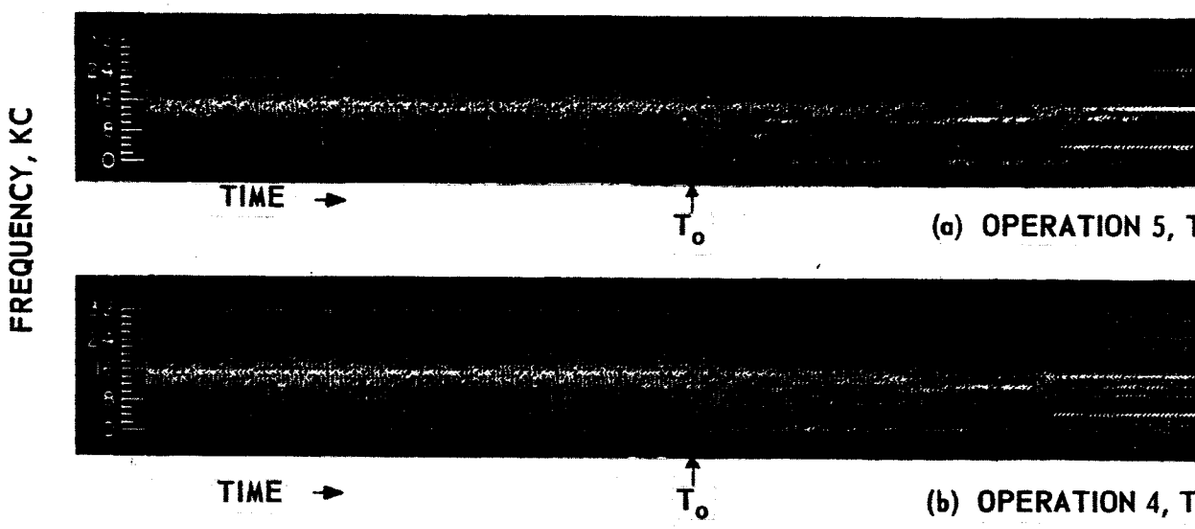

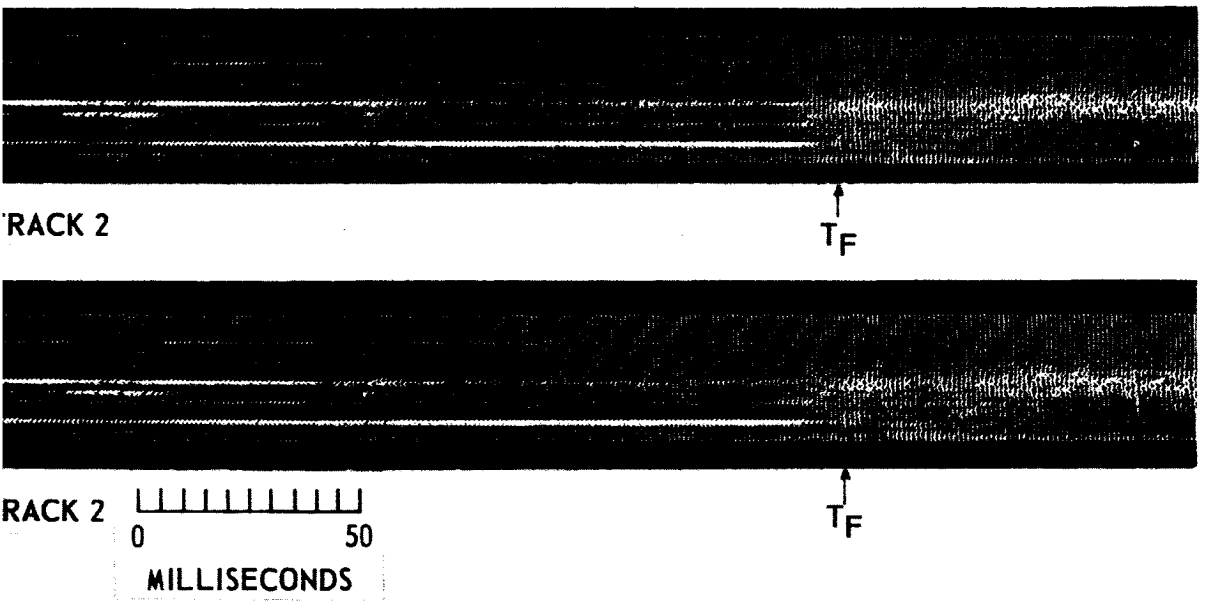

Figure 27. Spectrograms of Two F-1 Lox Valve Closings, Tape N8, Track 2. Operations 4 and 5.

E4074

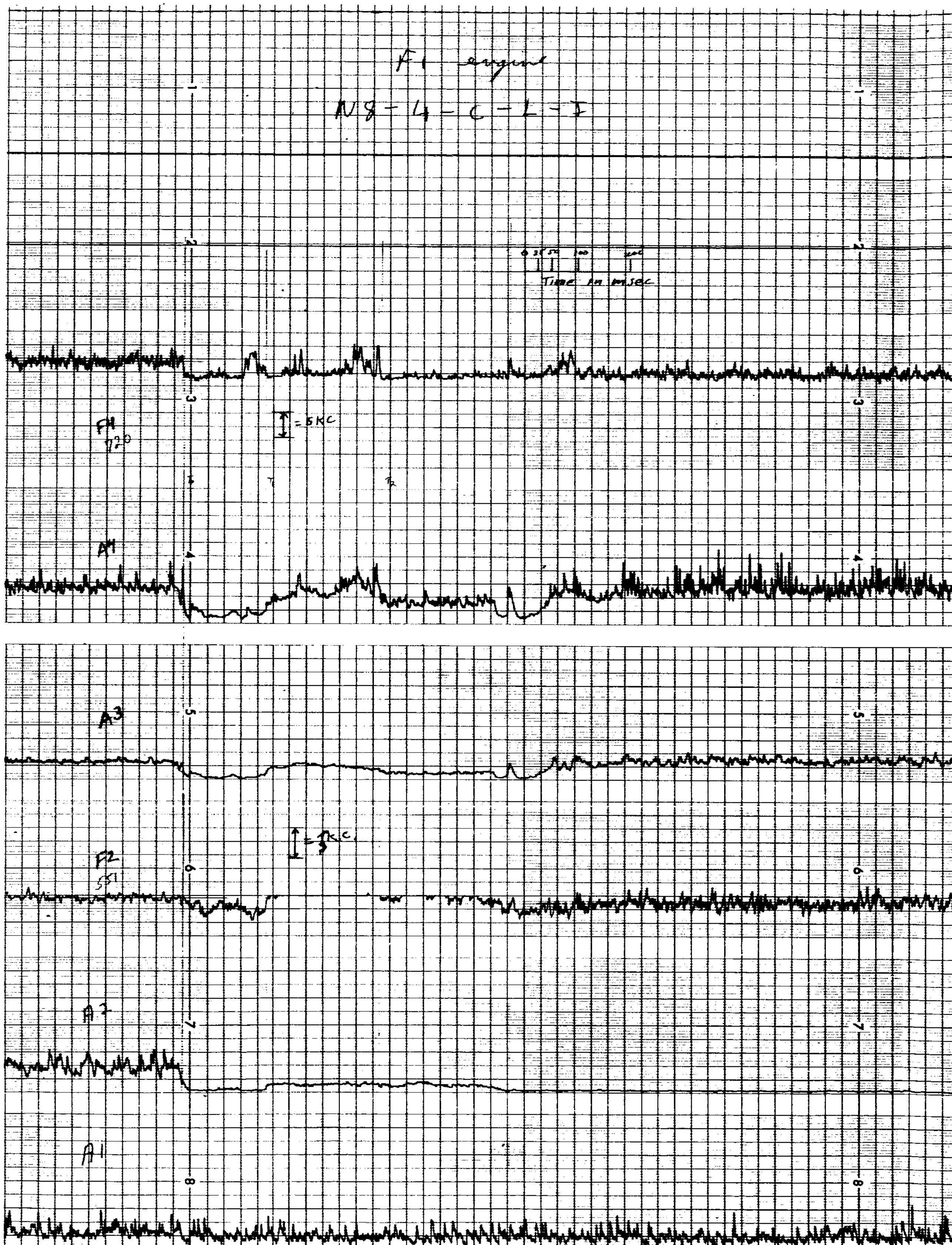

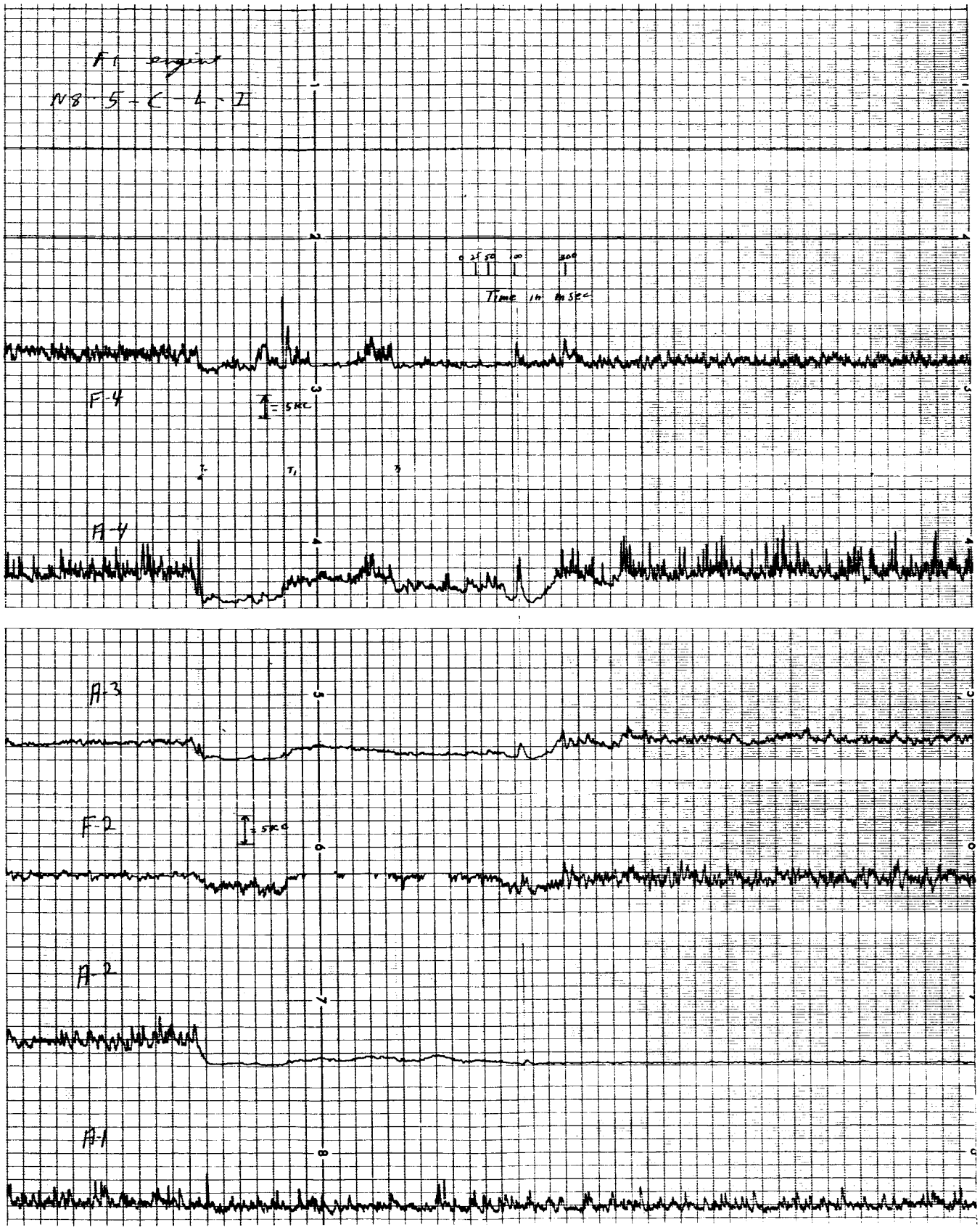

Figure 28, Parametric Plots of Two Typical F-1 Lox Valve Closings, Tape N8, Track 1. Operations 4 and 5.

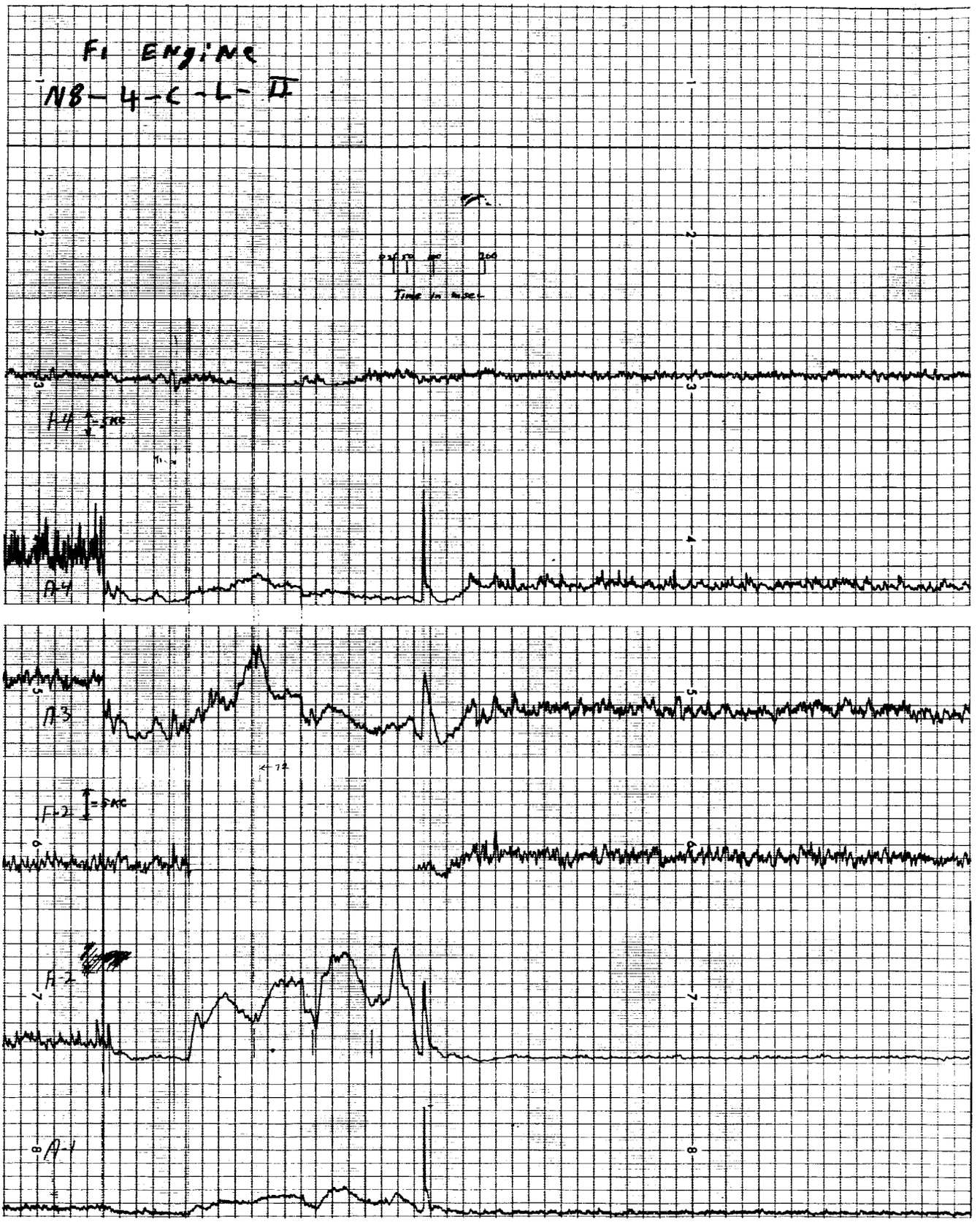
F1 ENGINE
NB-4-C-L-II
Time in msec
A-4
A-3
F-2
A-2
A-1

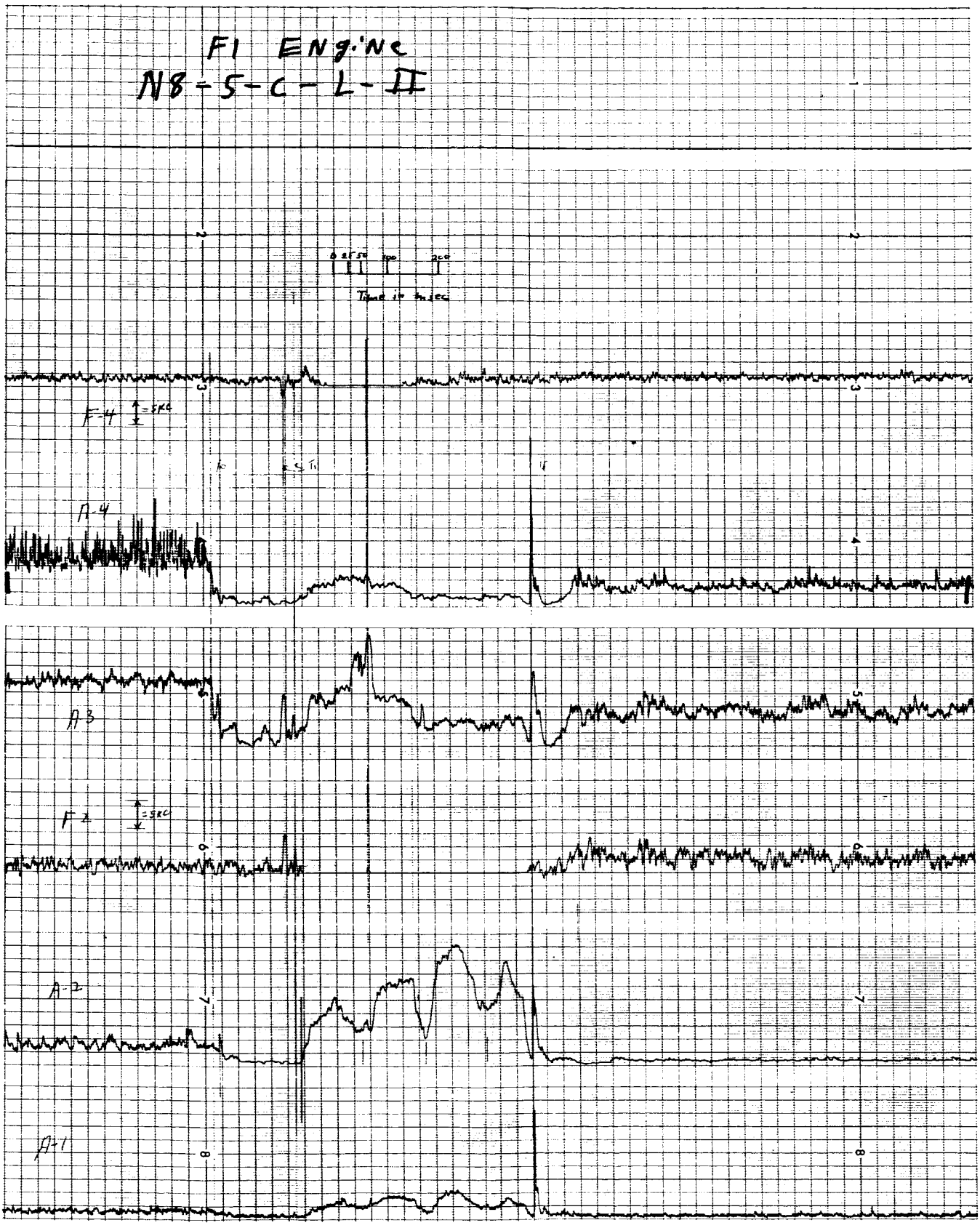

Figure 29. Parametric Plots of Two Typical F-1 Lox Valve Closings, Tape N8, Track 2. Operations 4 and 5.

F1 ENGINE LOX VALVE
PARA

Parameter Number	1	2	3	4	5	6	7	8	9	1
Event No.	T_1	T_2	T_F	P_F	$\overline{A2}(<T_o)$	$\overline{A2}\Big\|_{T_o}^{T_1}$	$\overline{A2}\Big\|_{T_1}^{T_F}$	$\overline{A2}(>T_F)$	$\overline{F2}(<T_o)$	$\overline{F2}$
1 *	144	306	731	N	10	1.5	1.5	1.0	6.34	5.1
2	174	381	628	93.7	10	1.0	3.5	1.0	6.2	4.4
3	172	364	610	106	10	1.0	3.0	1.0	6.16	4.4
4	155	365	608	97.2	9.5	1.0	3.0	1.0	6.16	4.4
5	164	369	612	100	10	1.0	2.5	1.0	6.12	4.7
$\bar{z}$	164	370	613	99	9.9	1.0	3.0	1.0	6.2	4.5
$\bar{\Delta}$	7	6	6	4.3	0.2	0	0.25	0	0.08	0.1
% Dev.	4.3	1.9	1.1	4.4	2	0	8.3	0	1.3	2.9

Parameter Number	19	20	21	22	23	24	25	26
Event No.	$\overline{A4}(<T_o)$	$\overline{A4}\Big\|_{T_o}^{T_1}$	$\overline{A4}\Big\|_{T_1}^{T_2}$	$\overline{A4}\Big\|_{T_2}^{T_F}$	$\overline{A4}(>T_F)$	$\frac{A4}{\overline{A4}}(T_o)$	$\frac{A4}{\overline{A4}}(T_F)$	$\overline{F4}(<$
1 *	14	4.5	8.0	6.5	14	4	1.7	22.2
2	13	3.2	13.0	8.0	14	4	6.0	22.3
3	13	3.5	13.0	8.0	15	3.0	4.0	22.3
4	13.5	3.5	13.0	8.0	14	3.5	5.0	22.5
5	13.5	3.5	12.0	8.0	13	3.2	7.6	22.3
$\bar{z}$	13.25	3.4	12.75	8.0	14	3.4	5.7	22.3
$\bar{\Delta}$	0.25	0.13	0.4	0	0.5	0.3	1.2	0.1
% Dev.	1.9	3.8	3.1	0	3.6	8.9	21	0.5

* This event differed significantly from all of the others analyzed. Hence, it is not included in determining $\bar{z}$ and $\bar{\Delta}$.

TABLE VII
LOSING EVENTS, TAPE N8, TRACK 1
IETRIC STABILITY

)	11	12	13	14	15	16	17	18	
T_1 T_o	$\overline{F2}\Big\|_{T_1}^{T_F}$	$\overline{F2}(>T_F)$	$\overline{A3}(<T_o)$	$\overline{A3}\Big\|_{T_o}^{T_1}$	$\overline{A3}\Big\|_{T_1}^{T_2}$	$\overline{A3}\Big\|_{T_2}^{T_F}$	$\overline{A3}(>T_F)$	$\frac{A3}{\overline{A3}}(T_o)$	
	6.1	5.5	6.5	2.0	4.0	2.0	7.0	3	
	6.62‡	5.7	7.0	1.0	4.0	2.5	7.0	3	
	6.62‡	5.5	6.5	1.0	5.0	2.5	7.0	2.5	
	6.62‡	5.5	7.5	1.0	4.5	2.5	7.5	2.6	
	6.62‡	5.7	7.0	1.0	4.0	2.0	7.5	3.2	
	6.62	5.6	7.1	1.0	4.4	2.4	7.25	2.8	
3	0	0.1	0.3	0	0.4	0.2	0.25	0.3	
	0	1.8	4.2	0	9.0	8.4	3.4	10.7	

	27	28	29	30	31	32	33	
$_o$)	$\overline{F4}\Big\|_{T_o}^{T_1}$	$\overline{F4}\Big\|_{T_1}^{T_2}$	$\overline{F4}\Big\|_{T_2}^{T_F}$	$F4(T_1)$	$F4(T_2)$	$F4(T_F)$	$\overline{F4}(>T_F)$	
	19.4	18.0	19.8	24.5	24.5	24.5	20.7	
	19.4	20.2	19.4	25.9	25.2	24.0	20.7	
	19.4	19.8	19.4	26.6	28.0	24.4	20.3	
	19.4	19.8	19.4	25.2	26.0	24.4	20.2	
	19.6	19.6	19.6	19.3	24.5	24.6	20.6	
	19.4	19.9	19.4	24.3	25.9	24.5	20.4	
	0.05	0.25	0.05	2.5	1.1	0.1	0.2	
	0.25	1.3	0.25	9.9	4.3	0.4	1.0	

‡ This event was monochromatic.

TABLE VII
F1 ENGINE LOX VALVE CLOSIN
PARAMETRIC ST

Parameter Number	1	2	3	4	5	6	7	8	9	10
Event No.	T_1	T_1'	T_2	T_3	T_F	ΔT_o	P_1	P_2	P_F	$A1(T_F)$
1	N	N	N	461	732	47	N	N		47
2	138/159	169	294	380	611	11	115	162	100	44
3	162	175	300	381	612	13	112	138	94	38
4	136	163	294	376	611	11	116	113	88	42
5	138/159	167	298	381	611	11	118	144	88	42
$\bar{x}$	157	169	297	380	611	11.5	115	142	93	41.5
$\bar{\Delta}$	7.3	3.5	2.8	4.5	0.25	0.75	1.75	14	4.5	2.0
% Dev.	4.6	2.1	0.9	1.2	0.04	6.5	1.5	9.9	4.8	4.8

Parameter Number	20	21	22	23	24	25	26	
Event No.	$\overline{A3}(<T_o)$	$\overline{A3}\Big\|_{T_o}^{T_1}$	$\overline{A3}\Big\|_{T_3}^{T_F}$	$A3(T_2)$	$A3(T_F)$	$\overline{A3}(>T_F)$	$\overline{A4}(<T_o)$	$\overline{A}$
1	29.0	13.5	12.5	N	31	18.5	20	4
2	28.8	11.0	14.5	50	33.5	17.8	20	3
3	29.0	11.5	13.0	46	33	17.5	19	2
4	29.2	11.5	13.0	42	32.5	18.5	19	2
5	29.2	11.0	14.0	47	33.8	18.5	20	2
$\bar{x}$	29.1	11.25	13.6	46	33.2	18.1	19.5	2
$\bar{\Delta}$	0.125	0.25	0.6	2.25	0.43	0.43	0.5	0
% Dev.	0.43	2.3	4.4	4.9	1.3	2.4	2.6	6

;S, TAPE N8, TRACK 2
.BILITY

11	12	13	14	15	16	17	18	19
$\overline{A2}(<T_o)$	$\overline{A2}\Big\|_{T_o}^{T_1}$	$\overline{A2}\Big\|_{T_1}^{T_F}$	$A2(T_F)$	$\overline{F2}(<T_o)$	$\overline{F2}\Big\|_{T_o}^{T_1}$	$\overline{F2}\Big\|_{T_1}^{T_F}$	$\overline{F2}(>T_F)$	$F2(T_1)$
8.5	4.0	3.0	23.5	7.8	8.9	7.8	8.8	N
8.0	2.4	23	27.0	7.8	7.6	6.62	9.1	13.8
8.3	2.8	26.5	30.0	7.8	7.7	6.62	8.9	13.8
8.0	2.5	25	31.0	7.7	7.7	6.62	9.0	11.0
7.5	2.4	26	30.8	7.7	7.7	6.62	8.8	12.9
8.0	2.5	25	29.8	7.75	7.7	6.62	9.0	12.9
0.2	0.13	1.25	1.3	0.06	0.04	0	0.43	0.9
2.5	5.0	5.0	4.3	0.8	0.5	0	4.7	7.0

27	28	29	30	31	32	33	34	35	36	37
$\Big\|_{T_o}^{T_1}$	$\overline{A4}\Big\|_{T_1}^{T_3}$	$\overline{A4}\Big\|_{T_3}^{T_F}$	$A4(T_F)$	$\overline{A4}(>T_F)$	$F4(<T_o)$	$\overline{F4}\Big\|_{T_o}^{T_1}$	$\overline{F4}(P_2)$	$\overline{F4}\Big\|_{T_3}^{T_F}$	$F4(T_1)$	$F4(>T_F)$
0	5.0	4.0	46	8.0	16.5	15.9	16.8	16.8	N.	16.9
0	9.0	3.5	45	7.5	16.5	15.9	14.7	16.0	12.6/13.1	16.8
5	7.5	3.5	46	8.0	16.5	15.9	14.7	16.5	14.2	16.9
5	7.0	3.5	44	8.0	16.5	15.8	14.7	16.8	13	17.1
5	8.0	3.5	43	8.0	16.4	15.9	14.7	16.4	12.3/13.8	16.8
6	7.9	3.5	44.5	7.9	16.5	15.9	14.7	16.5	13.5	16.9
18	0.6	0	1.1	0.18	0.025	0.03	0	0.43	0.48	0.08
7	7.6	0	2.5	2.2	0.15	0.2	0	2.6	3.5	0.45

2

(A) Track 1 Plots for F1 Lox Valve Closing

T_o - Standard time reference from which all intervals were measured. T_o is marked by various prominent indications which include: (a) a distinct drop in the F4 frequency from a mean of 21 kc to a mean of 19 kc; (b) a sharp drop in the A4 level. This drop is momentarily interrupted by an abrupt, steep peak which coincides with the F4 drop and then continues; (c) a drop in the A3 level also interrupted by a brief peak. This peak is coincident with the A4 peak, but is far less conspicuous; (d) a drop in the F2 level from a mean of 6.15 kc to 4.5 kc; (c) a marked drop in the A2 level accompanied by considerable subsequent smoothing of the random character of the track prior to T_o which reflects the presence of purging noise up to that time.

T_1 - This is marked by a sudden increase in the A4 amplitude and also by a simultaneous rise in the A3 amplitude. The A2 amplitude increases somewhat as well. The most dramatic signature marked by T_1 is an increase in $\overline{F2}$ from a mean of 4.5 kc to one of 6.62 kc. In all operations, except No. 1, F2 becomes virtually monochromatic at 6.62 kc and the significance of this will be discussed subsequently. In some, but not all operations, T_1 is also marked by a peak in F4 (this peak does not appear in operations 4 and 5).

T_2 - This marks the initiation of a period of change in the track 1 closing signatures of most traces. It is slightly preceded

by peaks in both A4 and F4 and followed by a distinct lowering of the level of each.

T_f - Except in the case of the first closing, T_f is marked by distinct peaks which occur simultaneously in F4, A4 and A3. Of these, the A4 peak is the most conspicuous. In the first closing, the A4 peak does not occur while the simultaneous peaks were observed in F4 and A3.

P_f - This is a period of relative"silence" following T_f and is well marked in A4 and A3.

(B) Track 2 Plots for F1 Lox Valve Closing

Many of the symbols employed for the track 2 plots are the same as for the track 1 plots, but in some instances the signatures which mark them differ. Because of this, all of them are defined below.

T_o - Zero time reference. It is marked by sudden intensity drops in A3 and A4 and by a slightly delayed drop in A2.

ΔT_o - Delay time of intensity drop in A2.

T_1' - This is marked by the onset of a sudden increase of A2 and the beginning of rapid perturbations, of low amplitude, in A4. T_1' is followed very shortly by a steady tone in F2 which becomes virtually monochromatic at a mean frequency of 6.62 kc. T_1' is believed to correspond to T_1 in the track 1 plots of the F1 lox valve closing event. The monochromaticity of F2 is interrupted by a small upward perturbation which occurs about the end of the first third of its duration.

T_2 - This is marked by a well defined maximum in A3 and the previously mentioned F2 perturbation which is simultaneous with it.

T_3 - This marks the onset of an amplitude plateau in both A3 and A4. It also indicates the termination of a monochromatic tone in F4 which had begun between T_1 and T_2.

T_f - Characterized by sharp, major peaks in all amplitude parameters.

P_1 - This is the period of a major, low frequency oscillation occurring in A2 during the interval from T_1 to T_f.

P_2 - The period of the monochromatic tone in F4 which begins after T_1 and ends at T_3.

P_f - This has the same meaning that it did for track 1. Subsequent to P_f stabilization of the purging noise levels is established.

Note: The features described above apply to all F1 valve closing operations except the first. The first F1 closing operation departed markedly from the remainder and is considered separately in the discussion that follows. Because it departed so radically, its behavior was not used in the estimates on feature dispersions.

V. Discussion of F1 Lox Valve Closings as Seen on Tracks 1 and 2.

Like the analysis of the opening event, the closing analysis was based on five operations. Study of the parametric plots indicates quite clearly that the first operation was rather different from the other four closings whose parametric patterns were in very good agreement among themselves. The first closing operation, (operation No. 1), differed in two

respects from the subsequent operations of the same valve. First, the operation time was distinctly longer. It was, in fact, more than 100 milliseconds in excess of the 613 millisecond mean operation time of the other closings. Second, many distinctive features which characterize F1 lox valve closings Nos. 2 through 5 do not appear in the parametric plot of operation 1. Among the missing signature details are the major peak in A3 at T_o, the monochromatic tones in F4 and F2 and the long period oscillations in A2 between T_1 and T_f. For these reasons, the first closing was judged to be "atypical" and the data derived from it was not used in computing the parametric mean values which are listed in Tables VII and VIII. The parametric plot of this atypical closing, as derived from track 2 data, is shown in Figure 30. If it is compared with the plots of two typical closings derived from the same data (see Figure 29), the abnormal character of the first closing signature becomes quite obvious.

For help in identifying the parameters employed in this analysis, a plot of closing operation No. 2 (a typical closing) is displayed in Figure 31 with most of the parameters marked on the display for convenient reference. Note that the figures which appear in association with each parameter, indicating the mean value and the mean deviation, are means for four events.

In a broad sense, the closing event is categorically similar to the opening in that it represents a parametrically definable interval between two different states of random purging noise. During the time the lox valve is in the open condition, prior to T_o, the purging noise pattern as reflected in the various parametric traces very closely resembles the signatures seen in the opening parametric plots subsequent to T_f. This is to be expected because

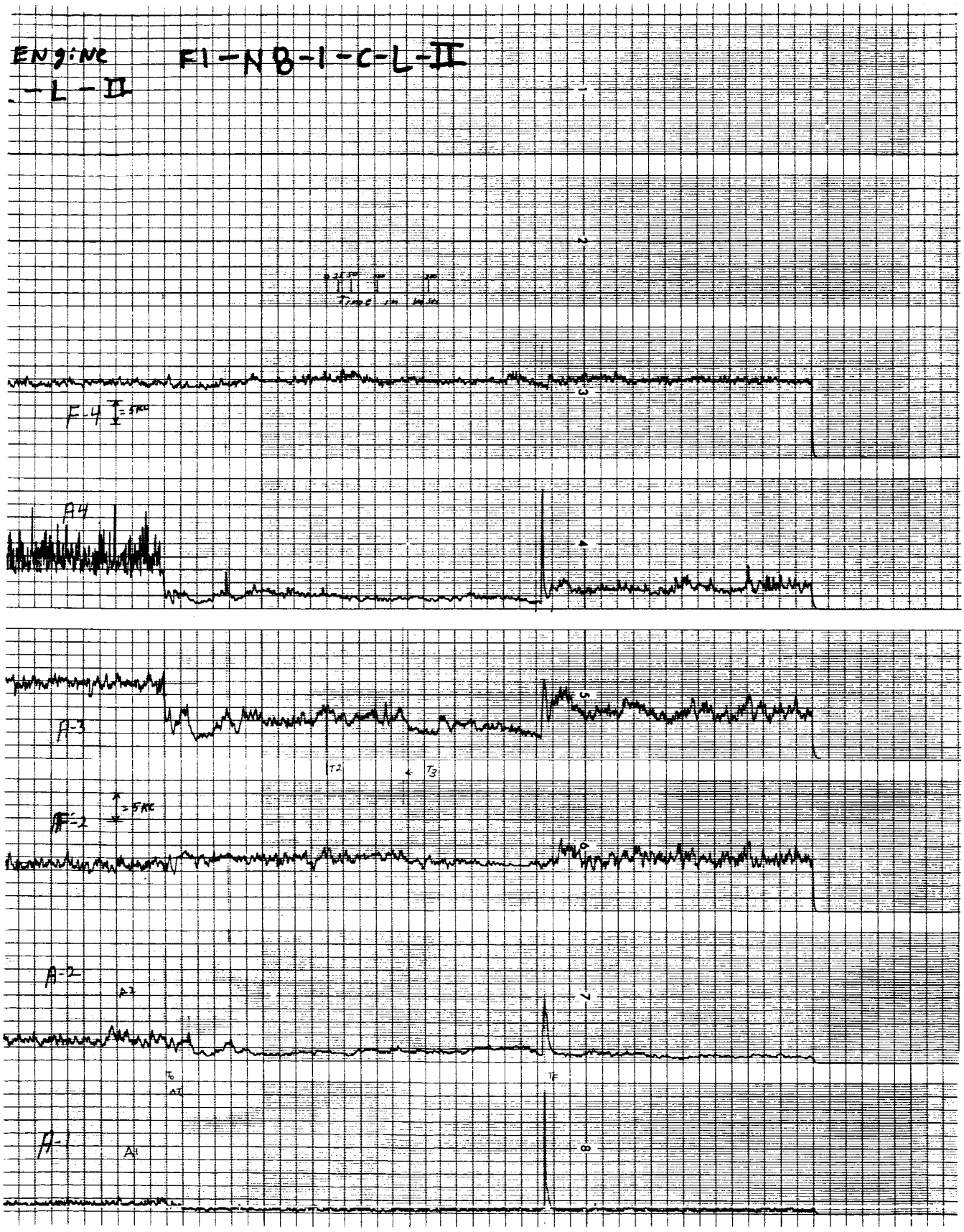

Figure 30. Parametric Plot of F-1 Lox Valve Atypical Closing, Tape N8, Track 2, Operation 1.

Figure 31. Parametric Plot of F-1 Lox Valve Closing Showing Parameter Identification, Tape N8, Track 2. Operation 2.

the gas, up to the time T_o for the closing operation is still flowing through the same port in the same direction. The relatively high level of the A2 trace associated with random perturbations of significant amplitude which persists prior to closing T_o appears in both the track 1 and track 2 derived plots and is characteristic of the open state. This is true even for event 1 which is atypical in other respects, as noted above. Details of the differences between the pre-T_o and post-T_f purging patterns will be described later. However, the point is made here that the A2 trace, even in the absence of other data, would provide an absolute indication of the valve state as would either $\overline{F2}$ or $\overline{F4}$. Other general features of the pre-T_o purging noise pattern are the essentially sustained levels of the A3 and A4 amplitudes as well as the fairly steady centroids displayed by F2 and F4. Fluctuations about these values, particularly in the cases of F2, A3 and A4 are more pronounced in the track 2 plots. The track 1 pre-T_o F2 centroid has a mean value of 6.2 kc while the track 2 F2 centroid has a mean of 7.75 kc reflecting the different resonances predominating at the different sensor locations. Note that these centroids are the same as those measured for the post-T_f values in connection with the opening event on the respective tracks. The pre-T_o F4 centroids have means of 24.3 kc for track 1 and 16.5 kc for track 2. Note that, unlike the case of pre-T_o F2 centroid, the higher frequency centroid value is associated with track 1. For track 1 the pre-T_o F4 closing centroid is close to the mean determined for the post-T_f opening value, the difference being about 200 cps. The track 2 F4 post-T_f opening and pre-T_o closing centroids are in equally good agreement (within about 200 cps).

As in the case of the opening events, T_o is believed to correspond to the time of actuation of the four-way reversing valve. At this point, the purging noise level drops in A2, A3 and A4 and these traces display conspicuously low amplitudes until T_1. In essence, the T_o to T_1 interval corresponds to the period called "silence" in connection with the analysis of the opening event. During the reversal period the excitation level of the system is low. Aside from the drop in amplitude of A2, A3 and A4, the traces become substantially smooth as the perturbations characterizing the purging noise either drop to a much lower frequency (for example, A3, track 2) or virtually disappear (for example, A2, track 1).

At the time T_1 the entire pattern changes in a manner to be described and it is virtually certain that T_1 marks the point at which gas has started to flow through actuator Port C and physical motion of the valve begins. One outstanding feature of the signature change is an energy increase in all amplitude bands (of both tracks) with the exception of A1 derived from track 1 data. The increase appears far more dramatically in the track 2 plots but is just as distinct, except for magnitude, in the track 1 plots. In particular, the A4 level in both plots rises with somewhat higher perturbations appearing in the track 1 trace. In the track 1 signature, A3 and A2 both show small increases, but in the track 2 plots A3 climbs quite rapidly to a maximum (at T_2) with rather violent excursions on the way. These excursions are of high amplitude, but relatively short period. A2 (track 2), of all the amplitude parameters, demonstrates the most remarkable behavior. The average level of the trace climbs, somewhat more slowly than that of A3.

But during the entire period from T_1 to T_f it exhibits extremely large amplitude oscillations of quite long period whose mean is 115 milliseconds. The other outstanding feature of the closing event signature following T_1 is the nearly perfect monochromatic line traced by F2. In track 2, F4 also displays a brief period of chromaticity (from T_2 to T_3), but the F2 trace is far more dramatic in that it persists during the entire interval of valve motion. In both tracks the frequency of this F2 tone (it is in fact a nearly steady state pure sinewave signal) is 6.62 kc. It was suspected that this signature corresponded to a longitudinal mechanical resonance and the length of the vibrating member was computed on the assumption of a half wavelength dominant mode. In this case,

$$L = \lambda/2$$

where L = the mechanical length and λ = the wavelength of resonance. Then,

$$L = c/2f$$

in which c = the velocity of propagation of sonic vibration in steel and f = frequency. The value of c is 5790 meters/second and, of course, f is known to be 6.62 kc. On inserting these values into the expression for length, one obtains the figure of 0.438 meters, or 17 inches. This turns out to be the length of the poppet valve shaft or stem. There seems little doubt that the signature corresponds to the so-called "slip-stick" friction with the intervals of maximum friction "grab" corresponding to the periods of A2 amplitude oscillation. During this same period there is a corresponding

oscillation in the A1 trace which is essentially in phase with that of A2 but of considerably lower amplitude. In the track 2 plots the F4 trace shows a well marked interval of monochromaticity. This falls wholly within the time range of the F2 monochromatic tone, but its frequency (14.7 kc) is somewhat too high to represent its second harmonic.

T_3 may possibly represent the time of disengagement of the pushrod at the end of the poppet shaft from the sequence port rocker arm. This is suggested by elapsed time considerations, but is not regarded as established. The significance of T_3, as a parametric indicator, is the termination of monochromaticity in F4 trace and the rather marked decline in A3 and A4 amplitude levels in track 2. T_f is believed to represent the finish of the F1 lox valve closing event and is characterized by major amplitude peaks in A1, A2, A3 and A4 as derived from track 1. This is true of all operations, including event No. 1 which has already been mentioned as atypical in other respects. The abrupt increase of energy in these traces seems to reflect the occurrence of valve seating. T_f can also be identified on the track 1 plots, but the indications are less conspicuous. With the exception of event No. 1, there are significant peaks in A3 and A4 and, including event No. 1, a distinct frequency peak in F4. A1, A2 and F2 do not display reliable indicators for T_f in any of the five events studied.

Subsequent to T_f, the closing parametric events are characterized by dips in the A3 and A4 levels, after which purging noise signals are resumed. The interval between T_f and stabilization of purging noise signatures is designated as P_f in the tables. It is of the order of 100 milliseconds.

VI. Purging Noise Characteristics Before and After F1 Valve Closing Event

As was done for the opening event, the differences among the purging noise patterns before and after the closings will now be discussed in terms of the different parameters with specific reference to the tracks from which they were derived. Again, it should be recalled that purging noise signals prior to closing - i.e., during the open state of the valve are results of the same excitation, both in terms of direction of gas flow and site of entry (actuator port) as existed subsequent to T_f for the opening events. And, of course, for the purging noise signals after closing, the excitation is the same as that which existed prior to T_o for the opening events.

A1 - Track 1 shows the same relatively large random excursions which were noted in connection with the opening events and these persist, incidentally, throughout the operation itself. The statement, made in the course of discussion of opening event purging noise signals, that the A1 trace derived from track 1 possesses little if any information, is sustained. Track 2 displays smaller amplitude perturbations both before and after the event and appreciable information during it. The post-event level is somewhat lower than the pre-event level.

A2 - As was true for the opening, track 1 and track 2 A2 data were very similar. The pre-event purging A2 signal displayed relatively large perturbations of random amplitude and period, while the trace subsequent to closing showed little activity. It tended to be essentially smooth and featureless and of quite

low amplitude. This is the reverse of the pattern observed for the opening event A2 purging noise signals. It will be recalled that these A2 purging noise patterns had been cited as diagnostically indicative of the valve state (open or closed) in themselves.

A3 - The pre-T_o A3 traces display considerable random activity for both tracks. The track 1 mean level, however, is markedly lower than the track 2 level and the perturbation amplitudes for track 2 are rather larger. The pre-T_o track 1 mean was only 7.1 while the track 2 mean was 29.1. Subsequent to T_f, the track 1 A3 signature differed only slightly from its pre-T_o pattern. The mean amplitude rose very slightly to 7.25 and the perturbations were somewhat more pronounced. On the other hand, the track 2 signature fell substantially to a mean level of 18.1 with, however, no significant change of perturbation amplitude. These figures are in substantial agreement for the A3 purging signal patterns observed for the opening events. For example, the opening pre-T_o mean level was 18.4 (compare with 18.1 above) and the opening post-T_f mean level was 6.4 (compare with 7.25 above).

A4 - The track 1 A4 trace displays the usual random pattern both before T_o and after T_f. The post-T_f excursions are somewhat larger and the mean level rises very slightly, being 13.25 before the closing event and 14 afterwards. This change is not

a significant one. However, the case of the track 2 A4 pattern is in marked contrast. Here, the pre-T_o random excursions are extremely large and relatively dense. The post-T_f perturbations are considerably smaller, having about one-half the amplitude of those characterizing the pre-T_o epoch. In addition, the axis crossing density is far less. These waveform differences are quite striking at a glance. Beyond the dramatic change in signal pattern, there is also a distinct shift of mean amplitude level. The pre-T_o A4 trace level has a mean value of 19.5 (with a percentage deviation of 2.6%). Following the closing operation, the post-T_f A4 level stabilizes at a mean value of only 7.9 (percentage deviation of 2.2%). If one now compares these levels with those measured for the opening event (still from track 2 data), one finds that the pre-T_o (for the opening) value has a mean of 8.6 and that the post T_f mean value is 18.6. Note that these levels are essentially consistent with the closing post-T_f and closing pre-T_o mean values respectively. One can quite confidently conclude, therefore, that as was true for the A2 trace, the A4 track 2 derived purging noise signal is a reliable indicator of the valve state (open or closed).

F2 - The F1 lox valve track 1 purging noise pattern for F2, prior to T_o, displays a relatively small, irregular frequency deviation about a fairly steady centroid whose mean value is 6.2 kc

and is quite consistent from closing to closing with a percentage deviation of only 1.3%. Subsequent to T_f the pattern is very similar except that the deviations are slightly greater and there is a small, but distinct drop in the frequency centroid to 5.6 kc (percentage deviation of 1.8%). In the case of the track 2 derived F2 trace, the signal also displays definite centroids before and after the closing event. The random deviations, however, are essentially more alike than in the track 1 data, but the difference between the centroids is appreciably greater, with the higher centroid following, rather than preceding the closing. The mean pre-T_o centroid frequency is 7.75 kc (with a percentage deviation of 0.8%) while the value of the post-T_f centroid is 9.0 kc (with a percentage deviation of 4.7%). The centroid levels for both tracks, before and after closing, agree closely with the values obtained after and before opening.

F4 - The pre-T_o and post-T_f F4 traces are, for a given track, quite similar. Definite centroids are exhibited as for F2 but, for each track, the pre-and post-event frequency deviations are far more alike, with the track 1 deviation amplitudes rather larger than those appearing in the track 2 derived F4 traces. Changes in the F4 purging noise centroids before and after the event do show differences, but these are small for each track, with the track 2 difference the lesser of the two. The pre-T_o

centroid for track 1 is 22.3 kc (percentage deviation of 0.5%) and the post-T_f centroid mean for the same track is 20.4 kc with a percentage deviation of 1.0%. In the case of the track 2 derived F4 trace, the pre-T_o centroid mean is 16.5 kc (percentage deviation of 0.15%) and the post-T_f mean is barely larger with a value of 16.9 kc (percentage deviation of 0.45%). Again, as for the other parametric traces, these values are in good agreement with the purging noise levels observed in connection with the F1 lox valve opening events. For example, in the case of the opening the pre-T_o centroid mean frequency is 20.7 kc (compared with 20.4 for the closing post-T_f value) and the post-T_f centroid mean is 22.1 kc (compared with 22.3 for the closing pre-T_o value).

VII. F1 Lox Valve Feature Timing Analysis

Having discussed some of the more significant features of the F1 lox valve opening and closing event parametric features in terms of trace patterns, we now consider the same events with respect to operation timing. It will be recalled that T_o - in the case of both the openings and the closings - was believed to mark the initiation of operation of the four way valve. This was seen parametrically as the beginning of a period of relatively low energy in the amplitude traces. This period, for the opening event, had a mean duration of 39.2 milliseconds (with a mean deviation of 4.1%) as measured on the track 1 plots and 40.8 milliseconds (with a mean deviation of 3.5%) as measured from the track 2 plots. The agreement between these means is quite close. The overall operation time required for the opening (T_o to T_f) as determined from

track 1 plots was 638 milliseconds (mean deviation of 0.2%) and from the track 2 plots was 624 milliseconds (mean deviation of 0.5%). It is noted that there is a discrepancy of 14 milliseconds between the two. This is large compared with the deviations among the track 1 and track 2 measurements respectively. It is believed that the track 1 mean time for the T_o to T_f interval (638 milliseconds) is correct and that the cues employed for the location of the T_f timing line on the track 2 plots were slightly obscured by the initiation of purging noise. On examination of the parametric plots for the opening events of the F1 lox valve as derived from track 2, it will be seen that the line indicating T_f corresponds to the time location of a slight dip in the A4 trace which just precedes a prominent peak. It is now fairly clear that this peak is a more accurate T_f cue. For the five events studied, the mean interval between the dip and the peak is about 1.5 millimeters as measured and this corresponds to 9.4 milliseconds in real time. This correction would bring the mean T_o to T_f interval (for the track 2 opening plots) to 632 milliseconds and the discrepancy would then be only 7 milliseconds, or roughly 1% between the two tracks which represents quite good agreement.

The T_o to T_1 interval as determined for the closing plots, is believed, it will be recalled, to represent the time required for reversal of gas flow to take place and corresponds, in effect, to the duration of operation of the four way valve. This interval, as derived from track 1 data, is in good agreement with the track 2 value. For track 1, the mean time was 164 milliseconds with a mean deviation of 4.3%. For track 2, the mean time for the apparently corresponding interval, i.e., T_o to T_1', was

169 milliseconds with a mean deviation of 2.1%. Note that the time required for operation of the four way valve to initiate closing is about four times the time required to initiate opening, if our interpretation of the parametric plots is correct. The interpretation is in large part based on the fact that in plots of both events, derived from both tracks, display an unmistakable drop of energy which is difficult to explain except in terms of a temporary reduction of the excitation level as would be expected during the interval of operation of the four way valve. The T_o to T_f intervals for the closing operation, as derived from both tracks, are in good agreement with each other and somewhat less than the time required for the opening operation. The mean interval for track 1 is 613 milliseconds with a mean deviation of 1.1%, while that derived from track 2 data is 611 milliseconds with a mean deviation of only 0.04%.

On the basis of the interpretation that the initial periods of low excitation energy which follow T_o for both the opening and closing events represent the operating time of the four way valve, it becomes possible to derive a good estimate of the actual motion time of the valve by subtracting these intervals from the corresponding T_o to T_f periods. In this way, we obtain values for the opening motion time as

From track 1 Plots ---- 598.8 milliseconds

From track 2 Plots ---- 591.2 milliseconds

For the closing motion time, we compute

From track 1 Plots ---- 449 milliseconds

From track 2 Plots ---- 454 milliseconds.

These figures are all mean values. If we now take the percentage deviation as derived from motion time differences and the average of the means, we find that for the opening motion it is 1.3 and for the closing 1.1. The striking fact is the briefer duration of the closing time as compared with the opening event. It should be recalled, however, that during opening, the gas pressure compresses the spring, while during closing the spring, in effect, exerts a force supplementing the driving pressure. This is believed to account for the shorter interval required for the closing motion.

2.5 Correlation of Sonic Signature Features with Mechanics of Valve Operation

In the foregoing discussions of the individual valve signatures, correlations were made, in many instances, between signature features and what was believed to be occurring mechanically within the valve. These correlations are reviewed below. Without having had the valves themselves directly available for detailed studies of their physical operation, these correlations are of necessity inferential, based on the taped data as processed taken in conjunction with drawings which were supplied.

In the course of analysis it was noted that certain features of the valve signatures were more clearly evident in one track than another. During the following review of signature correlation with mechanical operation, attention will be called to the influence of sensor location on the observed patterns. The parametric plots will be referenced exclusively in this review.

2.5.1 S3D Fuel Valve

Track 1 data was derived from a sensor located on the valve flange. The track 2 sensor was attached to the housing containing the actuator. Sensor locations are shown for the fuel and other S3D valves in Figure 32. In the case of this valve, the correspondence of T_o with start motion and of T_3 for the finish of motion for the opening event is given an "A" rating. The slight peak in A4 at T_o in the normal openings which is seen as a large peak in the abnormal openings, is quite consistent in occurrence with respect to the microswitch signal. This start of motion of the valve blade was transmitted fairly well through the main valve housing, but appeared only in a broad and ill defined manner in the track 2 data. It probably reflects a

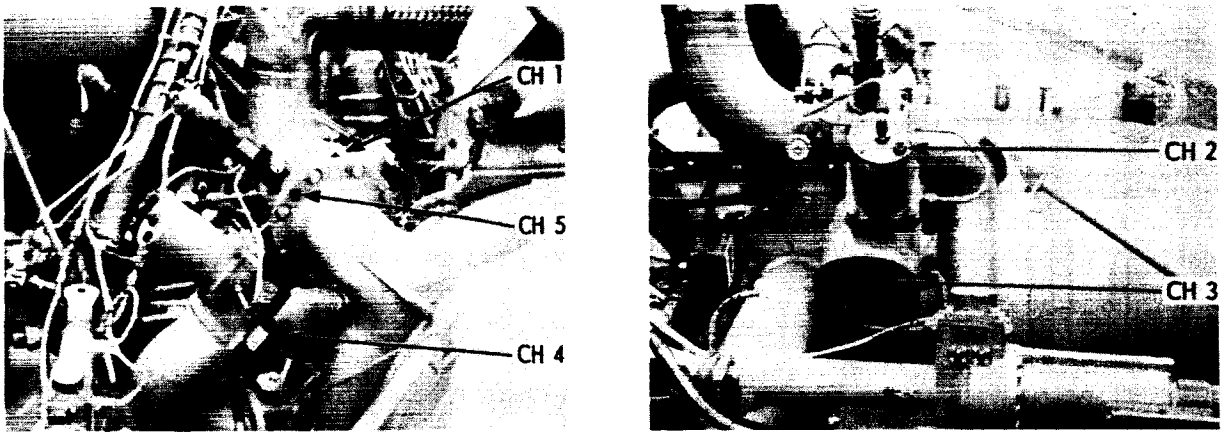

S3D FUEL VALVE

S3D LOX VALVE

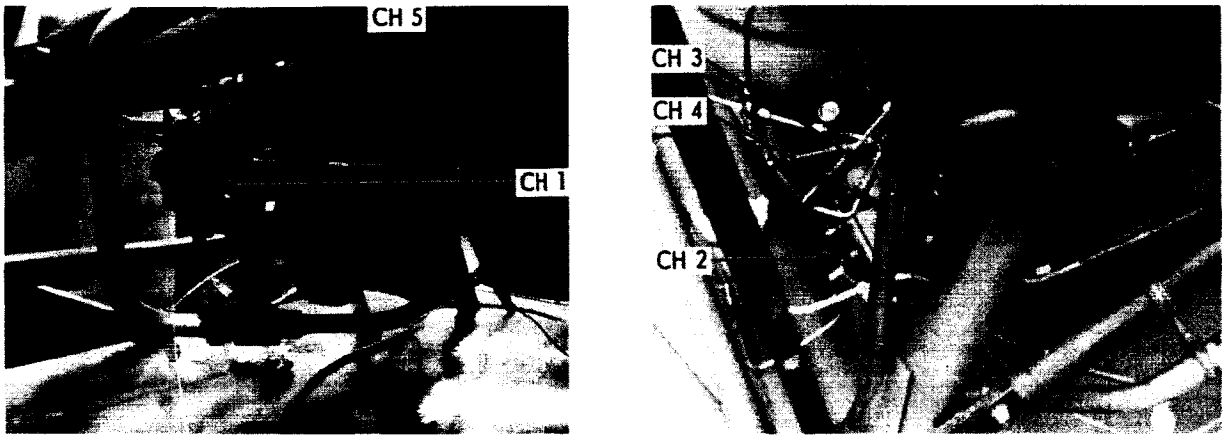

S3D GAS GENERATOR VALVE

Figure 32. S3D Valves with Sensor Locations Shown

resonance of the actuator case of extremely low amplitude. T_3, on the other hand, is well marked in both tracks, being identified by peaks of significant size in A1, A2 and A3. T_x which indicates the time of first detection of turbulence due to actuating gas flow is well marked by the sharp rise in F4 in track 1. This feature appears equally well in track 2 plots. The accompanying activity in F2 is even more sharply marked, probably because of the proximity of the track 2 sensor to the gas inlet. This conclusion is supported, to a degree by the greater amplitude observed in A2 in the track 2 data.

In the case of the S3D fuel valve closing, the T_o and T_f identifications which were based on major peaks in A1, A2, and A3 and on smaller, but significant and coincident peaks in A4 in the track 1 derived plots. These are believed to be reliable indicators. The small peak in F4, which determines T_p, is believed to indicate the occurrence of the bang caused by operation of the solenoid which controls the actuating valve. On some plots this peak was more marked than it appears in the ones shown. It can be seen only on the track 1 plots and is to a degree suspect for that reason. The absence of a correlated signal in A4 is not in itself conclusive negative evidence because the sensitivity of the axis-crossing detector from which the F4 trace was derived is considerably higher than that of the amplitude detectors. For example, note that there is a pre-event F4 trace (both tracks) as well as a post-event trace during a period of apparent total quiescence of A4. The time line denoting T_q marks the initiation of appreciable energy in A3 and A4 in the track 1 plots. Note that these signatures are even more pronounced in the track 2 plots which show a high level of A2 energy as well. These amplitude

features were interpreted as representing the take up of freeplay in the linkage (C). It is true, however, that they could reflect a high level of sonic energy due to the flow of gas in the actuating cylinder. In either case, one would expect the signal levels in track 2 to exceed their counterparts in track 1 and this is indeed the case. T_x which marks the sudden increase in F4 was, as in the case of the opening, believed to mark the first detection of turbulence caused by gas flow (A). Note, in this connection, that T_x precedes T_q by a significant interval (about 10 milliseconds). This would seem to support the suggested interpretation for T_x.

2.5.2 S3D Lox Valve

Plots for the S3D lox valve (and for the gas generator valve as well) were made only from track 1 data after examination of spectrograms derived from more than one sensor. It was concluded, after study of the spectrograms, that for these valves, accelerometers mounted on the main body would yield sufficient data both for timing purposes and for highlighting significant signature features.

For the lox valve opening event, T_o - believed to represent the start of motion - is well defined by simultaneous peaks in A2, A3 and A4. There is also a marked frequency peak in A2 and an abrupt frequency rise, leading to a plateau, in F4. The finish of motion (designated as T_f) is indicated by very prominent peaks in A4 and A3 as well as a significant peak in A2. On occasion there was a correlated peak in A1, but this did not appear with the reliability of the others. Confidence in the accuracy of this interpretation is very high. As with the fuel valve, a T_x timing line is identified by the abrupt increase in F4 which occurs somewhat after the initiating of the

timing signal. There is again considerable confidence that this represents the initial capture by the axis-crossing detector of turbulent gas flow in the actuating system.

For the lox valve closing, the T_o and T_f timing lines are marked by pronounced peaks in all four amplitude parameters and these times for start and finish of motion are believed to be well established. The T_x time line is believed to have the same significance that it did for the opening event; namely, the first detection of gas turbulence. The A3 and particularly A4 traces show considerable activity prior to T_o which was believed due to take up of freeplay in the linkage. However, the steady F4 centroid, beginning shortly after T_x, in advance of valve blade motion, and continuing somewhat past T_f may suggest an orificial source. The F4 centroid occurring during the opening event is also thought to be orificial. Trace A3 in the lox valve closing plots is interesting because of the slow oscillations following T_o of approximately 5 millisecond period. This oscillation is thought, possibly, to reflect a resonant effect involving the mass of the moving system and the compliance of the actuator piston spring.

2.5.3 S3D Gas Generator Valve

As for the fuel and lox valves, the T_o and T_f time lines which are believed to identify the start and finish of valve motion are marked by amplitude peaks in both the opening and closing events. These peaks occur in all amplitude traces. In the case of the opening, the T_o peaks are smaller than the T_f peaks, but for the closing they are essentially equal. As with the other valves, a T_x timing line is identified for both events and believed to indicate the initial detection of turbulence. In the gas generator valve

closings, as in the lox valve closings, a small peak in F4, whose time of occurrence is identified as T_p, is believed to denote the transmitted bang of the solenoid through the tubing. The prominent peaks in F4 (opening) are almost certainly of orificial origin. The second peak must be caused by the persistence of flow after motion has ceased. Note that in operation 4, the second peak is monochromatic, or nearly so. In the case of the closings, the first and third F4 peaks are both believed to be orificial. In the case of the third peak this is practically certain for the reason given in connection with the second F4 opening peak.

2.5.4 F1 Lox Valve

In the case of the F1 lox valve, data from two tracks was parametrically analyzed both for the openings and the closings. Figure 33 shows a longitudinal section of this valve. Note that the accelerometer associated with track 1 is mounted on the end cover near the sequence ports, while the track 2 accelerometer is located at purge port Y on the fitting bolted directly to the valve body casting.

For the opening event, T_o on both the track 1 and track 2 plots almost certainly corresponds to initial actuation of the four way valve and the period of silence (low level energy in A3 and A4) represents the time required for reversal of gas flow to take place. This interval is designated ΔT. Confidence in this interpretation is very high. It has been assumed that actual motion of the lox valve starts at the expiration of the silence interval or very shortly thereafter. For computation of the actual motion time, the former assumption was made. Based solely on timing considerations, it was suspected that T_3 might correspond to contact between the end

E4083

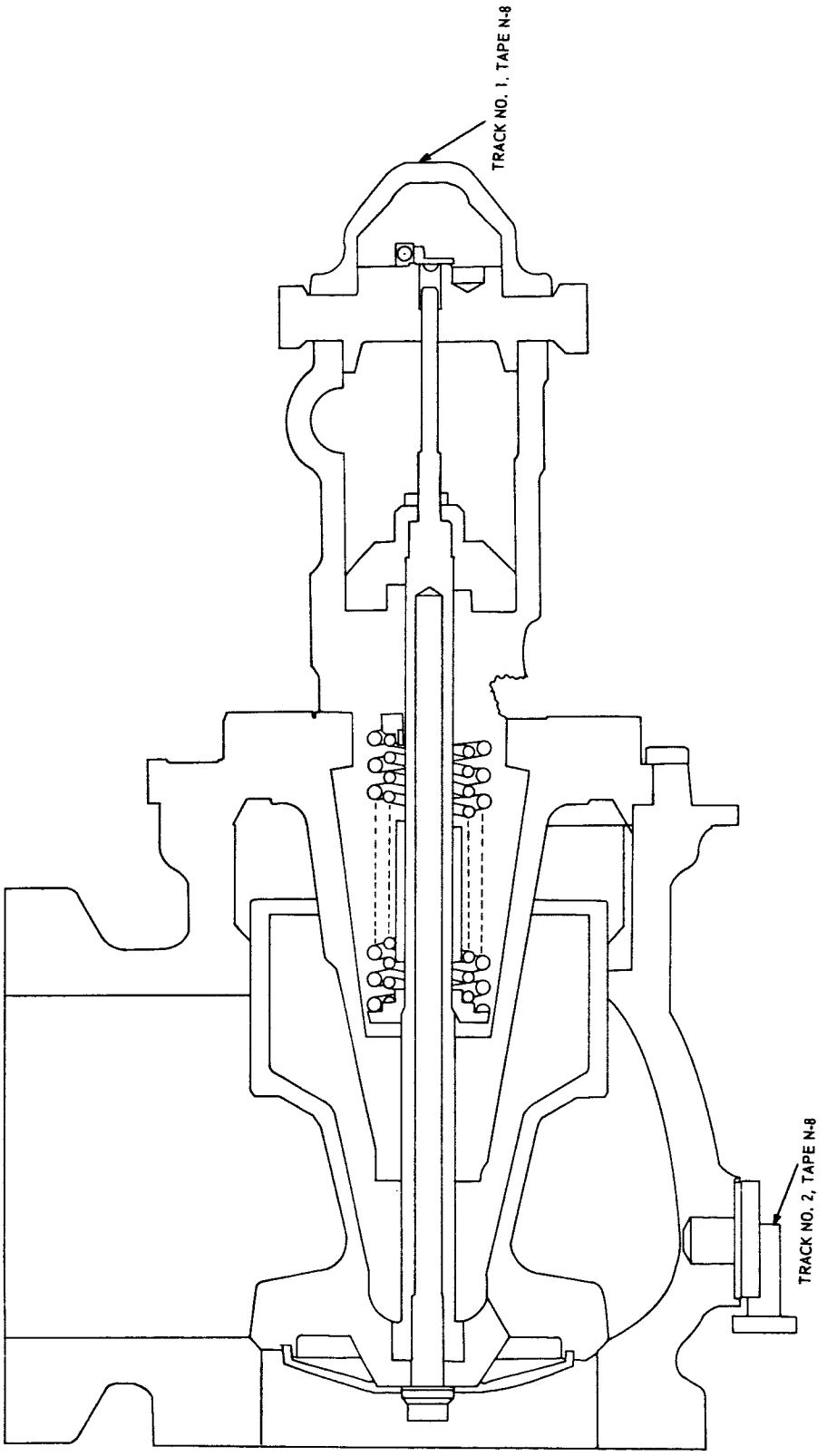

Figure 33. Longitudinal Section of F-1 Lox Valve Showing Sensor Locations for Tracks 1 and 2.

of the valve shaft and the sequence valve rocker arm. T_3 occurs at roughly the same time after T_o in the plots derived from both tracks, although the track 1 plots provide more clear cut cues for its identification. T_f (in the case of both plots) is believed to mark the finish of lox valve motion. This interpretation is considered to be well founded and, indeed, it is noted that the purging noise pattern resumes subsequent to T_f.

For the closing event, again T_o almost certainly marks the initiation of four way valve operation to achieve reversal of gas flow. The abrupt transition from the pre-T_o purging noise signatures to a period of relative silence (observed in plots from both tracks) can be due only to an interruption of system excitation. The termination of the silence period (designated as T_1 for the track 1 plots and T_1' for the track 2 plots) is, as was true for the opening event of the F1 lox valve, believed to represent the time at which gas begins to flow in the reverse direction. Again, as was true for the opening, it was assumed that the end of the silence interval marks the actual start of valve motion. If this assumption is incorrect, the error cannot be more than a very few milliseconds. Shortly after actual start of motion, there appears the remarkably steady F2 tone which has been attributed to a half-wave longitudinal resonance of the poppett valve stem excited apparently by "slip-stick" friction. In this connection, it is, as previously mentioned, believed that the accompanying long period amplitude variations in A2 (in the track 2 plots) represent periods during which the frictional resistance varies from minimum to maximum and back. The attribution of the monochromatic F2 tone to valve stem resonance is supported by the fact that the measured frequency of the monochromatic tone coincides exactly with the

computed half-wave resonance frequency for the valve stem. While this is not conclusive, it is strong presumptive evidence and a reasonably high measure of belief is assigned to this interpretation. The case for the interpretation of the periodic amplitude change in A2 (track 2) is not considered as strong. It is a reasonable assumption, particularly as it correlates with the A1 trace for the same plots, but is not supported by direct evidence. It should be noted that the monochromatic tone in F2 appears in plots derived from both tracks. However, the track 2 plots portray this tone in a far more pure form. That is, the tone as seen in the track 1 plots shows substantial amounts of momentary frequency deviation, particularly during the second half of its duration. On the other hand, the track 2 plots show a perfectly straight line (except for a slight positive peak at T_2) for F2 tone throughout its entire extent. It seems fairly certain that the location of the track 2 sensor on the main valve body favors sonic transmission of the signal because of the large cross section of the metal structure available for acoustic conduction between the valve stem and the track 2 accelerometer. T_f is definitely believed to mark the termination of valve motion. The large peaks in A4, A3, A2 and A1 (in track 2) are all coincident and are interpreted as reflecting the impact of the valve head on the seat. Some of these peaks also appear in the track 1 plots - principally A4 and A3 - with markedly lower amplitude. There is no question at all that the track 2 sensor position (at purge port Y) affords a superior indication of the finish of closing. Note that this position is, in fact, quite close to the valve seat.

In general, it would appear that, given a single choice of sensor location, that corresponding to track 1 might be preferred. This is due to the fact that track 2 data presents a clearer view of the activity of the critical sequencing valve while also providing clear indications of the operation of the four way valve, the start of motion and the completion of motion. However, for complete monitoring of both the opening and closing events there is always the possibility that a given malfunction might appear more conspicuously in the track 1 signature and therefore prudence would dictate employing both locations.

2.5.5 Orifice Resonance

As a supplement to the valve signature analyses, the orificial resonance of an airjet excited pipe was explored. This was done because some of the valve signature features were believed to be orificial in origin and it was considered important to examine a laboratory model of this effect. In this experiment, a piece of tubing, 30 millimeters in diameter, was used. An airjet was introduced at one end to supply sonic excitation. The acoustic output at the other end was picked up by a high quality dynamic microphone and tape recorded. The tape was then slowed down by a factor of 16 to 1 and the band from 0 to 1 kc was analyzed by the Melpar 100 channel filter bank. This band corresponded to 0 to 16 kc in "real" frequency and the resulting spectrogram is displayed in Figure 34. Detailed analysis, based both on this spectrogram and on others made with a Polaroid camera, indicated that most of the energy was concentrated within the frequency range of 2 to 6 kc. Predominate peaks occurred at 2.13 and 4.26 kc. H. S. Ribner[1] points out

1. Ribner, H.S., "Energy Flux from an Acoustic Source Contained in a Moving Fluid Element and its Relation to Jet Noise", JASA, Vol. 32, No. 9, Sep. 1960.

E4085

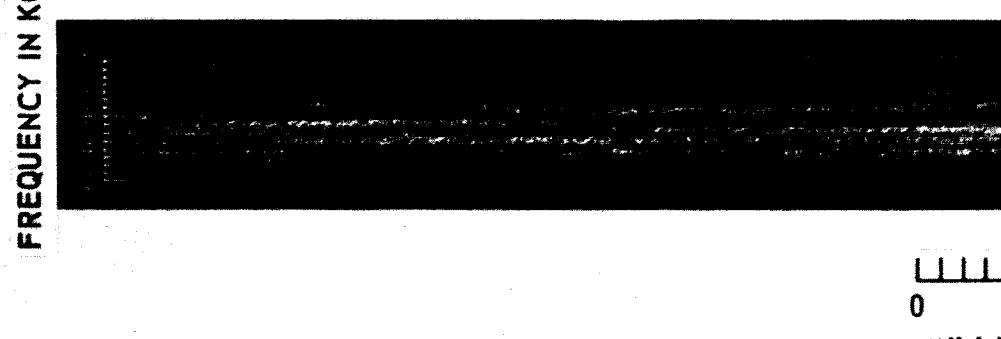

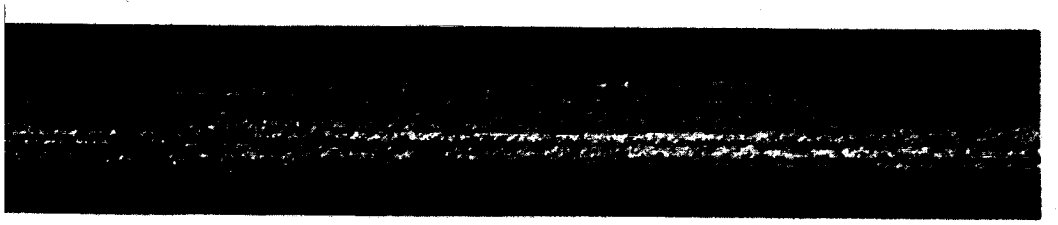

200

SECONDS

2

Figure 34. Spectrogram of Acoustic Output of Airjet Excited Pipe

that the principal sound frequency emitted by an eddy in a jet lies within a range between $c/2\pi R$ and c/R, where c is the sound velocity in the fluid and R is the radius of the jet. The first expression represents the circumferential resonance of the jet and the second a radial resonance. If a pipe radius of 1.5 centimeters is substituted in these expressions, with velocity taken as 1100 x 12 x 2.54 cm/sec, the circumferential resonance is found to be 3.56 kc and the radial 5.58 kc. These computations ignore edge effects and also the fact that the driving jet tends to increase the length of the path traveled by the sound. These factors would tend to reduce the computed values somewhat. The order of magnitude of agreement of the observed and computed values is good. If the orifice size is scaled downward to approximate values existing in the actual valves, the expected orificial resonances are consistent with the measured centroids which define the observed purging noise frequency bands. Ribner has also shown[1] on a semi-empirical basis that the energy distribution in the jet spectrum is reflected by an expression in which the square of the fundamental frequency appears. On this basis a double peak structure would be expected (fundamental plus second harmonic) and, as indicated, this was found. This distribution function is such that higher frequency components would also be anticipated and it can be seen, from the spectrogram, that these do exist.

---

1. Ribner, H.S., "On the Spectra and Direction of Jet Noise", JASA, Vol. 35, No. 4, April 1963.

3. QUALITY OF TAPES RECEIVED FROM NASA

Eight tapes containing valve operating sonic data were received from NASA. These were numbered at Melpar in order of receipt as N1, N2, N3 and so forth. Each of these was examined for signal quality and the best recordings were used for the analyses on which this report is based. In those cases in which the quality was below optimum, the difficulty was identified as either excessive noise, excessive signal amplitude causing overload or signal weak or absent.

A synopsis of tape quality, based on oscillographic examination, follows:

N1 and N2. These were F1 tapes. The signal/noise level was in general too low to permit satisfactory analysis.

N3. This was a tape of the S3D valves. Except for an occasional overload, the quality was excellent and this tape was selected for analysis.

N4. This was also an S3D tape. This tape had frequent overloads, usually on the direct record tracks. Because such overloads may generate erroneous spectral data this tape was not analyzed.

N5. This was an F1 lox valve tape. It was overloaded on two direct record channels and signals could not be found on two FM channels.

N6. Also an F1 lox valve tape. It was found similar to N5, except that one direct record channel (7) also had no signal recorded.

N7. This was also an F1 lox valve tape. Similar to N5. Good speech signal.

N8. This was the last tape received and was also an F1 lox valve recording. The signal quality of this tape was excellent and it was used as

the source of the F1 lox valve data contained in this report. No timing signals could be found on this tape.

4. CONCLUSIONS

4.1 General

It was the objective of this contractual effort to develop a method of analysis and the equipment for this analysis which would permit critical and comprehensive evaluation of the performance of mechanical and electro-mechanical devices aboard space vehicle stages as born by the information content in the acoustical signatures acquired by accelerometer sensors mounted judiciously about the device. This report covers Phase I of the program. This first phase was devoted to development of methods and techniques for analysis of the acoustical signatures. One of the principal areas to investigate was that of signature stability. That is, the closeness with which signatures for successive operations of the same valve under the same driving conditions would match one another. A second area of investigation pertained to the distinctive nature of the signature; i.e., the degree of clarity with which significant features of the signature represent the internal mechanical operating features of the valve thus permitting one to gain knowledge about the performance of internal valve mechanisms. Indeed the results show that one can literally obtain a time flow picture of the internal workings of the valve from the information content of the signature. Closely related to the investigation of the causes of distinctive signature features is the capability to sense signature changes that could be indicative of either an existing or potential future malfunction of a valve. A third area of significant interest is the influence of sensor location on the signature and the utility of using the outputs of a multiplicity of sensors for developing the complete signature. The fourth and final area

of significant interest lies in the development of an efficient means for retaining the significant information content of the signature, a means which will lend itself most efficiently to the development of on-site reliability test equipment designed to provide a pass-or-reject testing of all forms of missile engine valves. In the following paragraphs the findings with regard to each of the principal objectives mentioned above are summarized for the S3D fuel, lox and gas generator valves and for the F1 lox valve.

4.2 Signature Stability

In order to ascertain the degree of signature stability, a large number of operations of the fuel, lox and gas generator valves for the S3D engine and of the lox valve for the F1 engine were analyzed using both fine structure spectrum analysis and a specially developed parametric analysis, the latter designed to convert the information content of the acoustical signatures to a form most readily suited to automatic pattern recognition devices. For the S3D engine valves, it was found that the significant information content pertinent to assaying the performance of the valves for all three S3D engine valve types, fuel, lox and gas generator, lies in the frequency spectrum from 0 to 64 kc. For the F1 engine lox valve the significant information content was found to lie in the 0 to 32 kc range. These facts were determined by analyzing the acoustical signatures as acquired by Endevco Model 2227 and 2217 accelerometers mounted at various locations on the various valve bodies with the fine structure spectrum analysis equipment discussed in detail in Section 2.2.2 of this report. It should be noted that

this equipment is part of Melpar's signal analysis laboratory facility and was not constructed specifically for this contract. Typical spectrograms of the S3D valve signatures obtained by use of the fine structure spectrum analysis equipment are shown in Figures 3 and 9 for the S3D fuel valve openings and closings, Figures 13 and 15 for the S3D lox valve openings and closings, Figures 17 and 18 for the S3D gas generator openings and closings. For the F1 lox valve typical spectrograms are shown in Figures 21 and 22 for openings and Figures 26 and 27 for closings. Visual study of these spectrograms reveals that successive operations of the same valve type on both the S3D and F1 engines exhibit extremely strong similarity. In fact, one can overlay the photographic negatives of the spectrograms and observe qualitatively that the signatures deviate little from one operation to another. Thus, by this qualitative means, one is confident that the signatures are extremely stable. It is now important to point out that for the S3D fuel valve two operations did deviate markedly in their spectrographic pattern. Also a significant deviation from the mean pattern was observed in the case of the first closing operation of five F1 lox valve openings and closings subjected to analysis. In the case of the S3D fuel valve, the deviating operations were Nos. 1 and 11. In Figure 4, these operations are compared with other operations which appeared to be normal. As discussed in detail in Section 2.4.2 of the report, it appears that on opening operation Nos. 1 and 11, the S3D fuel valve blade hung up causing a delay in the initiation of blade motion of approximately 40 milliseconds beyond that typical of the remaining operations recorded. This diagnosis was made via the observation of energy bursts in the vicinity of 11.8 kc and 42 kc which consistently

accompany the break-away of the blade from the seated position. In the case of the first closing operation of the F1 lox valve, it was found to possess a duration from the instant of activation of the four way valve to the instant of attaining the fully open state that exceeded that typical of all others by 118 milliseconds. Also a "slip-stick" excitation of the poppet shaft fundamental resonance which was observed in all other operations analyzed, failed to occur. The details of the F1 analysis are discussed in greater detail in Section 2.4.5.

It is not sufficient to evolve only a qualitative evaluation of the signature stability. Rather, it is more satisfactory to obtain a quantitative estimate of the mean dispersion among a set of signatures which are considered to be typical of the event to be classified. To accomplish this end, and also to place the signature data in a form more suitable for automated recognition of malfunction, parametric data analysis instrumentation was developed. This instrumentation is discussed in detail in Section 2.2.3 of this report. For use with the S3D valves, it provides for the segmentation of the 0 to 64 kc spectrum into four bands. These bands are as follows: Band 1, 0 to 6.4 kc, Band 2, 5.76 to 12.8 kc, Band 3, 16 to 25.6 kc and Band 4, 28.8 to 64 kc except for the S3D gas generator for which Band 4 was 38.4 to 64 kc. The parametric analyzer determines the amplitude or intensity of the energy captured in each band. For the respective bands these amplitudes are designated as A1, A2, A3 and A4 for the respective bands. Also the frequency centroids in bands 2 and 4, designated as F2 and F4 respectively, are also determined. Frequency centroids in bands 2 and 3 were considered unnecessary and were not incorporated. Thus, six

parameters, viz; A1, A2, A3, A4, F2 and F4 are used to represent the significant information content of the acoustical signatures. Plots of these parameters as functions of time for the S3D fuel, lox and gas generator valves are illustrated in Figures 6, 9, 14, 16, 19 and 20 of the text. These parametric signatures allow for the statistical analysis of the time-amplitude-frequency characteristics of significant features in the signatures. The results of such statistical analysis are presented in Tables I, II, III and IV for S3D fuel, and lox valve openings and closings. The general technique is to select a distinctive feature in either an amplitude or frequency parameter and to record its time of occurrence, and amplitude or frequency value at that time. Also mean values of amplitude and frequency between various time boundaries considered pertinent in defining the signature were recorded. This procedure was performed on six S3D fuel valve openings and closings, and on six S3D lox valve openings and closings. The percentage dispersion in each feature class was computed for the entire set. These are summarized in Table IX below.

Table IX

Summary of Mean Dispersions in Percent Deviation from Mean Value Observed in S3D Valve Operation Acoustical Signatures

	Fuel Valve		Lox Valve	
Feature Class	Open	Close	Open	Close
Time	4.2	9	5.6	4.0
Frequency	11.5	10.3	4.6	5.0
Amplitude	37	22.5	31	15.0
Mean Frequency	—	—	3.7	2.5
Mean Amplitudes	—	—	33.4	7.0

It should be pointed out that the dispersions contained in Table IX are not produced by inaccuracy in the observation due to equipment limitations but are the result of the true variations in the event. The percentage deviations should thus be considered as specifying the degree of "blurring" occasioned in repetitions of the event. Any signature that deviates within the tolerance limits in all regards must of necessity be considered as a member of the normal category. An event deviating out of the indicated dispersion range for one or more of the factors used in establishing the mean dispersion chart would be automatically considered suspect. It should be noted that the dispersion is smallest for the times of occurrences of significant features. Thus timing would be an important factor in establishing the conformity or non-conformity of a given event signature to the baseline pattern. The next most desirable parameters having the next smallest dispersion are those involving frequency values. The parameter possessing the greatest dispersion and hence having the least influence on decision making is the amplitude parameter. Except for assisting in the establishment of the times of occurrence of various features in the signature, the absolute amplitudes are apparently of least value when viewed in the comparison with the small dispersion in timing and frequency values. However, it should not be interpreted from this that the amplitude data is not important in the decision making process. The timing data depends critically on the amplitude peaks observed at various times during the signature and without the amplitude parameters it would not be possible to confidently ascertain the times of occurrence of critical signature features. As a final note it

is interesting to observe that the deviations in timing for the atypical operations Nos. 1 and 11 for fuel valve openings were approximately 50%, thus far exceeding the mean dispersion for timing observed for the base-line pattern represented by the data in Table IX. It should be noted that the values that appear in Table IX represent averages of the critical feature timing dispersions and that in the case of selected critical features, such as the time of the initiation of motion of the valve blade, the dispersion was considerably less. The dispersion in the time of initiation of valve blade start motion was only 1% as compared to a mean value of 4.2% for the set of all timing dispersions for S3D fuel valve openings.

Consider now the same kind of data for the F1 lox valve. Table X shows the percentage dispersions noted in timing, frequency, amplitude, mean amplitudes and mean frequencies for F1 lox valve openings and closings as observed on track 1 (sensor located on the sequencing valve cover) and track 2 (sensor located on the valve body at purge port Y). In this case the

Table X

Summary of Mean Dispersion in Percent Deviation from Mean Value Observed in F1 Lox Valve Operation Acoustical Signatures

	Track 1		Track 2	
Feature Class	Open	Close	Open	Close
Time	2.0	2.4	2.5	2.6
Frequency	5.7	5.0	3.3	5.3
Amplitude	35.0	13.5	16	3.6
Mean Frequency	1.5	1.1	2.1	1.1
Mean Amplitude	6.8	3.3	5	3.4

analysis bands were Band 1, 0 to 3.2 kc, Band 2, 2.9 to 6.4 kc, Band 3, 8.0 to 12.8 kc and Band 4, 16 to 32 kc. A review of the data in Table X reveals that the overall signature stability of the F1 lox valve opening and closing signatures is considerably better than that for S3D fuel and lox valves. The one atypical closing (operation 1) as seen on both track 1 and 2 data departed so markedly from the base-line pattern in all respects as to leave no doubt that the departure would have been detected by automated recognition equipment designed to recognize such departures by pattern matching techniques.

Another very important factor should be mentioned with regard to the F1. This type of valve is characterized by the continuous presence of purging noise generated by the presence of continuous actuation gas flow through the driving piston. Initially, some concern was expressed that the purging noise might obscure the valve signature. Indeed this concern was without foundation. Not only did the purging noise in no way interfere with the identification of significant features of the valve signature, but by virtue of the distinctive nature of its spectral structure it actually proves valuable in identifying whether the valve is in the open or closed state.

4.3 Distinctive Feature Correlates

It was one of the purposes of this investigation to establish, where possible, relationships between distinctive features of the sonic signatures of the valves during operation and the corresponding mechanical events. Many such relationships were, in fact, found and are discussed

throughout Section 2.4 of this report. A summary of these findings appears in Section 2.4.5.

The physical valves themselves were not available for mechanical study and operational analysis, but assembly drawings were supplied. For the purpose of correlation between sonic features and mechanical events, the parametric plots were found particularly valuable.

In general, the behavior of the amplitude traces on these plots provided excellent cues to event timing. Although the amplitudes of specific peaks in these plots varied somewhat during successive similar valve operations, their times of occurrence were found to be quite stable. In the cases of the S3D valves, start and finish of blade motion could be determined with considerable accuracy. The behavior of the highest frequency centroid (F4) was also a valuable timing cue because it permitted detection of the first sonic recognition of turbulence caused by the actuating gas flow well in advance of the start of blade motion. In the F1 lox valves studied, amplitude cues permitted virtually positive identification of three critical timing features. These were the start of operation of the four way valve which reverses direction of actuating gas flow, the finish of operation of this valve (with direction of gas flow reversed) and the finish of motion of the lox poppet valve. There was a slight uncertainty (of only a few milliseconds) about the timing of the start motion of the poppet valve, but this was established as occurring either at the conclusion of, or very shortly after the conclusion of, resumption of gas flow following reversal. It was also possible, at least to estimate the time of contact between the end of the poppet valve shaft and the sequence actuator arm for both the

opening and closing events of the fuel valve.

Aside from timing information, other insights could also be inferred from study of the parametric plots. For example, during the closing event of the F1 lox valve, a nearly monochromatic tone was observed in one of the frequency parametric traces (F2). This tone occurred consistently at 6.62 kc and could be correlated with the half wavelength resonance of the poppet valve shaft which was believed to be excited by "slip-stick" friction. In other valve operation, characteristic frequency centroids suggested orificial resonances rather than vibrational motion of mechanical parts because they were found to occur over an interval during which the valve motion was known to have ceased.

When this investigation was first begun, it was hoped that data from valves known to be defective in one way or another could be provided for analysis. It was desired to compare the signature features of such valves with those produced by valves considered essentially normal. Unfortunately, data from known defective valves could not be made available. However, this in no way vitiates the favorable prediction for feasibility of successful malfunction detection by automated means because the deviations occurring within the course of successive operations of normal valves display so small a spread that a significant departure could not possibly escape recognition. This is unquestionably true of event timing and positive proof lies in the fact that during the operations of the normal valves, three specific instances of aberrant behavior occurred and were quite easily detected. Two of these involved the S3D fuel opening events. In operations 1 and 11, the time from first detection of actuating gas turbulence

was markedly longer than normal. The valve blade motion time, on the other hand, was decidedly shorter. The conclusion was virtually certain that in the cases of these two events there had been momentary sticking or binding of the valve mechanism and that the gas pressure had to build up to a higher value before motion started. When it did start finally, the mechanism moved at a faster than normal rate, thus completing the motion time of the event in less than the usual time. The timing deviations were of the order of tens of milliseconds. Such periods are easily detected because the measurement procedures employed permit a precision of less than one millisecond. The other abnormal or atypical event concerned the F1 lox valve and occurred during the first closing event of a series of successive operations. In this case the duration of the event was about 100 milliseconds longer than the mean of the other closings which were in excellent agreement among themselves. In addition, the monochromatic tone in F2 (previously mentioned) and certain other distinctive features of the other closing event signatures were missing.

Thus, it was entirely possible, in many instances, to correlate valve signature features with mechanical aspects of valve operation, even though the valves themselves were not available for study. In particular, it was found possible to determine timing of critical valve events with very high precision. This was true both for the S3D valves and for the F1 lox valve analyzed. It is of particular significance that the lox valve purging noise did not significantly impair the determination of event timing and other mechanical features of importance.

4.4 Influence of Sensor Locations

In each of the valves studied, data was simultaneously derived from various sensors (Endevco accelerometers) attached to judiciously selected sites on the valve bodies and on related parts such as actuator housings and the like. In general, for a given valve event the overall signature corresponding to a given sensor location will differ significantly from that derived from another location. This is because both distance from the site of origin of a specific sonic event and the effects of local cavity resonances, where present, tend to modify the signature pattern as it is detected at one sensor location or another.

The relation between sensor location and the consequent signature is discussed in Section 2.5. As an example of the influence that location plays in determining signature pattern, the F1 lox valve may be sited. In this case, the data analyzed was derived from two sensors. One was located at purging port Y which is near the poppet valve seat. The other was located on an end housing near the sequence valve actuator assembly. It was judged that data derived from the second sensor would, under normal circumstances, be sufficient to define timing and other important parameters associated with normal valve operation. The other sensor, because of its position near the seat, produced more marked amplitude peaks in the parametric plots associated with the seating events. However, in terms of the real goal which is not merely that of feature analysis but malfunction detection, regardless of specific source within the valve or associated mechanism, it cannot be urged too strongly that multiple sensors be employed in a practical automated accept/reject system. At least two locations should be used, preferably one on the

valve body at some strategic point and another located so that it can easily detect sonic signals from actuating or other peripheral valve parts. The use of more than one sensor would greatly enhance the reliability of malfunction detection by enhancing the probability of detecting a significant abnormal cue.

4.5 Summary of Conclusions

The results leave no doubt that for all acoustical signatures examined under this effort, for both the S3D and F1 valves, the potential is extremely great for the instrumentation of an automatic flaw detection system which will reject valves that deviate by a given preassignable threshold from a base-line pattern with an extremely high degree of confidence. The signatures thus far examined are stable in their representation, are interpretable in terms of known mechanical features of the valves and can be presented in an efficient parametric form suitable for the implementation of an automatic system capable of rejecting faulty operating valves.

An important piece of instrumentation has been developed for accommodating automatic pattern recognition. In the text, it is referred to simply as the parametric analyzer. This parametric analyzer performs a function that is critical to the future implementation of a completely automatic flaw detection system for valve acceptance or rejection. It extracts from the relatively complicated spectrum pattern a set of parameters that more efficiently retain the pattern information content and therefore are more suitable for implementation of an automatic pattern recognition system. Because of the important role played by the parametric data processor, and because of its unique design, incorporating principles established by Melpar prior to the performance of this contract, the special name "SONACODER" has

been selected to identify the device. It is closely modeled after principles developed by Melpar for its work on the Formant Vocoder.

5. RECOMMENDATIONS

The investigation performed thus far has revealed that acoustical signatures generated by appropriately located accelerometer-type transducers are bearers of significant information that can be related to internal features of the valve.

As indicated in the foregoing, the goal has been to develop a base-line pattern against which individual operations of the valve are compared for classification as acceptable or non-acceptable. To emphasize this base-line concept, a sketch of a pattern called a Skeleton Diagram, that results from the statistical analysis of the F1 lox valve openings on track 2 is illustrated in Figure 35. Indicated on this diagram are the graphical counter-parts for each of the measures used in the statistical analysis as tabulated in Table VII. Both the mean value of each measure and its dispersion are indicated. Actually, in implementing an automated recognition system the description of such a pattern would be effectively stored in the recognizer and decisions as to the acceptability or non-acceptability of a valve would be based on the measure of the deviation of the acoustical signature from the base-line patterns. Recognition is achieved by first determining effect-ively the difference between each parametric measure on the acoustical signature to be recognized and that established for the base-line weighted inversely in accordance with the observed dispersion for that parametric measure and then summing these to establish an overall "miss-distance" estimate. If this miss-distance estimate is less than a pre-established threshold, then the valve is acceptable. If it is greater, the valve is rejected. Our pattern recognition technique also permits the introduction of cost weighting data which effectively permits the introduction of apriori

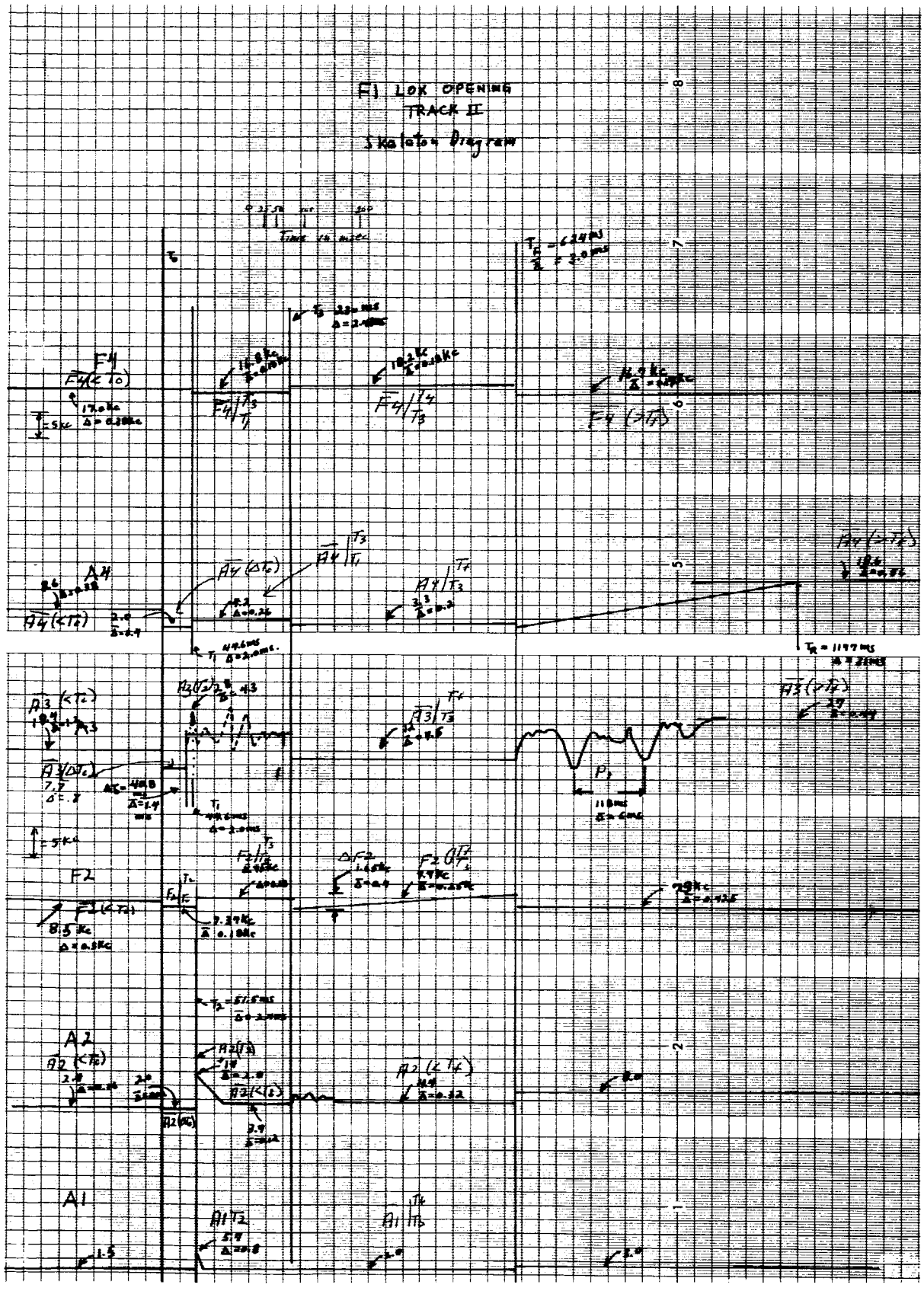

Figure 35. Skeleton Diagram of F-1 lox Valve Opening, Track 2

estimates of the relative importance of individual feature characteristics to establishing the recognition process.

It is recommended now, that a more concentrated effort be initiated to firmly establish base-line patterns for all valve types on the F1 engine. The effort expended in Phase I has accomplished its principal objective, namely, that of demonstrating the existence of significant and reliable information content in acoustical signatures. The effort was mainly concentrated on valves of a single, obsolete S3D engine and on too few samples of a single F1 engine lox valve. What is now required is a concentrated and expanded effort to analyze several varieties of valves on several engines.

An opportunity appears to exist in connection with the Saturn 5 program. A Saturn 5 is now being assembled at the Marshall Space Flight Center in Huntsville. Its five F1 engines, each possessing two sets of lox, gas generator and fuel valves, offer an ideal situation in which to establish base-line pattern recognition data for each of the F1 engine valve types. If indeed data can be obtained from all valves on all five engines, sufficiently large samples of different engine signatures could be accumulated to permit the establishment of an absolute base-line signature for use as an acceptance or rejection criterion for each F1 engine valve type. A minimum of 20 operations of each valve on each engine should be used for establishing the base-line reference patterns. This number will assure a high degree of confidence in establishing both the base-line pattern and the dispersion from the base-line pattern. Of course, it is recommended that multiple sensors should be mounted on each valve. Assuming for the moment that data from four sensors is analyzed for each valve operation, the total

number of signatures to be analyzed for the six valves is 2400. This is of course a very great number of signatures to consume and to accomplish the effort it is intended to employ digital computer computation extensively, using as input data to the computer the outputs generated by the parametric data processor (Sonacoder).

It is the conviction of the investigators responsible for the performance of this study that a very significant contribution to assure that all space vehicle engine valve units will operate properly at the instant of vehicle launch lies in pattern recognition analysis of the acoustical signature. It also appears that the critical analysis of valve operation made possible by study of the spectral pattern of the acoustical signature will serve as a valuable new tool in research on space vehicle engine valve design.